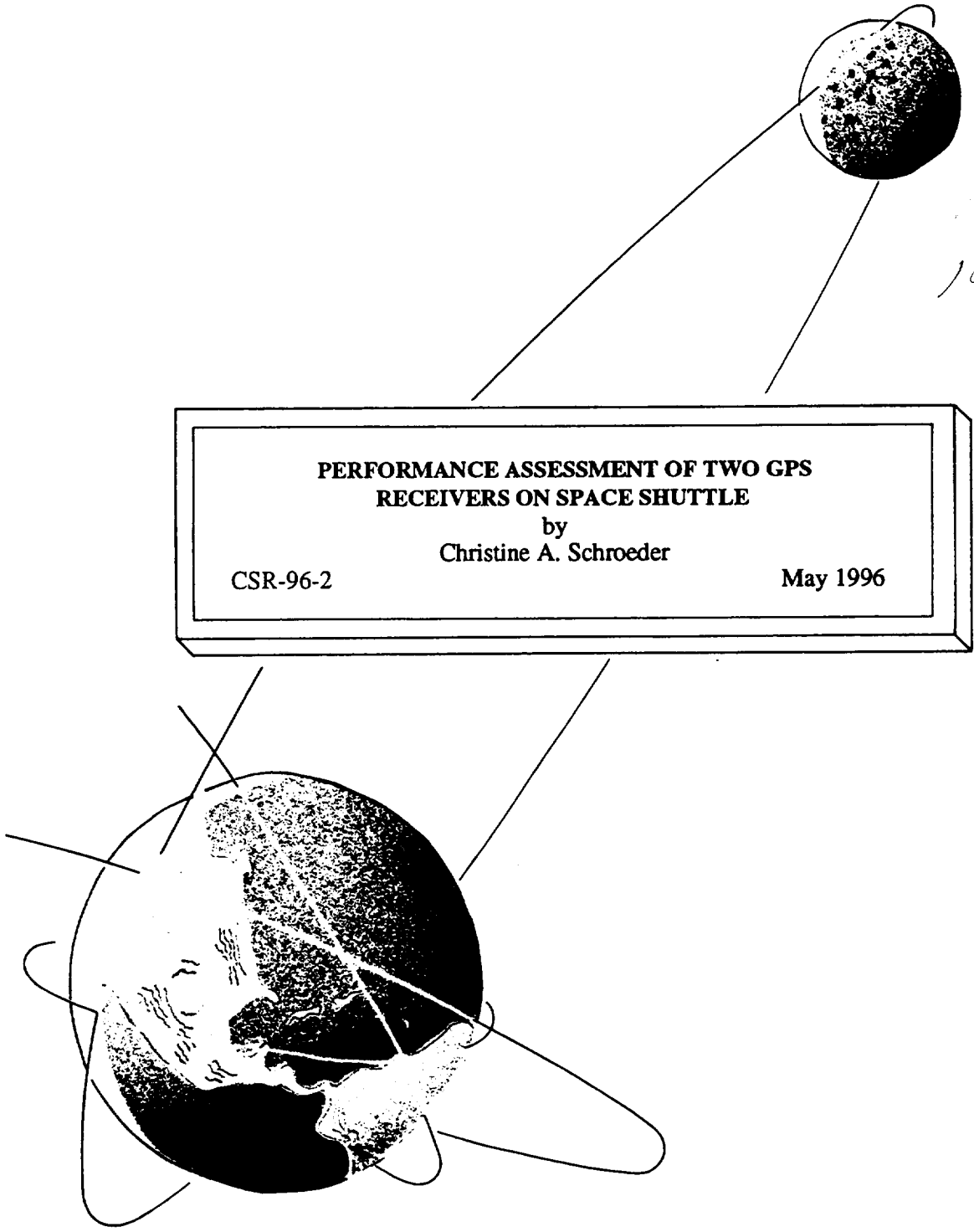

PERFORMANCE ASSESSMENT OF TWO GPS RECEIVERS ON SPACE SHUTTLE

by
Christine A. Schroeder

CSR-96-2 May 1996

CENTER FOR SPACE RESEARCH
THE UNIVERSITY OF TEXAS AT AUSTIN AUSTIN, TEXAS

PERFORMANCE ASSESSMENT OF TWO GPS RECEIVERS ON SPACE SHUTTLE

by

CHRISTINE A. SCHROEDER

Center for Space Research

The University of Texas at Austin

May 1996

CSR-96-2

This research was supported in part by

Grant No. 9-750

for the

NASA Johnson Space Center
Houston, Texas

by the

Center for Space Research
The University of Texas at Austin
Austin, Texas 78712

Principal Investigator:

Bob E. Schutz

Acknowledgments

This study would not have been possible with out the gratefully accepted support of NASA Johnson Space Center (JSC) Grant 9-750. The Wake Shield is supported by NASA Grant NAGW-977. The WSF-02/GPS experiment was support, in part, by the Texas Space Grant Consortium, directed by Byron Tapley. Mike Exner from University Corporation for Atmospheric Research (UCAR) provided the TurboStar receiver plus extensive expertise during some great trouble shooting sessions. Tom Meehan, Charles Dunn and Courtney Duncan provided assistance on the TurboStar receiver operation. Mike Cooke and Samantha McDonald of JSC designed the GPS data recorder and provided invaluable guidance during hardware integration. Russell Carpenter at JSC helped coordinate the experiment and provided, with Ray Nuss, very helpful information regarding the Collins receiver. Nick Combs from the University of Houston Clear Lake assisted in his role as WSF-02 Payload Manager and peace keeper. Anita Ramos at JSC provided key information on the Shuttle Remote Manipulator System and Bill Tracy, also from JSC, provided Shuttle state and center of mass information. John Ries from the Center of Space Research assisted with UTOPIA and MSODP runs. Timothy Valdez reproduced the experiment hardware figures shown in this study. P. A. M. Abusali was available through out the entire research for discussions and guidance. Most importantly, Bob Schutz provided support and guidance on a daily basis while also granting rare opportunities to participate in every aspect of the experiment. This study was a truly great experience because of the dedication of Bob Schutz.

May 1996

Abstract

Space Shuttle STS-69 was launched on September 7, 1995, carrying the Wake Shield Facility (WSF-02) among its payloads. The mission included two GPS receivers: a Collins 3M receiver onboard the Endeavour and an Osborne flight TurboRogue, known as the TurboStar, onboard the WSF-02. Two of the WSF-02 GPS Experiment objectives were to 1) assess the ability to use GPS in a relative satellite positioning mode using the receivers on Endeavour and WSF-02 and 2) assess the performance of the receivers to support high precision orbit determination at the 400 km altitude. Three ground tests of the receivers were conducted in order to characterize the respective receivers. The analysis of the tests utilized the Double Differencing technique. A similar test in orbit was conducted during STS-69 while the WSF-02 was held by the Endeavour robot arm for a one hour period. In these tests, biases were observed in the double difference pseudorange measurements, implying that biases up to 140 m exist which do not cancel in double differencing. These biases appear to exist in the Collins receiver, but their effect can be mitigated by including measurement bias parameters to accommodate them in an estimation process. An additional test was conducted in which the orbit of the combined Endeavour/WSF-02 was determined independently with each receiver. These one hour arcs were based on forming double differences with 13 TurboRogue receivers in the global IGS network and estimating pseudorange biases for the Collins. Various analyses suggest the TurboStar overall orbit accuracy is about one to two meters for this period, based on double differenced phase residuals of 34 cm. These residuals indicate the level of unmodeled forces on Endeavour produced by gravitational and nongravitational effects. The rms differences between the two independently determined orbits are better than 10 meters, thereby demonstrating the accuracy of the Collins-determined orbit at this level as well as the accuracy of the relative positioning using these two receivers.

Table of Contents

List of Tables

List of Figures

Chapter 1

Introduction

1.1 THE STS-69 FLIGHT

The Space Shuttle Endeavour was launched September 7, 1995, at 10:09 CDT from Pad 39A at Kennedy Space Center (KSC) on an eleven day mission in which one primary objective was to deploy and retrieve a free-flyer spacecraft. This free-flyer was the Wake Shield Facility (WSF), a 4-meter diameter stainless steel disk designed to conduct an experiment in developing ultra pure semiconductor materials within the spacecraft's wake. The Endeavour flight, referred to as STS-69, was the second flight of the Wake Shield, designated WSF-02. The first flight occurred in February of 1994. There are two other missions planned to fly a total of four times through 1999 in order to achieve the Wake Shield's ambitious goals.

The start of STS-69 was typically delayed. Originally scheduled to launch in late July of 1995, an issue surfaced after the launch of Space Shuttle Discovery on July 13. Apparently, the primary O-ring in a nozzle joint on the left Reusable Solid Rocket Motor (RSRM) of Space Shuttle Atlantis had been singed sometime during the June 27 mission. NASA postponed Endeavour's launch until flight hardware related to the O-rings could be reviewed on Atlantis and Discovery [Campion, et al., 1995]. However, this was not the only delay.

Once the O-ring issue was resolved, Mother Nature ordered up a record number of tropical storms for the summer of 1995. One of these storms developed into Hurricane Erin and Endeavour was rolled back from the launch pad to the Vertical Assembly Building on August 1, only the tenth roll back in shuttle history. Endeavour was returned to Pad 39A on August 8.

The launch was scheduled for August 31, but a failure of one of the three Endeavour fuel cells forced the mission management team to scrub the launch

prior to initiation of tanking operations. Fuel cell number 2 was replaced and the launch countdown was started on September 4.

Finally on September 7, Endeavour and its crew were ready to go. The commander of the mission was three-time Shuttle veteran David Walker with pilot Kenneth Cockrell, an Austin born University of Texas graduate! The three mission specialists were James Voss, James Newman and Michael Gernhardt, the sole rookie. Together they carried out STS-69 Spartan-201 deployment and retrieval up through September 11 when WSF-02 deployment occurred.

The WSF-02 was released for a total free-flight duration of 72 hours. During this free-flight, a nitrogen thruster on WSF-02, and subsequent Endeavour orbital maneuvers, eventually increased the separation between Endeavour and WSF-02 to more than 40 km. The nominal free-flight attitude of WSF-02 oriented the velocity vector normal to the disk. The orbit of WSF-02 was nearly circular at about 400 km with an orbit inclination of 28.5°.

This design of WSF-02 and its orbit characteristics made it a suitable platform for other experiments. With the primary thin film growth experiment set on the back side of the WSF-02, the Texas Space Grant Consortium (TSGC) took advantage of the opportunity to store payloads on the opposite side. TSGC is a joint program between NASA and three Space Grant Colleges: The University of Texas at Austin, Texas A&M, and the University of Houston. It is comprised of 56 Texas organizations ranging from industrial, educational and government backgrounds. One of TSGC's main objectives accomplished here is "To foster high quality graduate level space research at consortium academic institutions" [TSGC, 1996].

Three payloads were chosen by TSGC to be collectively known as TexasSat-01. The first experiment was Baylor University's Cosmic Dust/Orbital Debris Monitor (CoDEM). The CoDEM was used to capture orbital debris to be brought back to Earth for further study. The second was a joint experiment between The University of Texas at Dallas and Lamar University. They flew a Neutral Mass Spectrometer (NMS) used to measure the environment surrounding the WSF-02, including monitoring the wake area and the distribution of gases

released from the Shuttle. The University of Texas at Austin proposed a third payload consisting of a high precision Global Positioning System (GPS) receiver.

1.2 SPACEBORNE GPS

Spaceborne GPS is an advancement that has caught the interest of space entrepreneurs all over the world. Beyond the original goal of surface positioning, many space based applications have been developed for research in various scientific communities. Among these are onboard positioning and attitude determination, precision orbit determination (POD), Earth gravity model improvements, atmospheric sounding (occultation), and ionospheric imaging, just to name a few. There are several examples of these successful applications to support future activities with spaceborne GPS.

A recent development in attitude positioning involved a single frequency C/A-code receiver flown on the U.S. Air Force satellite RADCAL which reported attitude accuracy of better than 0.5° [Cohen, et al., 1993]. POD for altimetry missions reached new levels of accuracy exceeding 4 cm rms radial orbit accuracy when a dual frequency P-code receiver was flown onboard the joint U.S.-French TOPEX/POSEIDON at 1335 km. The orbit accuracy assessment was reached through analysis of tracking data from non-GPS sources, analysis of altimeter data and comparisons of results produced by independent software. These results were described by Taply et al. [1994], Melbourne et al. [1994], Yunck et al. [1994], Bertiger et al. [1994] and Schutz et al. [1994]. More recently, a TurboStar flown on the UCAR's orbiting GPS/MET at 750 km produced atmospheric profiling via GPS occultation measurements with estimated accuracy of about 1° K over a range of altitudes [Hajj, et al., 1995].

Success stories such as these have encouraged the continuous exploitation of GPS capabilities. However, even with the rapid growth in GPS applications, there have been few reported flights in low Earth orbit with a high precision GPS receiver. Nevertheless, several applications have been proposed and were reviewed by Yunck [1995].

One such idea was dedicated to improving the model of the Earth's gravity field. Errors in the gravity model inhibit applications with high orbit accuracy requirements. The well known nature of these errors can be characterized by dependencies on altitude and orbit inclination. Since modern gravity fields have relied on precise tracking of high inclination satellites, errors in the gravity field exist at low inclination where few satellites have contributed to gravity field determination. For example, the satellite content in JGM-3 [Tapley, et al., 1996; Tapley, et al., 1995] shows the correlation between satellite inclination, altitude and uncertainty in the gravity coefficients. The flight of a GPS receiver at low inclination and low altitude would provide a unique contribution to current gravity models.

There are also other applications with various levels of orbit determination requirements. Altimeter satellites, for example, have high radial orbit accuracy limitations in order to achieve their scientific objectives. Rendezvous and docking activities requires accurate knowledge of the relative position of two spacecraft, such as required for future Space Shuttle and International Space Station activities. The Space Shuttle also offers an opportunity to experiment with new spaceborne orbit sensitive instruments and refine their design before committing them to free-flight operation. With these incentives, the Shuttle program is now involved in an effort to investigate the benefits of utilizing GPS and has thus configured the orbiter fleet with GPS receivers. However, little experience has been acquired with using the Shuttle Collins 3M GPS receiver to support such operations. Knowledge of the expected orbit accuracy from the Collins 3M will be important for general Shuttle orbital operations as well as for supporting experimental scientific payloads.

Another important application is the use of GPS to obtain temperature profiles of the atmosphere. The technique is based on the measurement of GPS signals as they pass through the atmosphere, a technique that has now been demonstrated with MicroLab I carrying the GPS/MET experiment. However, the number of profiles from a single satellite is limited and the increased number of

measurements from multiple satellites could advance the fundamental information used in climatological models.

1.3 OBJECTIVES

The examples given in the preceding section for continuous operation of a spaceborne GPS receiver at low altitude and low inclination are completely compatible with the technical aspects of the STS-69/WSF-02 mission. As noted previously, the GPS Experiment on WSF-02 consisted of a high precision GPS receiver, known as the TurboStar. A second receiver, a Collins 3M, was carried on Endeavour during the STS-69 flight.

The technical objectives of the WSF-02/GPS experiment were to:

- assess the ability to use GPS in a relative satellite positioning mode using the WSF-02/GPS receiver and the separate receiver on Endeavour,
- assess the performance of the WSF-02 and Endeavour GPS receivers to support high precision orbit determination,
- assess the low altitude space environment, particularly the level of unmodeled forces experienced by Endeavour,
- assess the potential of gravity model improvements due to WSF-02,
- use the GPS signals to obtain atmospheric temperature profiles in an "occultation" experiment.

This report discusses the procedures used and results obtained for the first three objectives. The next chapter describes the WSF-02/GPS experiment on STS-69, including the equipment used, the pre-mission preparation, and then the actual in-flight WSF-02/GPS experiment. Chapter 3 describes GPS theory relevant to the analysis of the WSF-02/GPS experiment data. In particular, the procedures for navigation solution calculations, double-differencing of measurements, and ionospheric corrections are described. Ground tests of the two receivers used during the mission are discussed in Chapter 4, while Chapter 5 describes a similar in-flight calibration test. The sixth chapter finally examines precision orbit determination of the combined vehicle, Endeavour and WSF-02, through the use of the independent GPS receivers.

Chapter 2

The WSF-02/GPS Experiment

2.1 THE SET UP

The WSF-02/GPS experiment required several pieces of equipment, which were either borrowed or built specifically for the mission. Coordinating instrument compatibility, testing all components, and developing hardware to satisfy conflicting requirements was a challenge. The end result was an experiment that accomplished all mission objectives stated in Section 1.3. In the following sections, the major components and their integration will be discussed: the WSF-02, the WSF-02 TurboStar receiver, the Shuttle Collins receiver, the WSF-02 and Shuttle antennas, and a data recorder stowed on the WSF-02.

2.1.1 The WSF-02

The Wake Shield Facility, developed by the University of Houston's Space Vacuum Epitaxy Center and built by Space Industries, Inc., (SII) has three main objectives. One objective is to prove the feasibility of creating an ultra-vacuum away from the Shuttle. With the vacuum of space being in the range of 10^{-6} to 10^{-7} torr, the WSF-02 was expected to create a vacuum of 10^{-14} torr. This was accomplished by flying the "ram" side of a disk into the wind. This aligned the velocity vector normal to the disk plane which created a wake behind the shield. Figure 2.1 shows the WSF-02 in its nominal orbital attitude.

Within this wake-induced vacuum, a second objective was to use a process called epitaxy to grow a series of very pure and atomically ordered thin films of semiconductor compounds, such as gallium arsenide. Four, three-inch diameter wafers were successfully grown as a result of the WSF-02 flight [McKenna, 1995].

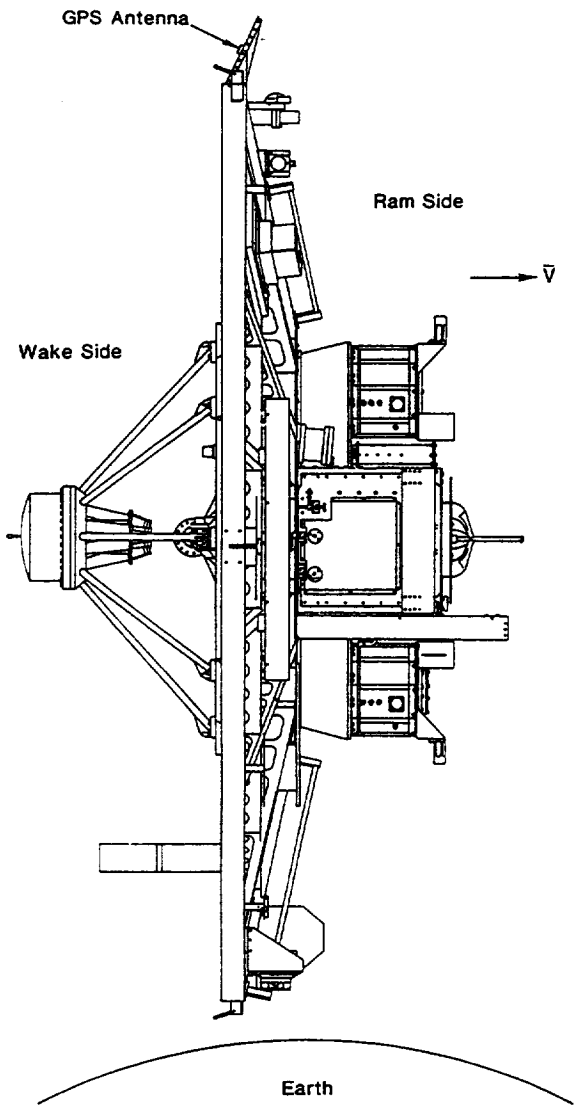

Figure 2.1 Side View of WSF-02

The third main objective was to support any secondary/auxiliary payloads. Fortunately, extra storage space on the WSF-02 ram side provided an excellent opportunity for additional experiments from both industry and academia. Figure 2.2 shows the ram side of the WSF-02 with several examples of secondary payloads labeled. Of most importance to this study is the WSF-02/GPS experiment.

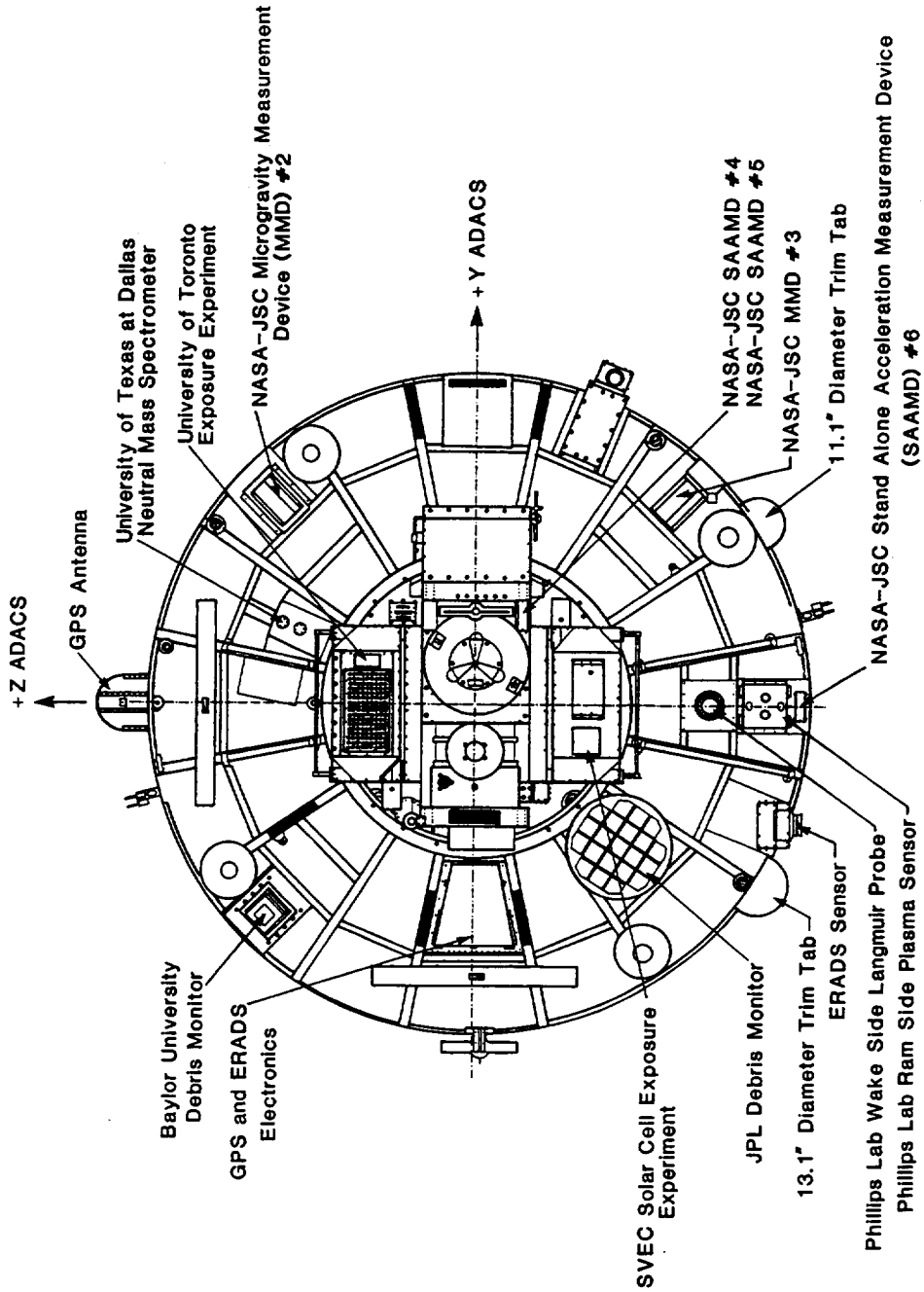

Figure 2.2 View of WSF-02 Ram Side

2.1.2 GPS Equipment of the WSF-02

The WSF-02 GPS Receiver

The WSF-02 GPS receiver was the flight version of the Allan Osborne TurboRogue, which has heritage based on JPL receiver designs. The flight version is marketed as the TurboStar and is shown in Figure 2.3. For the WSF-02 flight, the receiver was lent by the University Corporation for Atmospheric Research (UCAR). This receiver was the backup unit to the primary unit on the MicroLab I satellite launched in April 1995 for the GPS/MET meteorological experiment [Ware, et al., 1995].

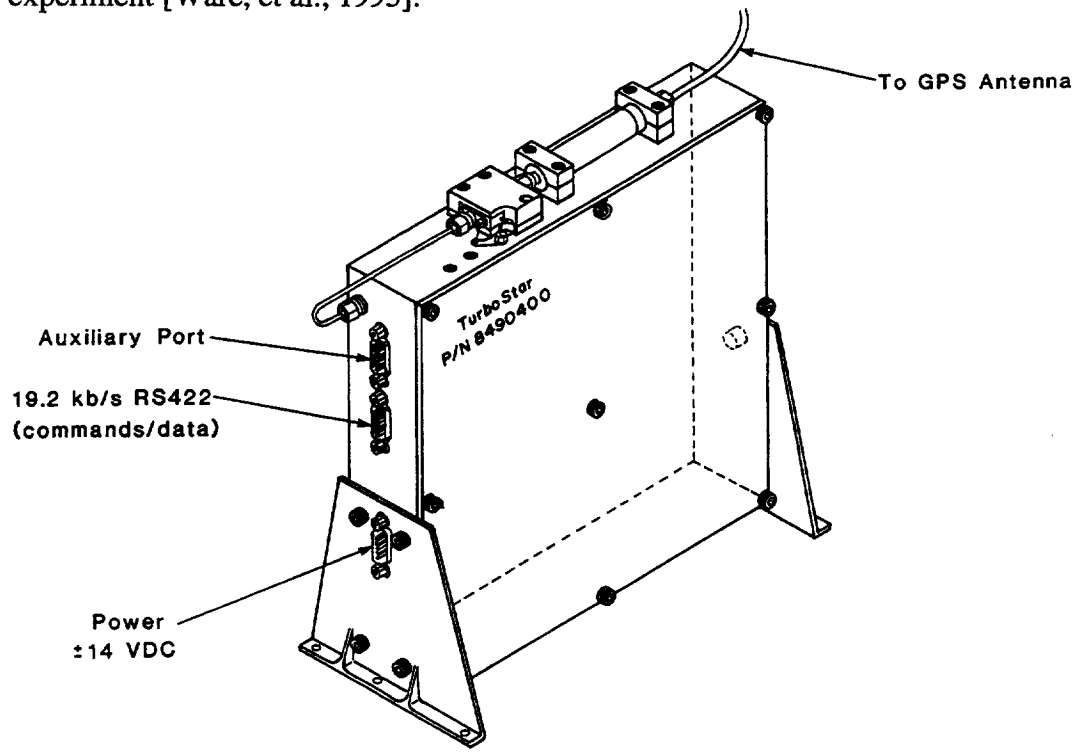

Figure 2.3 TurboStar Receiver

The WSF-02/GPS receiver design, tracking circuits and software were developed at JPL for NASA and flight software enhancements were implemented by JPL under contract to UCAR. The WSF-02 flight unit serial number was 105. The receiver mass was 2.3 kg in a 25x25x10 cm volume, using an average of 17

watts. The WSF-02/GPS receiver was tested in the pre-launch period for thermal conditions similar to those expected in the orbit environment. It was also tested for vibration loads exceeding those expected during Shuttle launches.

The WSF-02 TurboStar can track both the L1 (1575.42 MHz) and L2 (1227.60 MHz) signals from the GPS satellites. It is a precision code (P-code) receiver, but in the presence of anti-spoofing (AS), or encrypted P-code, the receiver tracks the coarse acquisition (C/A) code. When this occurs, the TurboStar can use a cross-correlation technique to construct a delay between the L1 and L2 measurements. This delay is then added to the L1 measurement to create a "pseudo" L2 measurement. Receiver's with this capability are often referred to as "codeless" receivers since they are able to make an L2 measurement without knowledge of the encrypted code.

The TurboStar measures both pseudorange and carrier phase on both frequencies for as many as eight simultaneous GPS satellites. Table 2.1 is an example of data from the TurboStar taken during the STS-69 flight. In this example, receive time is as follows: year, month, day, hour, minute, and second. The PRN list is the GPS satellites tracked during the sample time. (P1) and (P2) are pseudorange measurements corresponding to carrier frequencies L1 and L2, respectively, while (L1) and (L2) are carrier phase measurements corresponding to carrier frequencies L1 and L2, respectively. In the presence of anti-spoofing (AS), C1 is the pseudorange measurement made with the C/A-code. Since PRN 12 is a Block I satellite, it transmits only P-code. Hence, an L1 pseudorange measurement is given in the (P1) column.

Table 2.1 TurboStar Data

Receive Time: 95 09 11 11 00 55.0000000

PRN	(L1)	(L2)	(P1)	(P2)	(C1)
15	-24098675.50	-18778185.24	0.00	23018437.92	23018437.57
12	-28622690.97	-22303383.28	22205911.88	22205912.82	0.00
7	-28826558.24	-22462246.67	0.00	21211199.68	21211199.40
9	4619199.32	3599384.09	0.00	26642575.97	26642577.06
26	-414443.31	-322938.66	0.00	26680360.78	26680360.42
2	-40475645.46	-31539460.08	0.00	20248635.72	20248635.63

One additional issue remains to be addressed to understand the operation of the TurboStar. Because receiver clocks are not precisely synchronized with GPS satellite clocks, corrections need to be made to the measurement times of the receiver. The TurboStar has a capability known as "clock steering". In other words, the clock error does not grow with time but is self adjusting and controlled toward GPS Time. When the TurboStar does not have enough measurements to compute a navigation solution, no clock steering occurs. The quartz oscillator used by the receiver starts to "free-run" and a larger clock correction results (T. Meehan, JPL, personal communications, 1996). Figure 2.4 demonstrates typical clock steering of the TurboStar. This figure illustrates the departure of the receiver clock from GPS Time. Note that the magnitude is less than ± 1 microsecond.

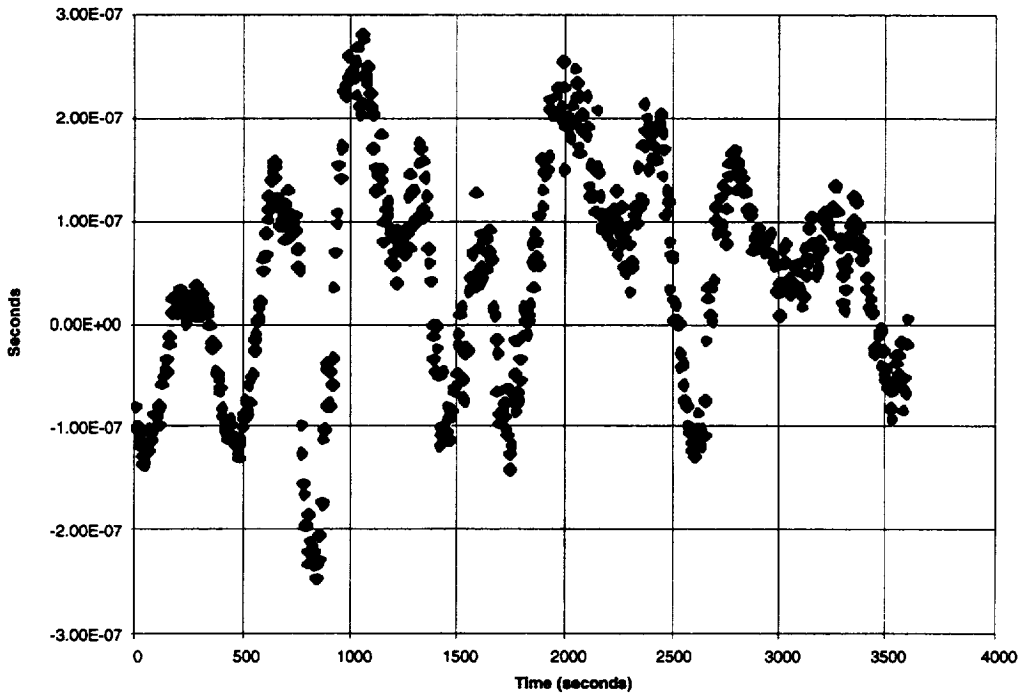

Figure 2.4 TurboStar Clock Corrections

The GPS Data Recorder

Because of a limited bandwidth on the WSF-02 telemetry system, especially during the film growth experiments, transmitting all of the GPS receiver data in real time was not possible. An onboard recorder was designed and constructed for the experiment by engineers of the NASA Johnson Space Center (JSC). To support a separate real time experiment, the recorder was also designed to extract "snapshots" of data in real time. These snapshots were transmitted over the WSF-02 telemetry stream on ground command when opportunities became available. Because of both telemetry bandwidth considerations and limited access to the WSF-02 telemetry, only a small number of additional receiver commands could be implemented.

The recorder was designed to store 80 megabytes on solid state flash memory. This enabled storage of the receiver's pseudorange and carrier phase measurements at an interval of every five seconds, in addition to handling occultation measurements which were taken at a frequency of 50 Hz. Occultation measurements occurred when a tracked GPS satellite underwent occultation by Earth's atmosphere. The receiver recognized occultation when the GPS satellite dropped below a pre-set elevation.

The TurboStar had a tracking mode called "hi rate" in which the receiver occultation parameter AZ Width was set to 90°. This enabled a higher number of occultation observations. In "lo rate" mode, AZ Width was set to 30°. Since the receiver provided more measurements in hi rate, a "hi-rate-to-lo-rate" command was programmed into the recorder to ensure sufficient storage space for the duration of the experiment. The hi-rate-to-lo-rate command could be activated from the Commercial Payload Operation Control Center (COMPOCC) using a software code 159.

Other communications allowed with the recorder during the mission are listed in Table 2.2. Not every command required a software code. "Power on" simply supplied power to the recorder from the WSF-02. "Acquisition on" enabled the recorder to transmit data to COMPOCC on command. There were three command codes needed to reformat the recorder disk if desired, which

would erase any existing data. As it turns out, at the start of the mission the recorder's disk space was about 4% full, but this was considered minimal and the disk was not reformatted. The last two commands terminated the experiment: "Acquisition off" and "Power off".

Table 2.2 Recorder Commands

Command	Code
Power On	N/A
Acquisition On	N/A
hi-rate-to-lo-rate	159
Reformat Disk	7, 25, 93
Acquisition Off	N/A
Power Off	N/A

Other amenities in the recorder design included PC-based software for pre-flight testing and on-flight operations. In most cases, the software was on a laptop computer. One software capability allowed the user to monitor real time data, i.e. navigation solution or pseudorange measurements. This option was an important health status flag for the receiver/recorder. If no data were displayed (either during an on-ground test or during an in-flight snap shot), the user would know the system was malfunctioning.

Other recorder health status variables were displayed as well, including recorder temperature and a recorder counter to demonstrate recorder power in the event of a receiver failure. Both the ground test and on-flight software recorded all data seen by the laptop in "log" files. During the flight, laptop recording only occurred during snap shots.

The WSF-02 GPS Antenna

The GPS antenna on WSF-02 was a micro-strip antenna made by Ball Aerospace and is shown in Figure 2.5. Its location on the shield was selected as a result of various compromises. For precision orbit determination, a full-sky view of the zenith direction is optimal, but for the atmospheric profiling objective, an

antenna orientation in the anti-velocity vector direction is optimal. Other considerations included avoidance of signal multipath sources and clearance of the wake region. With these factors in mind, the antenna was placed on the zenith side of the disk rim, with the ground plane oriented 26 ° with respect to the zenith, as shown in Figure 2.1. This orientation required trim tabs to offset an aerodynamic torque introduced by the protruding antenna ground plane to which the strip antenna was attached.

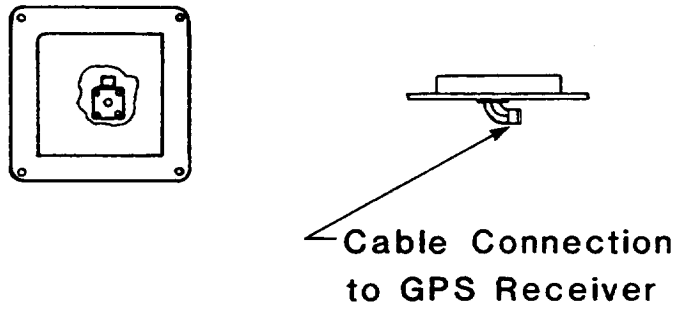

Figure 2.5 WSF-02 GPS Antenna Without The Ground Plane

Integration of the GPS Equipment

The TurboStar, data recorder, and antenna were integrated as shown in Figure 2.6. The auxiliary port was not used during the flight but was used in conjunction with another laptop during all hardware integration tests on ground. Note the receiver power supply was the recorder. The recorder required 28 V of which 15 V was supplied to the receiver. Also, all communications to and from the receiver traveled through the recorder.

Figure 2.7 is an actual photo of the integrated receiver and recorder on the WSF-02 taken at Hangar AE, KSC. These two pieces of equipment were then shielded with an aluminum cover to protect them from overexposure to the sun in space. It should be noted that the cover did not completely enclose the

equipment. Figure 2.8 is an actual photo of the GPS antenna attached to the WSF-02. The blue cable shown is the antenna cable which connected to the TurboStar.

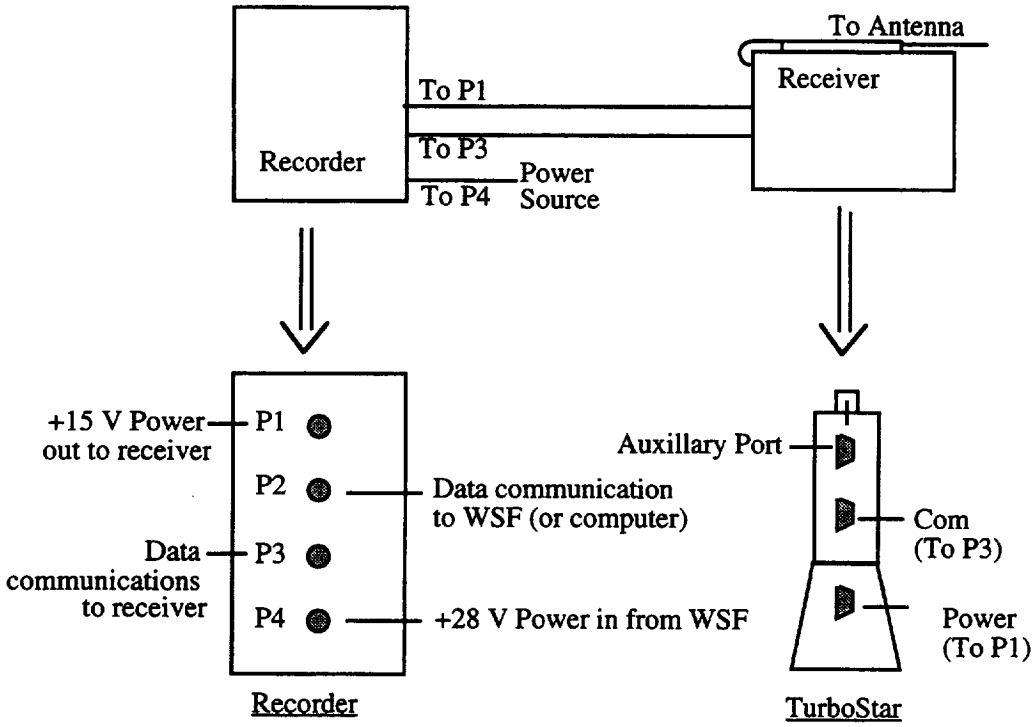

Figure 2.6 Receiver, Recorder and Antenna Integration Schematic

Figure 2.7 Installed Receiver and Recorder on WSF-02

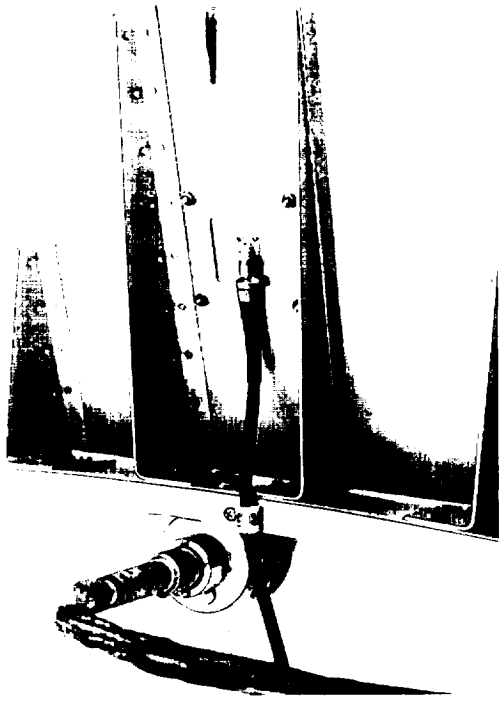

Figure 2.8 Installed WSF-02 GPS Antenna

2.1.3 GPS Equipment of the Space Shuttle Endeavour

The Collins 3M Receiver

The Endeavour spacecraft, designed to accommodate GPS, carried a Collins 3M GPS receiver. The receiver measures pseudorange and a differenced range with the capability to track up to five satellites, where the fifth channel is a "roving" channel. The Collins receiver is a dual frequency, P-code receiver. The L1 frequency is tracked on the first four channels, while the fifth channel uses L2 P-code. When the P-code is encrypted, the receiver only tracks the C/A-code on the carrier frequency L1. The serial number of the Collins 3M used on Endeavour is 001. The serial number of the model used for the ground tests was 98. Both had a mass of about 5.4 kg in a 8x18x30 cm. volume, using on average 28 watts.

Table 2.3 is an example of the assumed interpretation of the raw data obtained from the Collins receiver as shown in Appendix 1. It was assumed (PA) and (PB) were pseudorange measurements and (LA) and (LB) were differenced range measurements, but it was not obvious which frequency was being used. In this example, however, since it was known that P-code was encrypted (except for PRN 12), the measurements were C/A L1 pseudorange and differenced range and the second PRN 12 measurement was assumed to be an L2 measurement in the fifth channel.

Table 2.3 Collins Data

Receive Time: 95 9 11 11 0 54.9508563

PRN	(PA)	(PB)	(CA)	(LA)	(LB)
19	-4077183.380	0.000	0.000	720.427	0.000
12	-5032639.996	0.000	0.000	1494.610	0.000
15	-4219820.498	0.000	0.000	-4743.849	0.000
2	-6989795.783	0.000	0.000	-1050.212	0.000
12	-5032641.456	0.000	0.000	1494.634	0.000

The other issue with the interpretation of the raw Collins data shown in Appendix 1 is the time tag. It was first assumed that a receiver clock correction

needed to be calculated for each set of measurements (see Section 3.1). However, one result of the research that will be presented in Chapter 6 demonstrates that the receiver clock correction was accounted for in the time tag. Unfortunately, as shown by the negative pseudorange values in Table 2.3, the measurements are *not* consistent with this interpretation. This could be a misinterpretation of either the raw data, or a feature of the software that creates the spread sheet data in Appendix 1. As a consequence, the results presented hither do not involve a solution for the Collins clock correction. In other words, the receive time was interpreted as already being corrected to GPS Time.

The Shuttle Antennas

Because the orbiter operates in many spatial orientations, it is configured with two antennas: one on top above the crew cabin and the other directly below on the Shuttle's "belly". In Shuttle terminology, the two antennas are referred to as the "upper-hemi" and the "lower-hemi". Figure 2.9 illustrates the location of the upper-hemi.

For most in-flight applications, both antennas receive signals. The consequence of this design is that the five channels of the Collins will usually contain data from both antennas. However, the receiver has been shown to meet or exceed the Shuttle requirements, even in the presence of Selective Availability (100 m positioning). For most operations, the position requirements are several kilometers, with the exception of entry requirements being in the vicinity of 100 m (R. Carpenter, JSC, personal communications, 1996) so the association of antenna with tracked satellites is not important. In the POD problem, however, this distinction is important at the meter level.

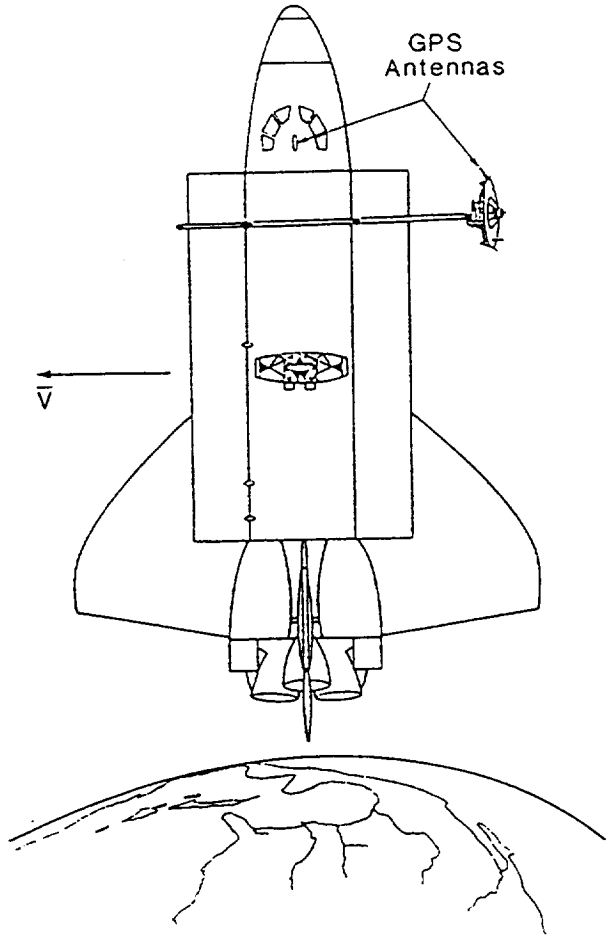

Figure 2.9 Shuttle Upper-hemi Antenna and WSF-02 Antenna

2.2 A TIMELINE OF PRE-FLIGHT EVENTS

The initial planning and establishment of hardware requirements took place in Summer 1994. Various hardware designs were considered and accepted or rejected. Several meetings were held between JSC, University of Texas and University of Houston personnel to resolve design issues. In Fall 1994, the design was established, as shown in Figure 2.6. Agreements were obtained in which

UCAR would loan the TurboStar receiver and JSC would design and construct the data recorder. Tests needed to be executed to verify compatibility and ensure all components were properly functioning. Once in flight, the experiment was basically passive; therefore, verification of every possible aspect of the mission prior to flight was a necessity.

In December of 1994, radio frequency interference (RFI) tests were conducted at SII, the contractor managing the WSF-02 project. These tests included simultaneous operation of all components to evaluate their response to RFI. No sources of RFI that would adversely affect the TurboStar were found.

At the turn of the new year in 1995, the TurboStar passed thermal and vibration tests at Ball Aerospace in Boulder, Colorado. These tests included vibration levels that exceeded those expected during launch and temperature effects reaching 65°C.

In March at JSC in Houston, Texas, an orbital flight signal simulator test was performed. This was the first joint test of the TurboStar and recorder system. In this test, a hardware signal simulator generated L1 and L2 P-code signals consistent with those that an orbiting receiver on the Shuttle would acquire. Although a few problems were discovered with the recorder, NASA engineers quickly modified it for another test in April.

The April test also included the Collins in an attempt to calibrate the two receivers and characterize their performance before the flight. A final test of the TurboStar and recorder on April 14 showed the units were functioning fine together. Analysis of the recorded data verified this successful operation.

By the end of the month, both the recorder and the TurboStar were ready to be integrated with the WSF-02 at the Cape Canaveral Air Force Station in Hangar AE near KSC. Despite many incidents (see April report in Appendix 2), the integration was a success. Finally in May, a final test of the receiver/recorder system was performed at Hangar AE and the latest version of flight software for the TurboStar was installed. This version of flight software had been validated in flight on the GPS/MET receiver. A different set of problems were encountered

due to the test environment, but the final flight preparation was a success (See May report in Appendix 2).

After the Shuttle's eleven day journey starting on September 7, 1995, preliminary results were rushed to the 8th International Technical Meeting of The Satellite Division of The Institute of Navigation [Schutz, et al., 1995]. Then in early October, both the TurboStar and recorder were removed from the WSF-02 in Hangar AE. Both were taken to JSC for data extraction and instrument analysis. While the hardware was at JSC, another TurboStar/Collins calibration test was performed as part of a post-flight analysis. This test concluded the WSF-02/GPS experiment. By mid to late October, the flight data became available allowing data analysis to begin and the TurboStar was returned to UCAR. Results of the experiment were presented at the AAS/AIAA Astrodynamics Meeting in early February [Schroeder, et al., 1995] and an additional test of the TurboStar was conducted in March 1996 at UCAR. The mission related events are summarized in Table 2.4.

Table 2.4 Timeline Of Events

Summer 1994	Initial Planning
Fall 1994	Experiment Design Finalized
December 1994	Equipment RFI Tests
January/February 1995	TurboStar Thermal/Vibration Tests
March 1995	Orbital Flight Signal Simulation
April 1995	TurboStar & Collins Calibration
April 1995	Final Recorder Test
April 1995	Hardware/WSF-02 Integration
May 1995	Last Flight Software Upload
September 1995	STS-69 Flight
September 1995	ION Meeting
October 1995	Equipment Retrieval
October 1995	TurboStar & Collins Calibration
February 1996	AAS/AIAA Astrodynamics Meeting
March 1996	Final TurboStar Checkout

2.3 THE FLIGHT EXPERIMENT

This section describes the actual turn of events and conduct of the experiment during the mission. Launch of STS-69 took place at 10:09 CDT, on September 7, 1995.

About three and a half days into the mission, on September 11, 1995, the Shuttle was placed into a gravity gradient (GG) attitude as shown in Figure 2.9 which remains stable without Shuttle thrusting. This enabled Endeavour to remain stable while WSF-02 operations took place, providing an uncontaminated environment for the WSF-02. The Remote Manipulator System (RMS), or Shuttle arm, grappled the WSF-02, lifting it out of the cross-bay carrier into a hover position at 254:05:44 UTC. There it hovered for about fifteen minutes before being slowly maneuvered into a position called "ram cleaning". Ram cleaning consisted of maneuvering the WSF-02's wake side into the direction of flight so that the "wind" of atomic oxygen could clean away any impurities collected during launch. After more than an hour and a half of cleansing, the WSF-02 was carefully moved to ADACS checkout (C/O) orientation where the WSF-02's Attitude Determination and Control System (ADACS) was to be tested. After ADACS C/O maneuvers, GPS acquisition was initiated since the WSF-02 was in an orientation similar to free-flight. With the arm quietly supporting the WSF-02 for an hour and a half as it waited to maneuver its payload into the release position, the receiver was powered on. Using information loaded into the receiver four months earlier, the receiver "found itself" by tracking and locking onto GPS satellites.

The WSF-02 was released into free flight at about 254:11:26 UTC. With the constraint of the Shuttle not being allowed to fire any thrusters for fear of contamination of the space around the thin film growth experiment, the WSF-02 used small nitrogen thrusters to maneuver away from the Shuttle. This was the first time a payload had maneuvered away from the Shuttle. With the WSF-02 at a safe distance, the Shuttle then maneuvered itself to further increase the relative distance to almost 40 km. During the first twenty hours of free flight, the WSF-02 mission permitted few occasions for snap shots of GPS data to be transmitted via

telemetry. However the data transmitted appeared normal and the recorder appeared to be working. Unfortunately, at 255:07:49 UTC a power converter failed in the recorder that provided power to the receiver (see Appendix 3 for further details). This failure ceased all data collection and snap shot telemetry capabilities; however, no prior data were lost. At the time of the failure, the cause was uncertain, so several attempts were made to revive the experiment in flight, to no avail. The receiver and recorder were eventually powered down. The WSF-02 was retrieved by the arm on September 14 after about 72 hours of free flight, and then returned to Earth on the 17th.

Chapter 3

Relevant GPS Theory

There are many aspects of GPS theory which could be discussed and then applied to numerous scenarios. For example, one could discuss: the several measurement types, the various measurement processing techniques, the error sources, how to account for each error source, the timing issue, the many applications of GPS , the expected accuracy for different applications, and so on. Here only the immediately relevant GPS theory subjects will be covered in order to establish the foundations of the analysis used in this study.

3.1 NAVIGATION SOLUTION METHODOLOGY

The position determination problem involving GPS is characterized in Figure 3.1. The receiver tracks a varying number of satellites, where the number of satellites is dependent upon the receiver capabilities and visibility of the satellites. For a simple kinematic solution of X_R, Y_R, and Z_R in the Earth Centered Inertial (ECI) True Of Date (TOD) frame, one might assume that the minimum observations necessary would be three, resulting in three equations for three unknowns. The nature of GPS however, induces clock errors that must be taken into account and thus four observations is the necessary minimum, not three.

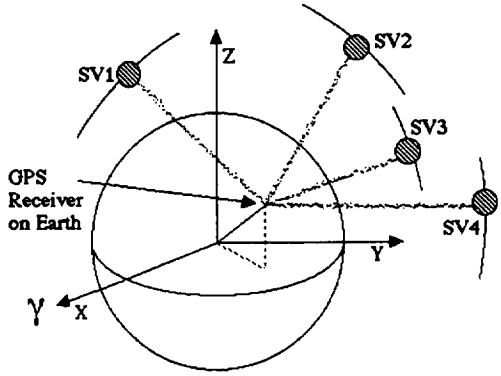

Figure 3.1 GPS Navigation Scenario

3.1.1 Clock Errors

Though most GPS clocks are either Cesium or Rubidium atomic standards, there still exist clock errors for each satellite which is usually modeled as a quadratic polynomial in the form of Eq. (3-1),

$$\delta t_T = T_T - t_T = a + b(T_T - T_0) + c(T_T - T_0)^2 + \eta \qquad (3\text{-}1)$$

where T_T is the true transmit time, t_T is the transmit time according to the GPS satellite clock, T_0 is a reference time, a is a constant offset, $b(T_T - T_0)$ is a drift term, and $c(T_T - T_0)^2$ is a nonlinear term. The constants a, b, and c, along with T_0 are superimposed onto the transmitted signal with other information as a "broadcast ephemeris". In order for Eq. (3-1) to be an equality, η represents other contributions, such as random effects and intentional dithering of the clocks, known as Selective Availability (SA). Because these other contributions are usually hard to model, they are neglected for this discussion.

A GPS receiver also has a clock error which could be modeled similar to the transmitting clock error. However, because the receiver clocks have no centralized entity that provides clock correction terms like the transmitter clocks, a receiver clock error must be estimated along with the position at each observation epoch. This additional parameter constrains the minimum necessary observations to four.

In the situation where the receiver has more than four channels, and GPS satellites lend themselves to visibility, the number of observations can exceed the number of unknowns. The problem becomes an overdetermined system of nonlinear equations and requires a method like least squares to be formulated.

3.1.2 The Formation of Least Squares

An observation/state relationship can be defined such that,

$$y_i = O_i - \rho_i \quad \text{for } i = 1, \ldots, \text{n total observations} \qquad (3\text{-}2)$$

where y_i is defined as a residual, O_i, the observed range, and ρ_i, the computed range. This residual is an indication of how well the estimated state compares with the actual observation since the computed range is dependent on the nominal state. Obviously, the better the estimated state, the closer ρ_i will match the observation, O_i, and the residual will approach zero. This residual can be used in a function that evaluates the performance of an estimation process, otherwise known as a performance index. For the least squares method, the performance index, J, is written as the sum of the squares of the residuals and needs to be minimized: thus, the name *least squares* has been adopted, where

$$J = \sum_{i=1}^{n} y_i^2 \tag{3-3}$$

This performance index is minimized when its derivatives with respect to each state being estimated are zero, namely,

$$\frac{\partial J}{\partial X_R} = \sum_{i=1}^{n} 2(O_i - \rho_i)\left(-\frac{\partial \rho_i}{\partial X_R}\right) = 0 \tag{3-4}$$

$$\frac{\partial J}{\partial Y_R} = \sum_{i=1}^{n} 2(O_i - \rho_i)\left(-\frac{\partial \rho_i}{\partial Y_R}\right) = 0 \tag{3-5}$$

$$\frac{\partial J}{\partial Z_R} = \sum_{i=1}^{n} 2(O_i - \rho_i)\left(-\frac{\partial \rho_i}{\partial Z_R}\right) = 0 \tag{3-6}$$

$$\frac{\partial J}{\partial (\delta t_R)} = \sum_{i=1}^{n} 2(O_i - \rho_i)\left(-\frac{\partial \rho_i}{\partial (\delta t_R)}\right) = 0 \tag{3-7}$$

Hence, since ρ_i is a nonlinear function of the unknown position, these conditions represent four nonlinear algebraic equations with four unknowns. One method of solving this complicated system is to use the Newton-Raphson iteration (NRI) method. The NRI method iterates for the root of a function, which is exactly the case presented here. There are four scalar functions of which their

roots are the desired estimated state, however, the functions are coupled. That is, each equation is dependent on all four unknown parameters.

Labeling Eqs. (3-4) through (3-7) as four separate functions F1, F2, F3 and F4, respectively, the NRI method for a system of equations takes the form [Cheney, 1994],

$$\overline{X}_{k+1} = \overline{X}_k - \left[\frac{\partial \overline{F}}{\partial \overline{X}}\right]^{-1}_{\overline{X}k} \overline{F}\Big|_{\overline{X}_k} \tag{3-8}$$

where

$$\overline{X} = \begin{bmatrix} X_R & Y_R & Z_R & \delta t_R \end{bmatrix}^T \tag{3-9}$$

$$\overline{F} = \begin{bmatrix} F1 & F2 & F3 & F4 \end{bmatrix}^T \tag{3-10}$$

$$\left[\frac{\partial \overline{F}}{\partial \overline{X}}\right] = \begin{bmatrix} \frac{\partial F1}{\partial X_R} & \frac{\partial F1}{\partial Y_R} & \frac{\partial F1}{\partial Z_R} & \frac{\partial F1}{\partial (\delta t_R)} \\ \frac{\partial F2}{\partial X_R} & \frac{\partial F2}{\partial Y_R} & \frac{\partial F2}{\partial Z_R} & \frac{\partial F2}{\partial (\delta t_R)} \\ \frac{\partial F3}{\partial X_R} & \frac{\partial F3}{\partial Y_R} & \frac{\partial F3}{\partial Z_R} & \frac{\partial F3}{\partial (\delta t_R)} \\ \frac{\partial F4}{\partial X_R} & \frac{\partial F4}{\partial Y_R} & \frac{\partial F4}{\partial Z_R} & \frac{\partial F4}{\partial (\delta t_R)} \end{bmatrix} \tag{3-11}$$

Carrying out the derivatives of the matrix (3-11) demonstrates that each term in this matrix is a function of the residual. For example, the diagonal terms have the form of Eq. (3-12) while the off-diagonal terms have the form of Eq. (3-13),

$$\frac{\partial F1}{\partial X_R} = 2\sum_{i=1}^{n}(O_i - \rho_i)\left(\frac{-\partial^2 \rho_i}{\partial {X_R}^2}\right) + \frac{\partial \rho_i}{\partial X_R}\frac{\partial \rho_i}{\partial X_R} \tag{3-12}$$

$$\frac{\partial F1}{\partial Y_R} = 2\sum_{i=1}^{n}(O_i - \rho_i)\left(\frac{-\partial^2 \rho_i}{\partial X_R \partial Y_R}\right) + \frac{\partial \rho_i}{\partial X_R}\frac{\partial \rho_i}{\partial Y_R} \tag{3-13}$$

If one notes that the residual, or $O_i - \rho_i$, is small and can be neglected to a reasonable approximation, then the first term can be ignored and the resulting matrix is symmetric! It follows that

$$\left[\frac{\partial \overline{F}}{\partial \overline{X}}\right] \approx \begin{bmatrix} \sum_i \frac{\partial \rho_i}{\partial X_R}\frac{\partial \rho_i}{\partial X_R} & \sum_i \frac{\partial \rho_i}{\partial X_R}\frac{\partial \rho_i}{\partial Y_R} & \sum_i \frac{\partial \rho_i}{\partial X_R}\frac{\partial \rho_i}{\partial Z_R} & \sum_i \frac{\partial \rho_i}{\partial X_R}\frac{\partial \rho_i}{\partial (\delta t_R)} \\ . & \sum_i \frac{\partial \rho_i}{\partial Y_R}\frac{\partial \rho_i}{\partial Y_R} & \sum_i \frac{\partial \rho_i}{\partial Y_R}\frac{\partial \rho_i}{\partial Z_R} & \sum_i \frac{\partial \rho_i}{\partial Y_R}\frac{\partial \rho_i}{\partial (\delta t_R)} \\ . & . & \sum_i \frac{\partial \rho_i}{\partial Z_R}\frac{\partial \rho_i}{\partial Z_R} & \sum_i \frac{\partial \rho_i}{\partial Z_R}\frac{\partial \rho_i}{\partial (\delta t_R)} \\ . & . & . & \sum_i \frac{\partial \rho_i}{\partial (\delta t_R)}\frac{\partial \rho_i}{\partial (\delta t_R)} \end{bmatrix} \qquad (3\text{-}14)$$

If one defines a matrix H to be a partial derivative matrix of the state observation matrix, and then defines the state observation matrix, y,

$$H = \begin{bmatrix} \frac{\partial y_1}{\partial X_R} & \frac{\partial y_1}{\partial Y_R} & \frac{\partial y_1}{\partial Z_R} & \frac{\partial y_1}{\partial (\delta t_R)} \\ \frac{\partial y_2}{\partial X_R} & \frac{\partial y_2}{\partial Y_R} & \frac{\partial y_2}{\partial Z_R} & \frac{\partial y_2}{\partial (\delta t_R)} \\ \vdots & \vdots & \vdots & \vdots \\ \frac{\partial y_n}{\partial X_R} & \frac{\partial y_n}{\partial Y_R} & \frac{\partial y_n}{\partial Z_R} & \frac{\partial y_n}{\partial (\delta t_R)} \end{bmatrix} \quad \text{and} \quad y = \begin{bmatrix} O_1 - \rho_1 \\ O_2 - \rho_2 \\ \vdots \\ O_n - \rho_n \end{bmatrix} \qquad (3\text{-}15,\ 3\text{-}16)$$

then this notation allows for simplification of the previous NRI equations. H multiplied by the transpose of itself will be equivalent to Eq. (3-14) and H transpose multiplied by the residual matrix will produce $\overline{F}$, or

$$H^T H \approx \left[\frac{\partial \overline{F}}{\partial \overline{X}}\right] \quad \text{and} \quad \overline{F} \approx H^T y$$

Applying this to Eq. (3-8),

$$\overline{X}_{k+1} = \overline{X}_k - \left[H^T H\right]^{-1} H^T y \tag{3-17}$$

By assuming the residuals are nearly zero, it can be seen that the NRI method can be written in a more compact manner and in a form that is consistent with the minimum variance estimation results [Tapley, 1973]. The resulting Eq. (3-17) is actually more commonly referred to as the method of least squares.

Often Eq. (3-17) can be re-written as $\overline{X}_{k+1} = \overline{X}_x - \hat{x}$. This $\hat{x}$ is the correction term to the previous estimate, $\overline{X}_k$. The solution converges as $\hat{x}$ approaches zero if the update on $\overline{X}_k$ is made each iteration. Fortunately, the NRI method has quadratic convergence. The convergence criteria is usually based on changes in $\hat{x}$ between iteration or on the change in the root mean square, or rms, of the residuals,

$$rms = \sqrt{\sum_{i=1}^{n} \frac{y_i^2}{n}} \tag{3-18}$$

This method of least squares is used throughout this research to provide the navigation solution or kinematic solutions for position at a specified time, given at least four GPS pseudorange observations. With the convenient bonus of quadratic convergence, the method is well suited to the GPS navigation problem.

3.2 DOUBLE DIFFERENCE MEASUREMENTS

The GPS receivers used in this analysis measure pseudorange and carrier phase. One technique used to remove some of the errors present in these measurements is the formation of a "double differenced measurement" [Hoffman-Wellenhof, et al., 1992]. If two receivers collect data at nearly the same time from two GPS satellites in common view, a double differenced (DD) measurement can be formed to remove common effects. The major effects

removed in the formation of the DD measurement are SA and clock errors from both the receivers and GPS satellites.

Removal of SA is particularly important, since this intentional degradation will produce errors in the position estimates at the level of 100 m. SA is a technique used by the Department of Defense to degrade the accuracy of GPS to unauthorized users [Sandlin, et al., 1995]. This degradation is caused by dithering each GPS satellite's clock, where the dither parameters are available only to authorized users in a classified environment. This error can be canceled if measurements from the same satellite taken by different receivers are differenced, such as in the formation of a DD measurement.

The DD can be represented as

$$DD_{obs} = \left(\rho^{SV1} - \rho^{SV2}\right)_{R1} - \left(\rho^{SV1} - \rho^{SV2}\right)_{R2} \tag{3-19}$$

where ρ represents the measured pseudorange (or carrier phase), the superscripts $SV1$ and $SV2$ represent two different GPS satellites (space vehicles) and the subscripts $R1$ and $R2$ represent two different receivers. Furthermore, the quantities in Eq. (3-19) parentheses represent single differences (SD) between satellites and thus Eq. (3-19) can be rewritten as

$$DD_{obs} = (SD_{obs})_{R1} - (SD_{obs})_{R2} \tag{3-20}$$

Note that the SD in the above equation will remove common receiver effects, such as receiver clock errors, while the DD cancels transmitter clock errors, including SA.

Two other sources of error arise from atmospheric and multipath effects. The ionosphere is the layer of atmosphere approximately between 100 and 1000 km above the Earth's surface. The ionosphere causes the biggest error next to SA on a range of less than 1 m to over a 100 meters, depending mostly on solar activity and the state of the Earth's magnetic field [Klobuchar, 1991]. The troposphere, spanning from the Earth's surface to about 40 km, is more difficult to

model since this medium varies greatly with water vapor content. When the troposphere is not modeled, positioning errors are on the order of 10 - 20 m, depending on the elevation angle. Both are signal path dependent. For this reason, the errors are a function of GPS elevation. At lower elevations, the signal will travel through more atmosphere, thereby increasing the error.

Multipath occurs when signals reflect off nearby objects into the antenna, thereby supplying false measurements. These measurements incorrectly imply longer signal paths. Positioning errors can approach 10 - 20 m when using pseudorange measurements [Hofmann-Wellenhof, 1992]. For measurements differenced on a short "baseline", or distance between two GPS antenna phase centers, the error can be nearly canceled since the two receivers see a similar elongated signal path.

If the two receivers are connected to a common antenna, the resulting "zero baseline" removes these additional common errors in double differencing. Zero baseline tests are frequently used to assess relative receiver performance or to calibrate the receivers. If the two receivers are adequately synchronized in time and instrumental biases are characterized, then the DD on a zero baseline will exhibit only measurement noise, with zero mean.

If the receivers are attached to separate antennas that are separated by a distance, d, some contributions may not cancel as they do on the zero baseline. For example, the antennas may experience different multipath signals. The multipath effect can still significantly cancel for the DD measurements depending upon the source of the multipath and the location of each antenna with respect to this source. Atmosphere delays will cancel on very short baselines because the satellite viewing direction is nearly the same from both antennas. However as d becomes larger, each antenna collects data that are influenced differently and such delays will not completely cancel.

Although DD measurements are used to remove clock errors, the time tag of the respective pseudoranges introduces an effect that must be taken into account. For example, the effects of SA are not strictly removed by the DD unless the pseudorange measurements have a common transmit time, which is not

the case. Experience shows, however, that the spectral content of SA enables most of the SA-effect to be removed in DD if both receivers record measurements within about 1 ms of each other [Rocken, et al., 1991]. In principle, if the receivers are not synchronized to this level, DD still removes most SA effects. The SA removal is degraded as the time synchronization difference between receivers becomes larger.

Aside from the issues of SA, the time tag problem can be compensated by forming a DD residual though it has been shown that a time synchronization difference up to 100 ms between receivers will only produce SA residuals at the few centimeter level. The DD residual is formed from the difference between the observed DD and the computed DD, or

$$DD\ residual = DD_{obs} - DD_c \tag{3-21}$$

As shown in Eq. (3-19), DD_{obs} is simply the DD of the measurements obtained from the receivers. DD_c is not based on observations, but calculated quantities based on specified antenna coordinates and GPS ephemerides, or

$$DD_c = \left(\rho_c^{SV1} - \rho_c^{SV2}\right)_{R1} - \left(\rho_c^{SV1} - \rho_c^{SV2}\right)_{R2} \tag{3-22}$$

where, for example, ρ_c^{SV1} is,

$$\left[\left(X_R(T_R) - X_{SV1}(T_T)\right)^2 + \left(Y_R(T_R) - Y_{SV1}(T_T)\right)^2 + \left(Z_R(T_R) - Z_{SV1}(T_T)\right)^2\right]^{1/2} \tag{3-23}$$

The receiver and GPS satellite states are in a nonrotating frame evaluated at the time the measurement was received and transmitted, respectively. One must note, for the best results, these times are "true" times in which clock corrections have been included.

The DD measurements and residuals will be used in the receiver calibration tests described in the subsequent chapters.

3.3 ADDITIONAL IONOSPHERIC CORRECTIONS

As discussed earlier, ionospheric effects can be one of the major sources of error in GPS positioning. Using DD measurements can alleviate this problem if the baseline between antennas is small, perhaps several tens of kilometers. If one is working with a lone receiver, the DD technique can not be utilized. However, if this receiver is dual frequency, there is another technique used to essentially eliminate the ionospheric effect using data on *both* frequencies.

The ionospheric error varies with signal frequency: the higher the frequency, the smaller the ionospheric effect. In actuality, this relationship could be written as,

$$\rho_{L1} = \rho_{IF} + \frac{\alpha}{f_{L1}^2} + \ H.O.T.'s \tag{3-24}$$

$$\rho_{L2} = \rho_{IF} + \frac{\alpha}{f_{L2}^2} + \ H.O.T.'s \tag{3-25}$$

where ρ_{L1} and ρ_{L2} are actual pseudo-range measurements, ρ_{IF} is the theoretical ionosphere-free range, f_{L1} and f_{L2} are the GPS frequencies 1575.42 MHz and 1227.60 MHz respectively, and α is a parameter that represents the total electron content of the ionosphere. This situation has provided two equations with two unknowns of which one is the ionosphere-free range.

Upon manipulation of Eqs. (3-24) and (3-25) and ignoring higher order terms (H.O.T.'s), ρ_{IF} becomes,

$$\rho_{IF} = \frac{\rho_{L2} - \gamma\rho_{L1}}{1-\gamma} \qquad \text{where} \quad \gamma = \left(\frac{f_{L1}}{f_{L2}}\right)^2 \tag{3-26}$$

This correction technique will be used with the dual frequency TurboStar data for independent navigation solutions and in conjunction with DD measurements over long baselines where ionospheric effects do not fully cancel.

Chapter 4

Receiver Calibration: Ground Tests

In order to acquire information in a controlled environment that would aid in characterizing the GPS receivers used on the STS-69 experiment, three ground tests were conducted. Two tests were performed, before and after the mission, at the NASA JSC in Houston on the rooftop of Building 18. Although both tests used the same TurboStar receiver carried on the Wake Shield flight, the Collins receiver was not the flight unit. Nevertheless, the general receiver characteristics observed in the ground tests were expected to be representative of the flight unit as well. The third test was performed at UCAR in Boulder, Colorado after the mission. This test compared the TurboStar against a well characterized TurboRogue as a final validation of the TurboStar's performance.

4.1 PRE-FLIGHT RESULTS

The pre-flight ground test was conducted on April 13, 1995, using a short baseline between the respective receiver antennas shown in Figure 4.1. This collocation experiment had a duration of about two hours. The TurboStar receiver was connected to a Micropulse choke ring antenna while the Collins receiver was attached to an L1/L2 patch antenna. The choke ring was supported by a tripod and the patch antenna was placed on a mast attached to a roof guard rail. The antenna phase center separation, or baseline, was about 2.4 m (7 ft 10.5 in) with a height difference of 0.4 m (1 ft 4 in). The roof contained structures that could contribute

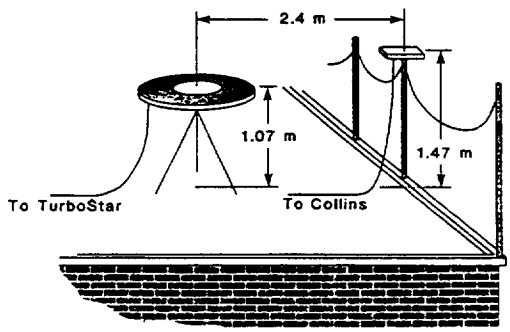

Figure 4.1 Pre-Flight Test Set Up

to multipath, but these effects will partially cancel because of the short distance between the two antennas, or baseline. The baseline vector was oriented in approximately the North/South direction.

Double difference (DD) residuals were computed according to the procedure described in the previous chapter, where R1 and R2 represent the TurboStar and Collins receivers. The computed DD was based on the GPS broadcast ephemerides and, for simplicity, an assumed zero baseline. In other words, the 2.4 m antenna separation was ignored for the computation of the DD, thereby introducing an error equal to the baseline length. A sample calculation can be found in Appendix 4. It should also be noted that the TurboStar data were recorded at an interval of 5 sec and the measurement time tags differed from GPS time by less than one microsecond. The Collins receiver recorded data at an interval of 1 sec, but the data sampling times were offset from the TurboStar by 0.262 seconds.

Figure 4.2 illustrates the pseudorange DD residuals obtained from two combinations of GPS satellites. As discussed in Chapter 3, the cancellation of common effects over a 2.4 m baseline should result in residuals that exhibit primarily measurement noise with zero mean. The measurement noise is immediately apparent in Figure 4.2 as the point scatter. TurboRogue receivers usually display pseudorange precision around 0.5 m, even with AS on, which is significantly smaller than the noted scatter. Therefore, DD noise is most likely to be dominated by the Collins, as verified by later tests.

It is quite evident that the residuals do not have a zero mean. As observed in Figure 4.2, the mean values vary between PRN combinations, although there appear to be some similarities. An example of the statistics for various combinations of GPS satellites is given in Table 4.1. Since the DD sign is determined by the order in which the differences are formed, it can be ignored for the moment. Obvious similarities between bias (or mean) values exist with 80 m (PRN 19:2, 31:15, 18:27), 30 m (PRN 18:19 and 15:27) and 63 m (PRN 2:15 and 18:15). The standard deviation in Table 4.1 is a good measure of the pseudorange precision, except in cases where the residuals have a linear slope.

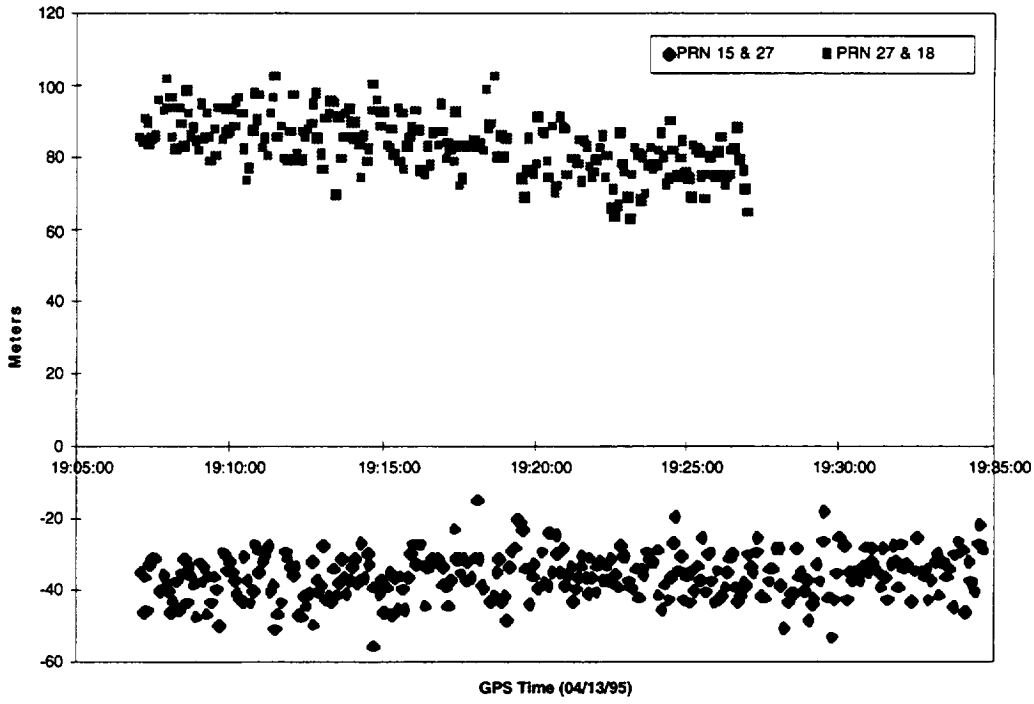

Figure 4.2 Pre-Flight DD L1/L2 Pseudorange Residuals

Table 4.1 Pre-Flight DD Residual Statistics

PRNs		Mean DD Residuals (m)	Standard Deviation	Number of Data Points
18	2	-108.76	7.81	56
19	2	-76.41	8.06	96
18	19	-29.85	9.56	93
2	15	62.11	9.50	28
31	15	-78.02	10.72	570
2	31	136.81	9.54	252
27	18	83.65	7.96	239
15	27	-35.70	6.40	422
18	15	-64.75	6.62	95

There are two possible explanations for the observed biases in the DD residuals. The first most obvious issue is the assumed zero baseline for the computed DD. The error introduced by this assumption is at most 2.4 m, so it can be eliminated as a significant contributor to the biases. The second explanation could be the existence of biases between tracking channels within the receiver.

Because tracking channels are not identical in construction, they must be calibrated within a given receiver during each power-up. For example, the Collins has its own calibration capability used for its navigation solution calculations. By initially tracking the same satellite on all channels, the Collins can determine channel biases to ensure all channel measurements match. After the calibration is complete, the tracking channels begin searching for other satellites. However, it is suspected that these calibration values are not included in the reported raw data such as pseudoranges. Therefore, these differences amongst channels will appear in the DD measurements since they have not been removed after calibration (R. Nuss, JSC, personal communications, 1996).

When comparing DD residuals common to a particular combination of tracking channels, the biases remained although different magnitudes were observed as shown in Figure 4.3. It might be concluded that the biases are not channel oriented; however, it is believed the channels referred to in Figure 4.3 are software assigned channels. In other words, the receiver software reads the data from a physical "hardware" channel and assigns the value to an arbitrary "software channel". Therefore, the output of raw data does not depict the actual hardware channels used to track the satellites.

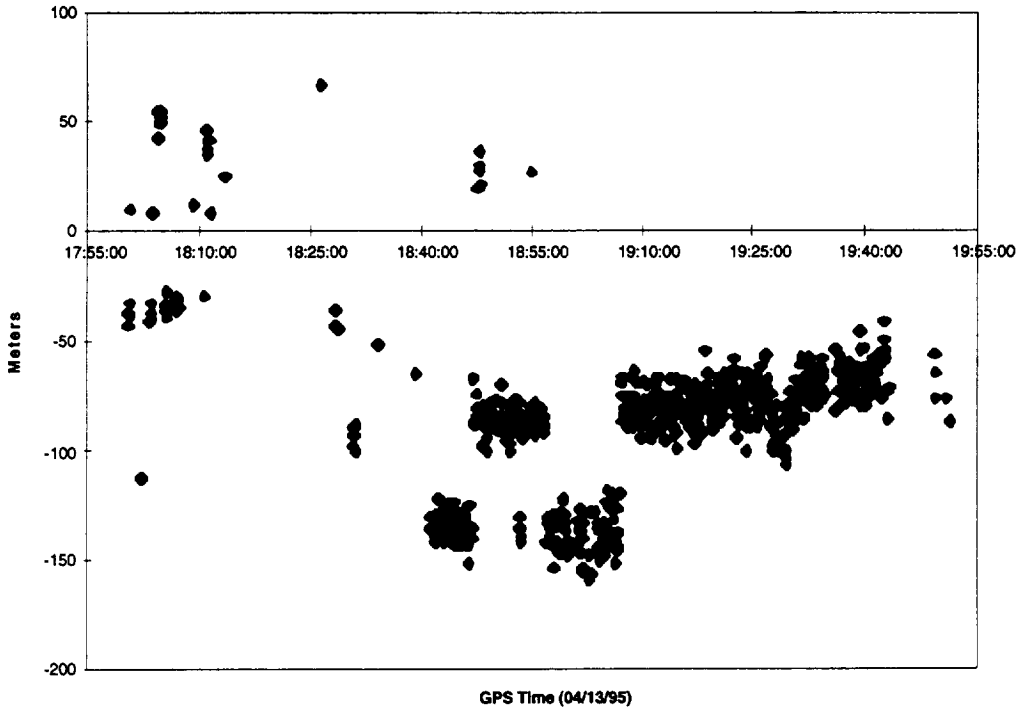

Figure 4.3 DD Residuals Between Software Channels 1 and 3

At this point, a hardware channel bias was regarded as the most likely explanation of the DD biases. If this explanation is correct, then the difference of two DD formed between three satellites, i.e. $DD^{1/3}$ and $DD^{2/3}$, would produce a third DD of the uncommon satellites, i.e. $DD^{1/3}$. In other words, applying Eq. (3-19),

$$DD^{1/3} - DD^{2/3} = \left[\left(\rho^{PRN1} - \rho^{PRN3}\right)_{R1} - \left(\rho^{PRN1} - \rho^{PRN3}\right)_{R2}\right] - \left[\left(\rho^{PRN2} - \rho^{PRN3}\right)_{R1} + \left(\rho^{PRN2} - \rho^{PRN3}\right)_{R2}\right] \quad (4\text{-}1)$$

$$= \left[\left(\rho^{PRN1} - \rho^{PRN3}\right)_{R1} + \left(\rho^{PRN1} - \rho^{PRN3}\right)_{R2}\right] \quad (4\text{-}2)$$

$$= DD^{1/2} \quad (4\text{-}3)$$

Note, Eq. (4-1) through (4-3) will be correct only if the DDs were formed with the hardware channels remaining locked on their respective satellites at the same

time. Table 4.1 demonstrates the feasibility of such an idea. For example, the mean DD residual between PRN 18 and 2 differenced with the mean DD residual between PRN 19 and 2, essentially give the mean DD residual between PRN 18 and 19.

There are situations when the differencing of two DD of three satellites do not produce the third. For example, the mean DD residual between PRN 18 and 27 differenced with the mean DD residual between PRN 15 and 27 do not give the mean DD residual between PRN 18 and 15. However, these DD were formed during completely different times as shown in Figure 4.4. This suggests that a hardware channel lost lock with one of the three satellites, and at a later time a different hardware channel picked up that lost satellite. For example, since the magnitude of DD PRN 15 and 27 appears rather consistent, PRN 18 might have been lost by one hardware channel and picked up by another.

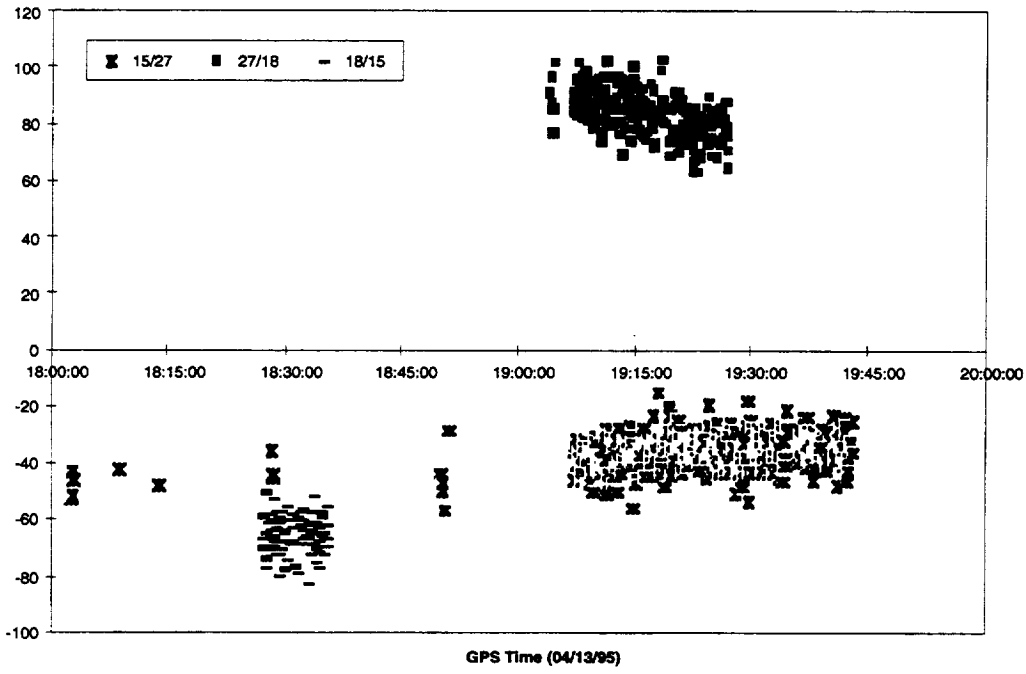

Figure 4.4 DD Residuals Between Three Common PRNs (m)

In principle, the biases could be produced by either or both receivers. However, based on the heritage of the TurboStar, it is unlikely that it is producing significant channel biases. Numerous tests have been performed using TurboRogues from the large pool of receivers in global use and biases at the level observed in the WSF-02 tests have not been reported. A test between a TurboRogue 8100 and a Trimble SSE operated from a common antenna (a "zero baseline") by the Center for Space Research at Galveston produced no significant DD bias (B. Schutz, UT Austin, personal communication, 1995). Nevertheless, a zero baseline between the WSF-02 TurboStar and a receiver in common use for ground applications was conducted and will be presented in the next section. If the biases are shown to exist in the Collins, it should be pointed out that, even with the observed biases, the receiver exceeds the Shuttle operations requirement. The biases will influence a navigation solution obtained from a four satellite minimum, but the observed bias magnitudes will still allow 100-150 meter positioning in the presence of SA.

One final observation can be made after analyzing the DD residuals. In addition to the noise scatter and biases, the residuals exhibit a small slope as well. Figure 4.2 also illustrates that the slopes for a given PRN combination are different. For example, the DD residuals formed between 27 and 18 have a slope whereas the DD residuals formed between 15 and 27 have a significantly smaller slope, perhaps even a zero slope.

The linear variation with time observed in some DD residuals is reminiscent of effects introduced by time tag errors, but other possibilities do exist such as doppler-dependent effects in the tracking loops. No evidence exists to suggest that such effects are caused by the TurboStar since the receiver design and time tagging has been thoroughly characterized. Additional Collins hardware information is required to enable assessment of these possibilities and this aspect will continue to be investigated. This time-dependent effect appears to be a function of the satellite combination used in DD or the tracking channels involved in the DD.

4.2 POST-FLIGHT RESULTS

Two post-flight ground tests were conducted in addition to the pre-flight experiment. One, being very similar to the pre-flight test, was performed on Building 18 of JSC, on October 13, 1995. The second was performed at UCAR in Boulder, Colorado on March 13, 1996.

4.2.1 Collins/TurboStar Calibration

Another ground test was performed at JSC after completion of the STS-69 flight using the same receivers used in the pre-flight tests. In this post-flight test, both receivers were attached to the same L1/L2 patch antenna for about 2.5 hours. With a common antenna (or zero baseline), all multipath and atmosphere effects will be removed in the formation of double differenced measurements. One additional difference between the pre-flight and post-flight tests was the absence of anti-spoofing (AS) in the GPS transmissions during the October test.

Similar results were obtained in the post-flight test compared to the pre-flight test, with the exception that the P-code tracking enabled by the absence of AS resulted in significantly smaller scatter in the residuals as shown in Figure 4.5. Experience with TurboRogue receivers shows a much smaller effect in measurement precision in AS and non-AS periods, so it is believed that the significant change in DD noise resulted from the Collins receiver. These residuals also show the existence of biases, which is further demonstrated by the statistics given in Table 4.2. In addition, the existence of small linear variations in the residuals are evident, as in the pre-flight test.

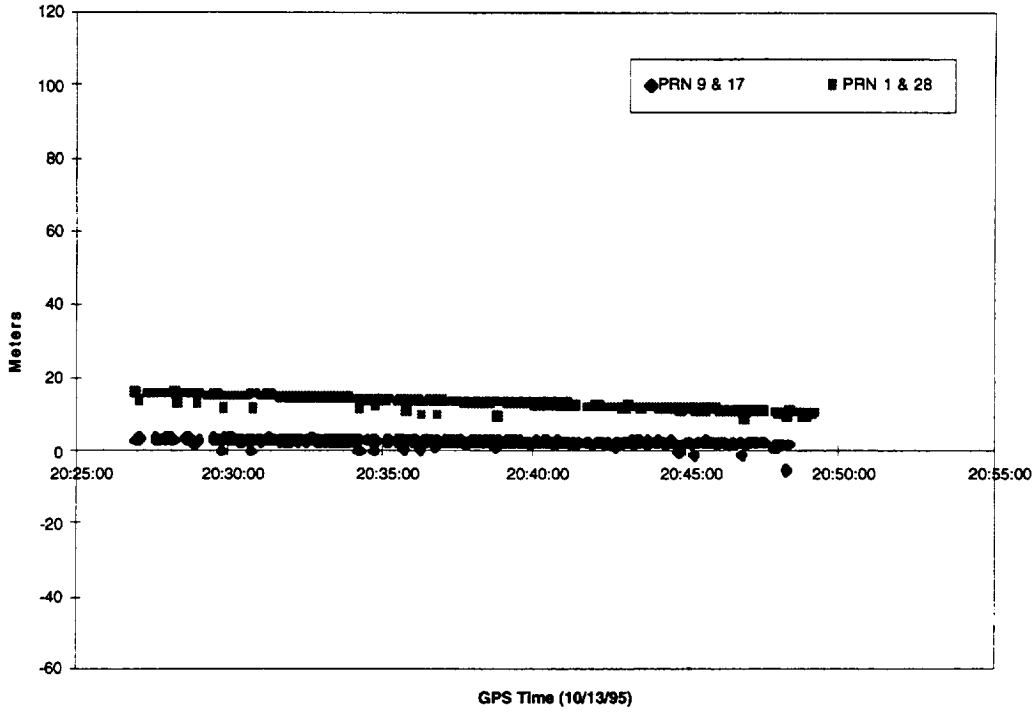

Figure 4.5 Post-Flight DD Residuals

Table 4.2 Post-Flight DD Residual Statistics

PRNs		Mean DD Residuals (m)	Standard Deviation	Number of Data Points
12	23	-38.74	0.42	206
1	23	52.91	1.94	139
12	1	-90.93	1.22	15
9	17	2.53	0.89	219
31	17	86.66	1.78	136
9	31	-81.34	1.01	293
1	28	12.79	2.15	250

4.2.2 Additional TurboStar Calibration

Knowing the TurboStar was a flight *version* of the TurboRogue model, one could not be one hundred percent certain the observed biases did not originate from the TurboStar. An additional ground test was conducted to evaluate this possibility. In this experiment, a zero baseline test was performed between the TurboStar and an "off-the-shelf" TurboRogue. The standard TurboRogue was number DS03 of the UNAVCO pool of receivers, with serial number 207.

Figure 4.6 is a sample of the DD L1 pseudorange residuals formed for an hour between channels one and two of the two receivers. During this test, AS was "on". For this sample, the mean was about 0.018 m and the standard deviation was about 0.23 m. All DD residuals formed had the same characteristics as demonstrated in Figure 4.6. This test was confirmation that the TurboStar did not cause the significant biases seen in the previous calibration tests.

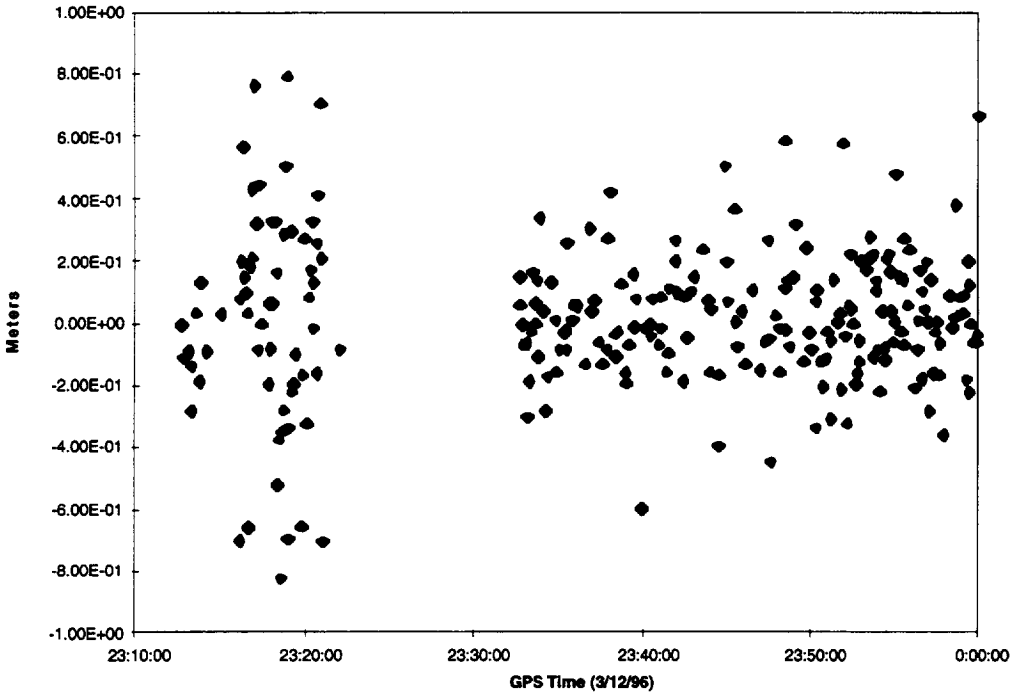

Figure 4.6 DD L1 Pseudorange Residuals

4.3 SUMMARY

The results obtained in the pre-flight and the post-flight tests are consistent, except for the influence of AS on the Collins measurement precision. The TurboStar/Collins calibration tests exhibit biases in pseudorange double differences and characteristics that may be the result of small errors in time tags. Based on the wide use and understanding of the TurboRogue design, these DD characteristics are believed to be associated with the Collins receiver. The TurboStar/TurboRogue calibration test confirmed this belief. The existence of biases in the Collins, however, can be mitigated by estimating bias parameters when DD measurements based on pseudorange are used. Other factors like the residual slopes cannot be completely accommodated in bias estimation alone. The slope source requires further investigation, though extensive evidence suggests that the biases are caused by channel biases in the Collins. Various tests have indicated that the pseudorange precision of the TurboStar is about 0.5 m or better in the presence of AS and slightly better when AS is off. The DD tests show that the Collins pseudorange precision is about 6 m in the presence of AS and about 1 m when AS is "off".

Chapter 5

Receiver Calibration: In-Flight Test

As has been shown, the ground tests provided a well controlled environment for receiver calibration and equipment surveillance. It is assumed that the ground test results would apply to the in-flight experiment but one could not be certain. For this reason, it was felt that an in-flight calibration test would increase confidence in the data received during the free flight portion of the experiment.

In order to be comparable to the ground tests, the in-flight calibration had to be similar in design. Basically, this required the Collins and TurboStar to be connected to antennas that were stationary with respect to each other and with an appropriate viewing time of a common celestial space. This scenario occurred during one of the phases of the WSF-02's deploy sequence and will be discussed in the following sections.

In addition to calibrating the receivers in a manner similar to the ground tests, powering the WSF-02 GPS receiver before release provided a grace period in which the receiver locked on to GPS satellites while mission experimenters checked receiver operations.

5.1 PRE-RELEASE OPERATIONS

Prior to the WSF-02 unberth activities on September 11 (Day 254), 1995, Endeavour was placed into a gravity gradient (GG) attitude orientation, as illustrated in Figure 2.9, with the Shuttle main thrusters on the Earth side. This GG attitude was maintained throughout the WSF-02 pre-release period and extending into the WSF-02 free-flight period. The GG mode enabled Endeavour to maintain a stable attitude without using the Shuttle attitude thrusters, thereby avoiding a source of WSF-02 contamination.

The Endeavour Remote Manipulator System (RMS or arm) was used to unberth the WSF-02 in preparation for release to free-flight. The RMS maneuvered the WSF-02 into four staging positions after grapple: hover, ram cleaning, attitude determination and control system (ADACS) checkout and, finally, release. The timeline for these positions is summarized in Table 5.1. Hover occurred immediately after removing the WSF-02 from the cross bay carrier in the payload bay as illustrated by the in-flight photo in Figure 5.1. The ram cleaning position consisted of maneuvering the WSF-02 wake side into the direction of flight so that the "wind" of atomic oxygen could clean away remaining impurities. In this orientation shown in Figure 5.2, the WSF-02 was held over the Shuttle port wing for about two hours with the GPS antenna on the Earth side, an undesirable orientation for GPS tracking.

Table 5.1 Periods Of Arm Movement

UTC: Day 254	WSF-02 Activity
05:44 - 05:52	Latch release to Hover
06:08 - 06:17	Hover to Ram Cleaning
08:35 - 08:46	Ram Cleaning to ADACS C/O
09:05 - 09:47	ADACS C/O Maneuvers
11:15 - 11:26	ADACS C/O through Release

The WSF-02 GPS receiver was activated during the ADACS checkout period, which was designed to evaluate the WSF-02 attitude system prior to release. The WSF-02 was held over the Shuttle starboard wing in an attitude similar to the free-flight configuration for over an hour and a half. The Endeavour/WSF-02 orientation during the ADACS period is illustrated in Figure 5.3. Following the ADACS C/O period, the WSF-02 was deployed to free-flight as shown in Figure 5.4.

After activation of the TurboStar receiver at 254:08:50 UTC, by 09:04 the receiver had locked on four GPS satellites. At 9:14, the receiver had locked on eight satellites. Because of the WSF-02 antenna orientation, the number of

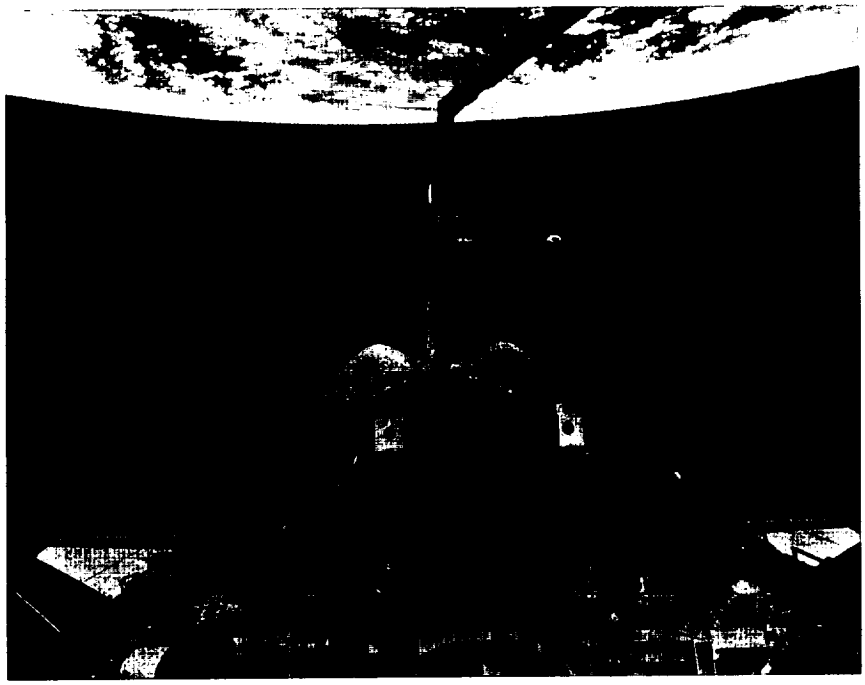

Figure 5.1 WSF-02 in Hover Position (NASA Photo)

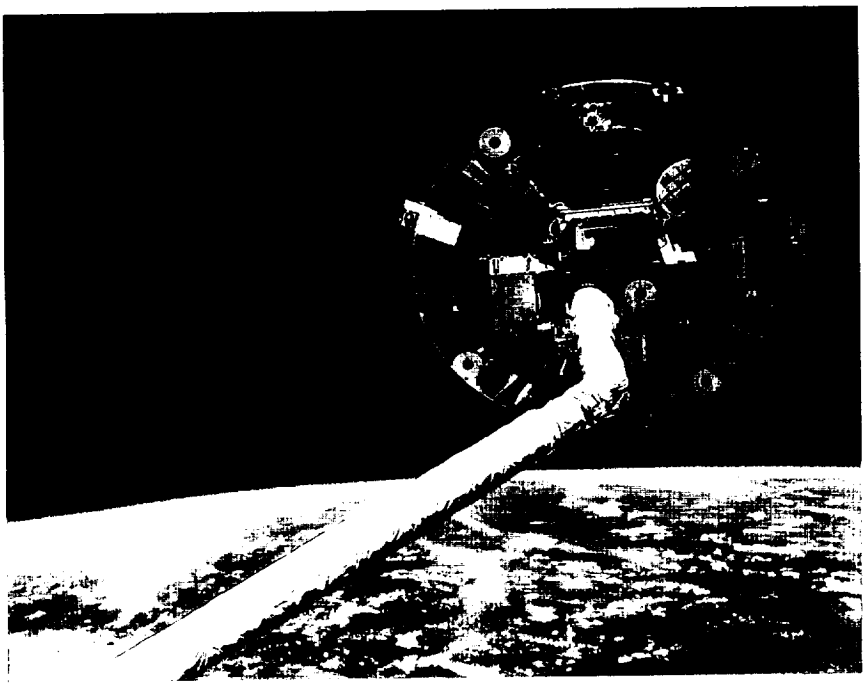

Figure 5.2 WSF-02 in Ram Cleaning Orientation (NASA Photo)

tracked GPS satellites varied between four and eight, with occasional periods in which fewer than four satellites were tracked.

The WSF-02 attitude and number of satellites tracked by the TurboStar are shown in Figure 5.5. Although this attitude record was obtained from the WSF-02 ADACS, the variations also represent the variations exhibited by the Endeavour attitude since the two vehicles were attached. The observed attitude variations in Figure 5.5 are attributed to librations of the Shuttle about the GG orientation. Also note there is a bias of 12° in pitch and a few degrees in roll. The bias in roll is normal since mission experimenters considered a "near-flight" WSF-02 attitude as within plus or minus six degrees of zero roll, zero yaw, and zero pitch. The pitch bias was the result of the WSF-02 not being returned to nominal flight attitude after the arm finished maneuvering the WSF-02 during ADACS C/O.

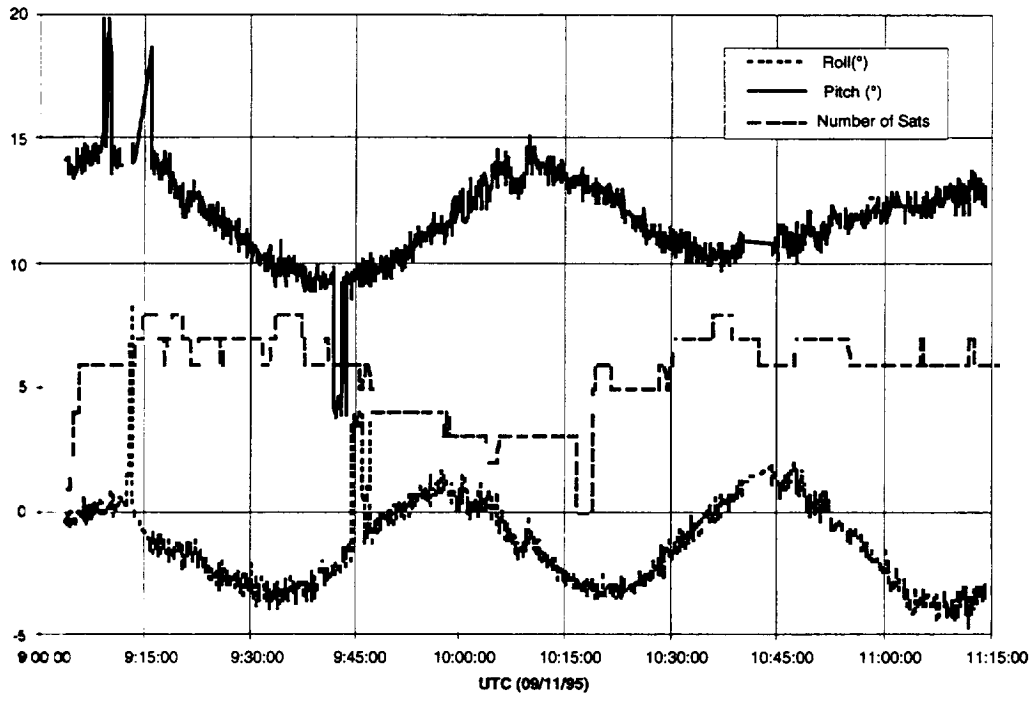

Figure 5.5 WSF-02 Attitude and GPS Tracking History

For reference, the WSF-02's attitude is in a local vertical, local horizontal (LVLH) system which can be depicted in Figure 5.6. The roll of the WSF-02 is a rotation of the disk about a vector orthogonal to the disk platform with positive being in the velocity direction. Pitch is a rotation about the WSF-02's orbital angular momentum vector positive to the "north". Yaw, not shown in Figure 5.5, is a rotation about the WSF-02's zenith vector, positive being in the zenith direction (T. McCusker. SII. personal communications, 1995).

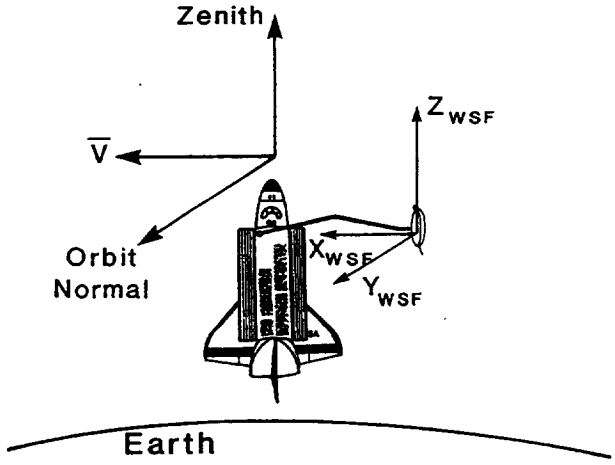

Figure 5.6 WSF-02 LVLH Attitude

5.2 IN-FLIGHT DD MEASUREMENT CONSIDERATIONS

The method of DD residuals, similar to those calculated for the ground tests, is one approach for in-flight calibration. Necessary criteria for in-flight DD computations for this study included no arm movement and at least two common satellites observed by both the WSF-02 and Shuttle receivers. Correlating Figure 5.5 and Table 5.1, there is clearly one time interval where there are several observations with the TurboStar during a "no arm movement" period: 254:10:18 UTC to 254:11:14 UTC. This one hour arc was chosen as the interval for the in-flight calibration.

Several factors complicate the computation of in-flight DD measurements for this mission. First, with the Shuttle receiver using two different antennas

viewing a significantly different celestial space than the WSF-02, the existence of common satellites was uncertain. The odds of discovering common satellites between the receivers decreased knowing the Collins is only a five channel receiver rather than eight like the TurboStar.

In addition, variations in the Shuttle/WSF-02 attitude as shown in Figure 5.5 introduce another complication. If the oscillations are not correctly modeled, the DD measurements will contain errors representative of the displaced distance of the receiver from the nominal GG orientation.

Finally, during the pre- and post-flight calibration tests conducted at JSC, the DD residuals were computed using a set of antenna coordinates that were constant in an Earth-fixed coordinate system. The computed DD was obtained from these antenna coordinates and the GPS satellite coordinates generated from the broadcast ephemerides in the same coordinate system. The in-flight calibration, however, is more complicated because the orbital motion of the Endeavour/WSF-02 vehicle produces a time-varying position of the antenna in an Earth-fixed system.

The following few sections will discuss these issues in more detail. How they specifically apply to the WSF-02/GPS mission and techniques used to overcome these complications will be presented. A sample calculation is provided in Appendix 4.

5.2.1 Common Satellites Among Receivers

There are two factors that affect the determination of common satellites between the two receivers in this mission. One deals with respective antenna orientation and the other with receiver tracking capability.

First, with the two Shuttle antennas being 180° apart, the antennas together provide a full view of the celestial sphere even though each "antenna axis" is in the local horizon plane. (The antenna axis is the axis orthogonal to the ground plane intersecting the phase center of the antenna). Even though the WSF-02 antenna axis was 26° above the local horizontal, the orientation of the WSF-02 with respect to the Shuttle resulted in the antenna axis orientation approximately

perpendicular to the Shuttle antenna axes. In other words, the common view of the celestial sphere between the WSF-02 and a single Shuttle antenna could be roughly estimated as 90° as demonstrated in Figure 2.9. Second, the Collins receiver had five tracking channels, compared to eight channels in the TurboStar. This constrained the maximum number of common satellites to five.

With these issues in mind, both data sets from the TurboStar and Collins receivers were compared. Figure 5.7 shows the number of common satellites as a function of time during the in-flight calibration epoch. Fortunately, there were at least two common satellites for a majority of the time shown.

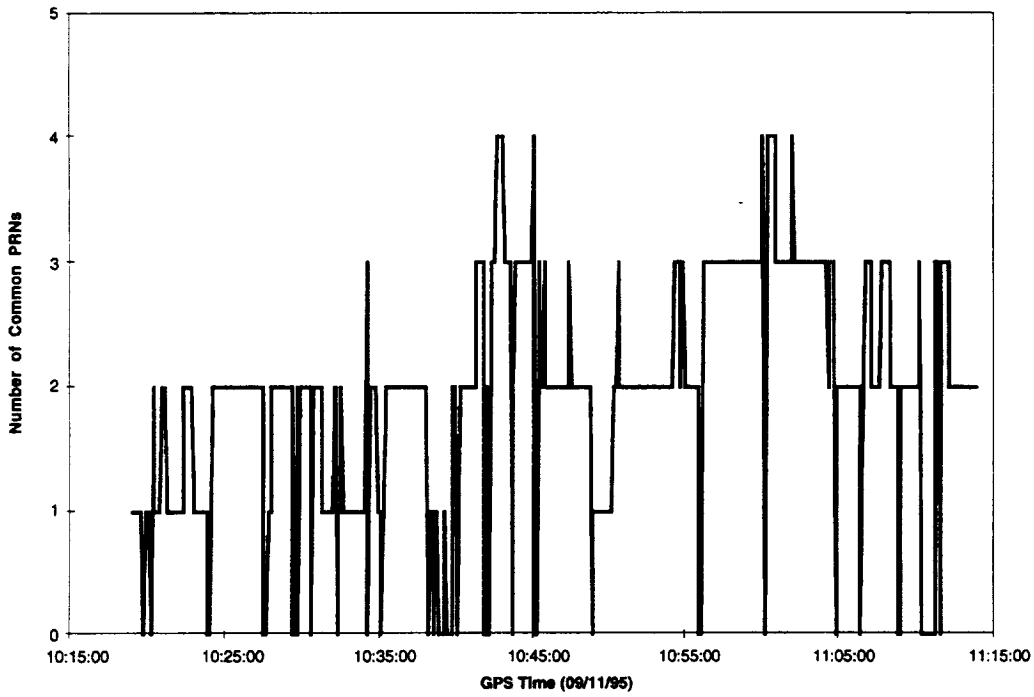

Figure 5.7 Number of Common PRNs Between the Collins and TurboStar

It should be noted that not all the observations with four common satellites were unique. For example, there are about fifteen observations with four satellites in common view but not all were truly unique satellite pairs. This is a result of the "roving" fifth channel in the Collins. An example of a repeat satellite is

shown in the data of the Collins and TurboStar in Tables 5.2 and 5.3. The Collins is tracking PRN 12 on two separate channels thereby giving the false impression of four satellite combinations between both receivers (PRNs 12, 15, 2, and 12).

Table 5.2 Collins Data

Receive Time: 95 9 11 11 0 54.9508563

PRN	(P1)	(P2)	(C1)	(L1)	(L2)
19	-4077183.380	0.000	0.000	720.427	0.000
12	-5032639.996	0.000	0.000	1494.610	0.000
15	-4219820.498	0.000	0.000	-4743.849	0.000
2	-6989795.783	0.000	0.000	-1050.212	0.000
12	-5032641.456	0.000	0.000	1494.634	0.000

Table 5.3 TurboStar Data

Receive Time: 95 09 11 11 00 55.0000000

PRN	(L1)	(L2)	(P1)	(P2)	(C1)
15	-24098675.50	-18778185.24	0.00	23018437.92	23018437.57
12	-28622690.97	-22303383.28	22205911.88	22205912.82	0.00
7	-28826558.24	-22462246.67	0.00	21211199.68	21211199.40
9	4619199.32	3599384.09	0.00	26642575.97	26642577.06
26	-414443.31	-322938.66	0.00	26680360.78	26680360.42
2	-40475645.46	-31539460.08	0.00	20248635.72	20248635.63

Because the DD_C requires the position vector of each antenna tracking the common satellite, it is necessary to know which antenna on the Shuttle is being used. This question was solved by taking the dot product of the common satellite's ECI (TOD) position vector with the Shuttle's orbital angular momentum vector. If the dot product was less than 90°, the GPS satellite was above the orbital plane. If the dot product was greater than 90°, the GPS satellite was below the orbital plane. Because of the Shuttle GG attitude as shown in Figure 2.9, the upper-hemi views above the orbital plane while the lower-hemi in the belly of the Shuttle views below the orbital plane. It can then be concluded, that when the dot product is less than 90°, the upper-hemi is being used to track the common satellite. If the dot product is greater than 90°, the lower-hemi is tracking.

Figure 5.8 shows the GPS satellites tracked by the Collins with the satellites common to the TurboStar hi-lighted. This figure not only reassured sufficient compatibility between the two data sets but further demonstrated that only the upper-hemi antenna shared common satellites during this experiment.

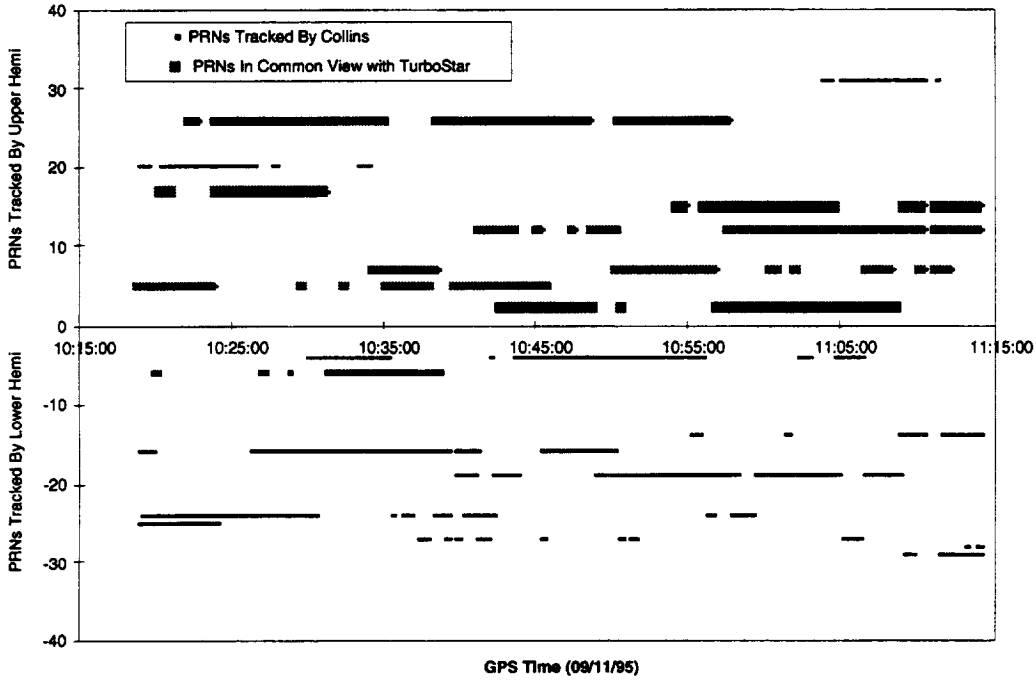

Figure 5.8 PRNs Tracked By the Shuttle Upper and Lower-hemi

5.2.2 WSF-02 Position Ephemeris

Since the position of WSF-02 is time-dependent in an Earth fixed system, the computed DD requires a nominal ephemeris for the position of the WSF-02's GPS antenna as discussed in Section 3.2. For this aspect of the calibration tests, a reference ephemeris was constructed from the "navigation solutions" generated with the method described in Section 3.1 using the TurboStar's in-flight measurements. This navigation ephemeris consists of the antenna positions (x, y,

z) in the WGS-84 reference frame and a corresponding receiver clock correction term that can be computed from a minimum of four pseudoranges. Because the solution is influenced by SA and viewing geometry, the navigation solutions were smoothed with the University of Texas Orbit Processor (UTOPIA). The expected level of position error from SA is about 100 m.

By treating the (x, y, z) navigation solutions as a set of "observations", the TurboStar navigation ephemeris was fit with UTOPIA to determine an orbit that fit the observations in a least squares sense. The nature of the problem is well-suited to a batch estimation procedure. The UTOPIA force modeling included geopotential perturbations computed to degree and order 70 from the JGM-3 gravity field [Tapley, et al., 1996], atmospheric drag from the Density and Temperature Model (DTM) [Barlier, et al., 1978] with a drag coefficient of 2.2, and solar radiation pressure with a reflectivity coefficient of 0.3. The combined vehicle mass and area used in UTOPIA were 108294.5 kg and 266 m^2 (see Appendix 8), respectively, which are consistent with the Shuttle characteristics during the GG period (B. Tracy, JSC, personal communications, 1995). It should be noted that UTOPIA assumes the observations refer to the center of mass (CM) of the spacecraft. This assumption, that the WSF-02 antenna was at the CM of the vehicle, induced a small error but for initial analysis was deemed negligible.

The fit of the navigation positions produced a root mean square (rms) value of 62.6 m, consistent with the expected level of SA. For this fit, the TurboStar data from 254:10:18 UTC to 254:11:14 UTC were used. The navigation solution differences with the UTOPIA-fitted orbit can be resolved into radial (R), along-track (T) and cross-track (N) components and are plotted in Figure(s) 5.9. The rms values of these components were: R 36.7 m, T 21.2 m, and N 48.1 m. This UTOPIA ephemeris was outputted in the Earth Centered Inertial (ECI) J2000 coordinate frame and eventually used for the computed ranges of the WSF-02 antenna.

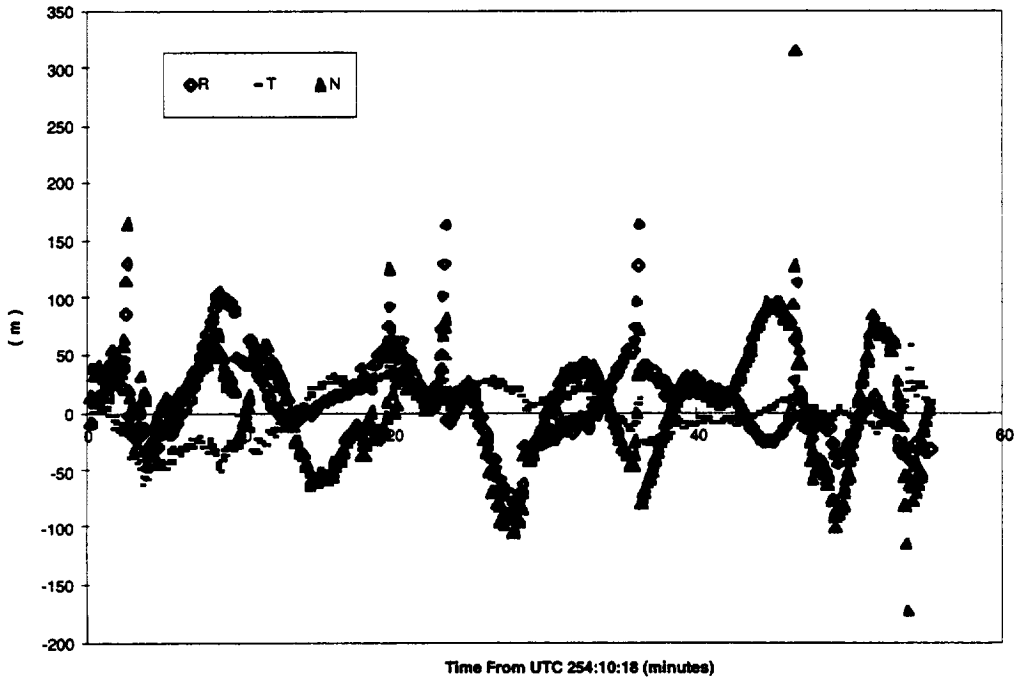

Figure 5.9 Radial, Transverse and Normal Residuals (WSF-02 Reference Ephemeris - Navigation Ephemeris)

5.2.3 Endeavour's Upper-hemi Position Ephemeris

In addition to the ephemeris for the WSF-02 antenna, an ephemeris for Endeavor's upper-hemi antenna was needed for the computation of DD residuals. This was accomplished through knowledge of the Remote Manipulator System (RMS). Using the Shuttle flight records, the RMS orientation was determined. With this RMS information, the position vector of the WSF-02 with respect to an Endeavour reference point was established in a Shuttle-fixed coordinate system. The distance between the upper-hemi antenna on Endeavour and the WSF-02 antenna was about 13 m. This relative position vector from the RMS data was added to the WSF-02 navigation solution to generate a separate (x, y, z) ephemeris for the upper-hemi. Because the two antennas were stationary with respect to each other, the relative position vector between antennas had constant components in a spacecraft-fixed coordinate system.

The Remote Manipulator System

The RMS is a mechanical "arm" on the port side of the Shuttle payload bay. One of the main functions of interest to this experiment is unberthing satellites from the payload bay and maneuvering them into a position to be deployed.

Monitoring and maneuvering the RMS requires flight controllers to track the position, attitude, rotational rates, and translational rates of the POR, or point of resolution. The POR is an arbitrarily selected reference point, be it on the arm itself or on the payload that the arm grapples. When the arm is unloaded, the POR is designated at the tip of the 15.32 m (50 ft 3 in) arm where the end effector is located. When the arm is loaded, the POR is designated as a point on the grappled payload usually defined by payload operators, or personnel responsible for the payload. For the WSF-02 experiment, the POR was defined at the center of the WSF-02. This chosen location corresponded to the origin of the WSF-02 PLOP coordinate system, to be defined in the following section.

Figure 5.10 shows the end effector and the six arm joints that contribute to the calculation of the POR's state. JSC flight controllers provided all RMS joint angles and POR position and attitude data during WSF-02/arm operations (A. Ramos, JSC, personal communication, 1995). The POR position and attitude information proved most useful.

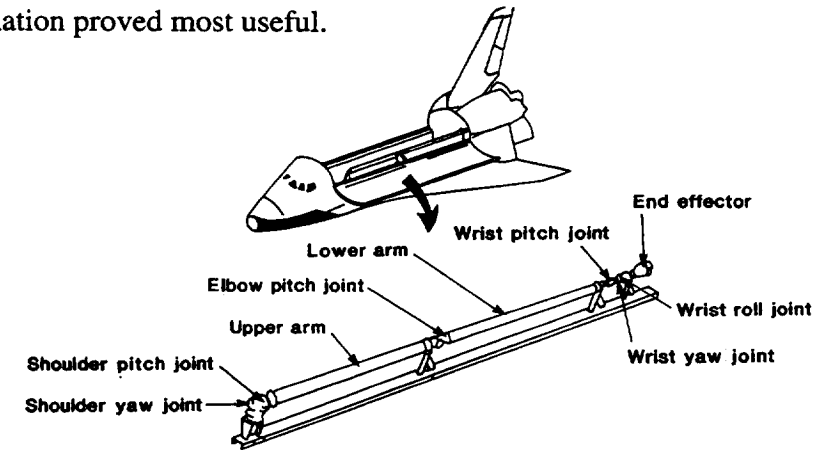

Figure 5.10 The Remote Manipulator System (RMS)

The accuracy of this information is difficult to specify for a given mission. In general, with the orbiter reaction control system (RCS) thrusters off, the RMS can deploy a 29500 kg (65000 lb.) payload within five degrees relative to the RMS shoulder joint and a payload angular rate, with respect to the orbiter, less than 0.015 dg/sec. If the arm is unloaded, the accuracy is ± 5 cm (2 in.) and ± 1 degree [Payload, 1988]. Since the Shuttle was required to maintain a non-contaminated space before and during WSF-02 deploy, no thrusting was performed. Also, the WSF-02's mass was only 2000 kg (4300 lb.). With these factors it can be assumed that the accuracy of the information was better than the conditions stated above. Also, since the POR data is calculated based on the joint angles, flexure due to the weight of a payload or thermal deformations is not considered.

The next section will describe how the arm data was used to calculate the position vector between the WSF-02 antenna and the Shuttle upper-hemi in a Shuttle body-fixed coordinate frame. This position vector will be referred to as the "relative GPS antenna position vector".

The Relative GPS Antenna Position Vector

In order to use the RMS information most effectively and efficiently, a clear understanding of the coordinate systems is required. Figure 5.11 shows three orbiter-fixed coordinate systems: Orbiter Body Axis System (OBAS), Orbiter Rotation Axis System (ORAS), and Orbiter Structural Reference System (OSRS). Note that all origins are outside the Shuttle structure, in front of and below the Shuttle nose. Fortunately, the payload has only one coordinate system of importance to this section: Payload Operating System (PLOP). Figure 5.12 shows the orientation of PLOP on the WSF-02.

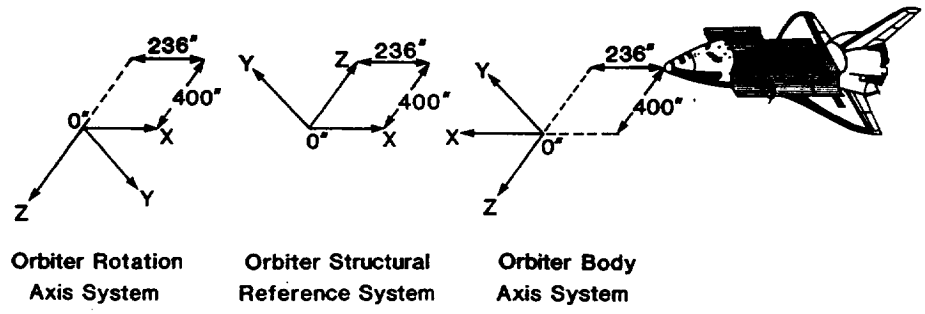

Figure 5.11 Shuttle Body-Fixed Coordinate Systems

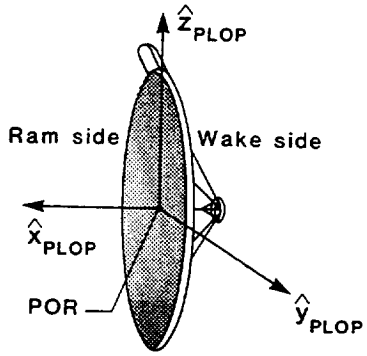

Figure 5.12 The Payload Operating System (PLOP) Coordinate System

As stated previously, the POR is the origin of the PLOP coordinate system in the WSF-02 as shown in Figure 5.12. The arm data provided by JSC is POR position in OBAS coordinates and WSF-02 attitude in the form of a transformation from ORAS to PLOP, that is:

$$T_{ORAS}^{PLOP} = [Roll][Yaw][Pitch] \tag{5-1}$$

$$= \begin{bmatrix} 1 & 0 & 0 \\ 0 & c_{roll} & s_{roll} \\ 0 & -s_{roll} & c_{roll} \end{bmatrix} \begin{bmatrix} c_{yaw} & s_{yaw} & 0 \\ -s_{yaw} & c_{yaw} & 0 \\ 0 & 0 & 1 \end{bmatrix} \begin{bmatrix} c_{pitch} & 0 & -s_{pitch} \\ 0 & 1 & 0 \\ s_{pitch} & 0 & c_{pitch} \end{bmatrix} \tag{5-2}$$

where c_α and s_α are cos(α) and sin(α), respectively, and T_{OBAS}^{PLOP} is the transformation from the OBAS coordinate frame to the PLOP coordinate frame. Eq. (5-2) can be rewritten as,

$$T_{PLOP}^{ORAS} = \left[T_{ORAS}^{PLOP}\right]^T \tag{5-3}$$

Because SII personnel provided the position of the WSF-02 antenna with respect to the Wake Shield, Eq. (5-3) was used to convert the WSF-02 GPS antenna position in PLOP to ORAS, or

$$\bar{R}_{ORAS}^{WSF/POR} = T_{PLOP}^{ORAS}\, \bar{R}_{PLOP}^{WSF/POR} \tag{5-4}$$

where the superscript *WSF/POR* indicates the position from the PLOP origin, or POR, to the WSF-02 antenna and the subscript *ORAS* is the respective coordinate frame. Equation 5.4 can be transformed again to the OBAS coordinate system,

$$\bar{R}_{OBAS}^{WSF/POR} = T_{ORAS}^{OBAS}\, \bar{R}_{ORAS}^{WSF/POR} = \begin{bmatrix} c_{180} & s_{180} & 0 \\ -s_{180} & c_{180} & 0 \\ 0 & 0 & 1 \end{bmatrix} \bar{R}_{ORAS}^{WSF/POR} = \begin{bmatrix} -1 & 0 & 0 \\ 0 & -1 & 0 \\ 0 & 0 & 1 \end{bmatrix} \bar{R}_{ORAS}^{WSF/POR} \tag{5-5}$$

Because the position of the POR is provided from the arm data in OBAS, now the position of the Wake Shield antenna with respect to the OBAS origin, O, can be expressed in OBAS coordinates,

$$\bar{R}_{OBAS}^{WSF/O} = \bar{R}_{OBAS}^{POR/O} + \bar{R}_{OBAS}^{WSF/POR} \tag{5-6}$$

The Shuttle antenna positions were given in OSRS coordinates (Davis, JSC, personal communications, 1995). Transforming them into OBAS,

$$\overline{R}_{OBAS}^{STS/O} = T_{OSRS}^{OBAS}\,\overline{R}_{OSRS}^{STS/O} = \begin{bmatrix} -1 & 0 & 0 \\ 0 & 1 & 0 \\ 0 & 0 & -1 \end{bmatrix} \overline{R}_{OSRS}^{STS/O} \tag{5-7}$$

Now a vector from the WSF-02 antenna to each Shuttle antenna can be calculated,

$$\overline{R}_{OBAS}^{STS/WS} = \overline{R}_{OBAS}^{STS/O} - \overline{R}_{OBAS}^{WSF/O} \tag{5-8}$$

Table 5.4 lists the Euler angles used in the transformation matrix from ORAS to PLOP. The asterisk in the table indicates POR position and attitude data obtained from JSC records corresponding to UTC 254:09:47. According to the records, this was the last time arm movement occurred before UTC 254:11:15. Table 5.5 lists the resulting vectors that produce the relative GPS antenna position vector, or $\overline{R}_{OBAS}^{STS/WSF}$. The upper-hemi is the Shuttle antenna used for "STS".

Table 5.4 Transformation Angles

From	To	Pitch (°)	Yaw (°)	Roll (°)
ORAS	PLOP	89.99°*	9.86°*	99.98°*

Table 5.5 Calculation of the Relative GPS Antenna Position Vector

From	To	Coordinates	X (m)	Y (m)	Z (m)
POR	WSF-02 Antenna	PLOP	-0.21	0.0	1.97
POR	WSF-02 Antenna	ORAS	-0.34	-1.95	-0.13
POR	WSF-02 Antenna	OBAS	0.34	1.95	-0.13
OBAS Origin	POR	OBAS	-16.89*	10.84*	-10.65*
OBAS Origin	WSF-02 Antenna	OBAS	-16.54	12.79	-10.77
OBAS Origin	Upper-hemi	OSRS	12.88	0.0	12.70
OBAS Origin	Upper-hemi	OBAS	-12.88	0.0	-12.70
WSF-02 Antenna	Upper-hemi	OBAS	3.66	-12.79	-1.93

* From JSC arm data

The accuracy of the vector components quoted in Table 5.5 are difficult to quantify. As previously discussed, one could assume the arm data to be correct within ± 5 cm (2 in), which implies the position of the WSF-02 with respect to the orbiter was known to within ± 5 cm. According to NASA engineers, the accuracy of the NASA supplied Shuttle antenna position vector was within a few inches as well. Another error source would include measurement error of the WSF-02 antenna with respect to the PLOP origin, POR. In general, it was concluded that the overall uncertainty was about 10 cm for the final relative GPS antenna position shown in Table 5.5.

As discussed earlier in this chapter, the position ephemeris for the WSF-02 was based on the navigation solutions calculated from the TurboStar pseudorange measurements which were then smoothed using the UTOPIA program. The Shuttle position ephemeris was formed by adding the relative GPS antenna position to the WSF-02 reference ephemeris. In order to do this, the relative GPS antenna position vector needed to be transformed from OBAS to the Earth Centered Inertial J2000 (ECI J2000) coordinate frame. The procedure for solving the transformation matrix from OBAS to ECI (J2000) is given in the following section.

Transformation From OBAS to ECI

A single transformation from OBAS to ECI (J2000) did not appear blatantly obvious, therefore, some assumptions along with a few intermediate transformations were developed. A coordinate system was defined with its origin at the center of the Earth, its radial unit vector ($\hat{u}_r$) pointing to the WSF-02 GPS antenna, its normal unit vector ($\hat{u}_t$) in the opposite direction of the orbital angular momentum vector, and a third vector to complete the right hand rule ($\hat{u}_n$) in the opposite direction of the velocity vector of the WSF-02 as shown in Figure 5.13. For lack of a better name, this coordinate system was named UNIT and the axes were assumed to be parallel with OBAS. Note that when the Shuttle is in a GG attitude, $\hat{x}_{OBAS}$ is aligned with the radial vector from the center of the Earth to the Shuttle's center of gravity. With the distance between the WSF-02 GPS antenna and the OBAS origin being extremely small relative to the radius of the orbit, this was assumed to be an adequate approximation. In actuality, this UNIT coordinate system is rotated about the $\hat{u}_n$ axis from OBAS by an angle on the order of 10^{-3} degrees. With this assumption, one can write,

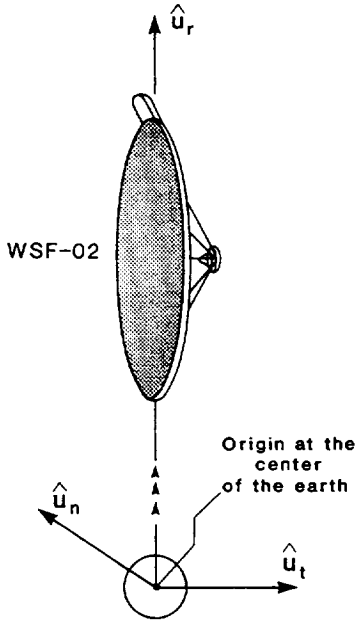

Figure 5.13

$$\bar{R}_{UNIT}^{STS/WSF} = \bar{R}_{OBAS}^{STS/WSF} \tag{5-9}$$

The next step was to transform this relative GPS antenna position vector to the more commonly known RTN coordinates (radial, transverse, and normal). This will allow the final transformation to ECI (J2000).

Because of the choice of the UNIT coordinate system, the transformation from UNIT to RTN is a single rotation about the radial unit vector,

$$T_{UNIT}^{RTN} = \begin{bmatrix} 1 & 0 & 0 \\ 0 & c_{180} & -s_{180} \\ 0 & s_{180} & c_{180} \end{bmatrix} = \begin{bmatrix} 1 & 0 & 0 \\ 0 & -1 & 0 \\ 0 & 0 & -1 \end{bmatrix} \tag{5-10}$$

Next, the transformation from RTN to ECI (J2000) is,

$$T_{RTN}^{ECI} = \begin{bmatrix} c_\Omega c_\theta - s_\Omega c_i s_\theta & -c_\Omega s_\theta - s_\Omega c_i c_\theta & s_\Omega s_i \\ s_\Omega c_\theta + c_\Omega c_i s_\theta & -s_\Omega s_\theta + c_\Omega c_i c_\theta & -c_\Omega s_i \\ s_i s_\theta & s_i c_\theta & c_i \end{bmatrix} \tag{5-11}$$

where θ is $\omega + f$, ω the argument of periapse, f the true anomaly, i the inclination, and Ω the right ascension of the WSF-02 antenna orbit. These elements were unknown for the Shuttle orbit. Therefore, the WSF-02 position ephemeris was used to obtain the elements since the WSF-02 and Shuttle were in the same orbit.

The elements needed for the OBAS to ECI (J2000) transformation can be computed from the following series of calculations,

$$\text{Radial unit vector of RTN} \rightarrow \hat{r} = \frac{\overline{R}_{ECI}^{WSF}}{\left|\overline{R}_{ECI}^{WSF}\right|} \tag{5-14}$$

$$\text{Normal unit vector of RTN} \rightarrow \hat{h} = \frac{\overline{R}_{ECI}^{WSF}(t_1) \times \overline{R}_{ECI}^{WSF}(t_2)}{\left|\overline{R}_{ECI}^{WSF}(t_1) \times \overline{R}_{ECI}^{WSF}(t_2)\right|} \tag{5-15}$$

$$\text{Transverse unit vector of RTN} \rightarrow \hat{\theta} = \frac{\hat{h} \times \overline{R}_{ECI}^{WSF}}{\left|\hat{h} \times \overline{R}_{ECI}^{WSF}\right|} \tag{5-16}$$

$$i = cos^{-1}\left(\frac{h_z}{|\overline{h}|}\right) = cos^{-1}\left(\left|\hat{h}_z\right|\right) \tag{5-17}$$

$$sin(\Omega) = \frac{h_x}{|\overline{h}|cos(i)} = \frac{\left|\hat{h}_x\right|}{cos(i)} \quad ; \quad cos(\Omega) = \frac{-h_y}{|\overline{h}|cos(i)} = \frac{-\left|\hat{h}_y\right|}{cos(i)} \quad \Rightarrow \quad \Omega \tag{5-18}$$

$$\sin(\theta) = \frac{|\hat{r}_z|}{\sin(i)} \quad ; \quad \cos(\theta) = \frac{|\hat{\theta}_z|}{\sin(i)} \quad \Rightarrow \quad \theta \tag{5-19}$$

Note the series of Eqs. (5-14) through (5-19) is independent of velocity. Usually one solves for the angular momentum vector ($\bar{h}$), and then uses the components (h_x, h_y, h_z) for these calculations, as in Eq. (5-17). However, these equations can be written in the form of the angular momentum unit vector, or "normal" unit vector ($\hat{h}$), as again demonstrated in Eq. (5-17). With the WSF-02 position ephemeris, $\hat{h}$ is adequately approximated using two position vectors in the orbit at neighboring times, i.e. Eq. (5-15). This approximation assumes two-body motion between t_1 and t_2, which for this analysis is an interval of five seconds.

Substituting these elements into the RTN to ECI (J2000) transformation matrix in Eq. (5-11), the final resulting Shuttle antenna position solution can be written as,

$$\bar{R}_{ECI}^{STS} = \bar{R}_{ECI}^{WSF} + T_{RTN}^{ECI} T_{UNIT}^{RTN} \bar{R}_{UNIT}^{STS/WSF} \tag{5-20}$$

This procedure was implemented for each epoch of the WSF-02 reference ephemeris thereby creating a shuttle antenna reference ephemeris that was consistent with the fixed relative distance between the shuttle and WSF-02 antennas.

5.2.4 Implementation of Position Ephemerides

Position Ephemeris Evaluation

In one attempt to check the position ephemeris for the WSF-02 antenna, the inclination and ascending node were compared to values obtained through the JSC Mission Control Center (MCC). Mission controllers calculated an average orbit inclination and ascending node of 28.5° and 16.9°, respectively (Tracy, JSC,

personal communications, 1995). Figure 5.14 shows that the inclination and ascending node calculated from the WSF-02 position ephemeris agree with MCC.

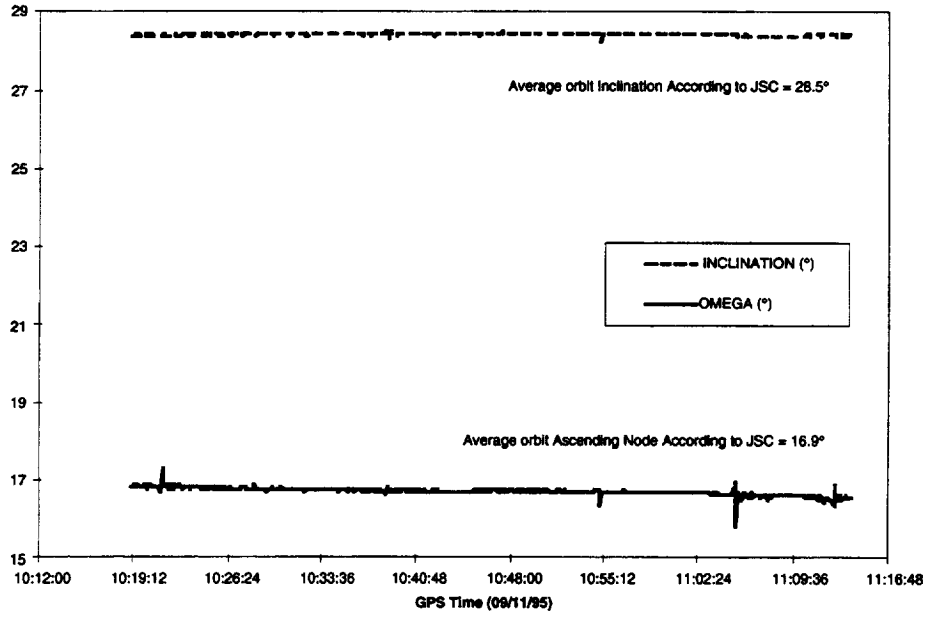

Figure 5.14 Orbital Inclination & Ascending Node Calculated From WSF-02 Position Ephemeris

Transforming Ephemerides from ECI to ECF

The final results thus far are reference ephemerides for the WSF-02 and shuttle upper antenna in ECI (J2000). However, as previously discussed, the DD_C requires positions in the ECF coordinate system. Therefore, the two ephemerides needed to be transformed. It was first assumed that the coordinate frames ECI True of Date (TOD) and ECI (J2000) were close enough for this first analysis since the mission was performed in 1996. Therefore, the transformation from the ECI frame to the ECF frame was a simple rotation.

The transformation from ECI (TOD) to ECF involves the Greenwich Meridian angle (θ_g), or angle from the Equinox to the Greenwich Meridian. Referenced to September 11, 1995 at 00:00 UTC [Astronomical Almanac, 1995],

$$\theta_g = 360.98536^{\circ}/_{day}(\Delta t) + 349.56798^{\circ} \qquad (5\text{-}12)$$

where Δt is the time interval past 00:00 UTC. This equation can then be used for the transformation from ECI (TOD) to ECF assuming the Z axes are aligned with the Earth's angular velocity vector as shown in Figure 5.15,

$$\overline{R}_{ECF}^{ANTENNA} = T_{ECI}^{ECF}\overline{R}_{ECI}^{ANTENNA} = \begin{bmatrix} c_{\theta_g} & s_{\theta_g} & 0 \\ -s_{\theta_g} & c_{\theta_g} & 0 \\ 0 & 0 & 1 \end{bmatrix} \overline{R}_{ECI}^{ANTENNA} \qquad (5\text{-}13)$$

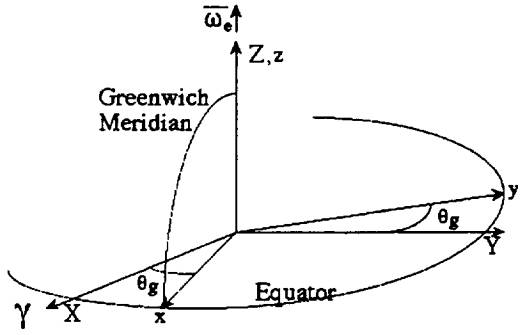

Figure 5.15 Coordinates ECF (x, y, z) and ECI (TOD) (X, Y, Z)

Interpolation Of Position Ephemerides

The position ephemerides for the WSF-02 and both Shuttle antennas were produced using a fixed time step increment of five seconds. This output frequency was chosen for UTOPIA to provide a smoothed ephemeris at points near the measurement times. Since these ephemerides are to provide the necessary data for DD_C computations, the epochs must match that of the DD_{obs} computations. The data required for DD_{obs} is directly obtainable from the GPS data for each receiver. This GPS data, however, is at different times. The Shuttle receiver records data at times offset from the WSF-02 receiver by 0.262 seconds.

Therefore, in order to obtain positions of each antenna at the correct time, an interpolation needs to be performed on the position ephemerides.

Since the data points are not widely spaced, i.e. five second interval, the method of interpolation chosen was Lagrange Polynomials [Hornbeck, 1975]. This method uses n+1 data points to produce a polynomial of degree n which approximates intermediate values between the n+1 data points. Based on research done by Engelkemier [1992], ten data points on a 15 second interval produced a rms of 3.13 mm for a satellite in an approximate 700 km circular orbit. Therefore, for this experiment, ten points on an interval of five seconds was deemed adequate. The Lagrange Polynomial interpolation method is described in more detail in Appendix 7 along with a sample of the interpolated data for the Shuttle ephemeris.

5.3 RESULTS OF IN-FLIGHT CALIBRATION

The ephemerides for Endeavour and WSF-02 described in the previous section were used to compute DD pseudorange residuals between the Collins and TurboStar. The procedure used was similar to the ground study, except the motion of the receivers in the ECF coordinate frame was accounted for in this analysis.

Examples of pseudorange DD residuals from the in-flight calibration test are shown in Table 5.6 and Figure 5.16. The TurboStar recorded L1 and L2 pseudorange and carrier phase at an interval of 5 sec, whereas the Collins receiver recorded L1 data at an interval of 1 sec. The DD residuals for this experiment were formed at a five second interval. The shorter time duration for satellite visibility, coupled with the viewing directions of the respective antennas, is illustrated in Figure 5.16. As in the ground test, if the receivers are correctly modeled in the DD residual computation, only receiver noise with zero mean should result, but it is evident that both biases and time variations exist. Although the reference ephemerides are in error by 100 m since they are based on the navigation solution, this error mostly cancels in the DD using a short baseline of 13 m. Furthermore, if an error exists in the baseline modeling, this would

produce, at most, a 13 m difference, considerably smaller than the characteristics shown in Figure 5.16. Based on the ground test, the existence of biases is not unexpected and can be attributed to the same unresolved source observed with the ground tests.

Table 5.6 On-Flight DD Residual Statistics

PRNs		Mean DD Residuals (m)	Standard Deviation	Number of Data Points
15	26	-109.58	2.42	25
2	12	-33.95	13.36	143
15	2	-110.31	6.44	75
5	12	8.12	3.57	17
17	26	45.63	13.26	76
26	7	57.94	30.63	81

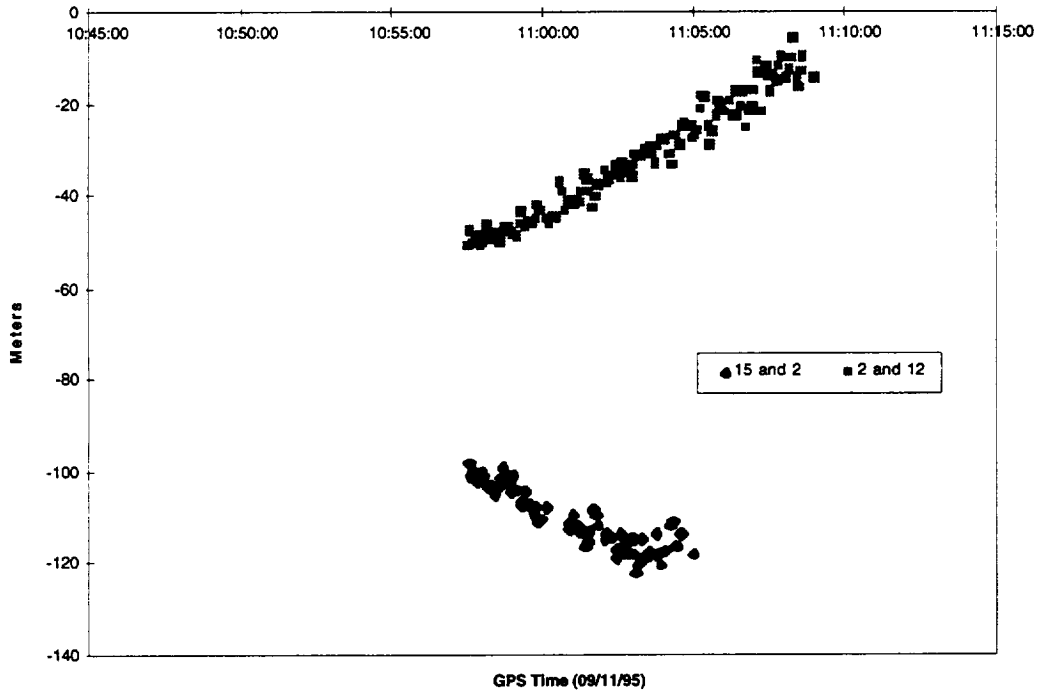

Figure 5.16 Post-Flight DD Residuals

The linear trends in Figure 5.16 could be an exaggerated effect produced by the source of the small linear trends seen in the ground tests, such as a doppler effect (the doppler component is larger in orbit) or an unknown time tag error in the Collins data. Another possible contributor is the modeling of the Endeavour attitude in the computed DD. The assumed attitude was strictly gravity gradient, yet the attitude history during this period shows librations about mean values (see Figure 5.5). These attitude variations produce changes in the spatial orientation of the relative antenna position vector that have not been accounted for in the DD computations. The pitch and roll variations shown in Figure 5.5 would transform into a DD variation of at most a meter (see Appendix 4 for sample calculations). However, Figure 5.17 shows the yaw of the WSF-02. Yaw varies from the original assumed value of zero by over 25°. This transforms into a DD variation of up to almost 7 m. This is significantly smaller than the total variation of the DD (for example, between 15 and 2 in Figure 5.16); however, it still could be a contribution.

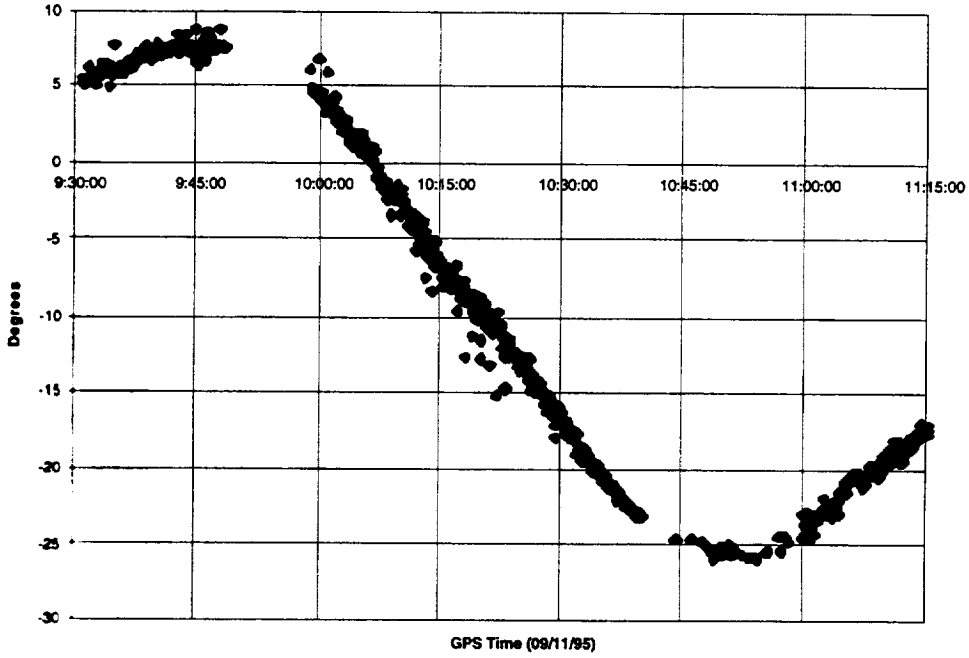

Figure 5.17 WSF-02 Yaw

Chapter 6

Shuttle/WSF-02 Precision Orbit Determination

An alternative calibration approach would be to form DD measurements between the two flight receivers and perform a relative positioning solution in which the time-dependent position of one receiver is assumed known and the other position is estimated. The estimated relative position could then be compared to the known position vector, as given in Table 5.5 of the previous chapter. However, since each satellite combination in the DD has a different bias, many bias terms must be estimated along with the relative position. The small number of common satellites described previously limits the usefulness of this technique.

Since the global network of ground GPS receivers enables another source of information to be used in double differencing, the number of common satellites between the flight GPS receiver and the ground GPS receiver is dramatically increased over the in-flight case. If double differences (pseudorange or carrier phase) are formed with one of the flight receivers as R1 (see Eq. (3-19)) and a ground receiver as R2, then the orbit of the flight receiver can be determined by a dynamic approach. Furthermore, this approach of determining the orbit using DD measurements can be applied to each flight receiver and the resulting independent orbits can be compared. If both orbits have been determined for the spacecraft center of mass, then the comparison between the two orbits should, in principle, yield zero. Of course, in practice, the result will not be zero because of the different receiver error sources, but the differences are a further calibration test of the two receivers. The dynamic technique of using DD measurements to determine the orbit is described, for example, by Schutz [Schutz, et al., 1994] for TOPEX/POSEIDON.

6.1 DOUBLE DIFFERENCING WITH IGS DATA

The International GPS Service for Geodynamics (IGS), in collaboration with numerous institutions, collects GPS data from a global network of stations. Most of the receivers used at these stations are TurboRogues programmed to record L1 and L2 pseudorange and carrier phase at an interval of 30 sec. The stations from the IGS network used in the STS-69 analysis are given in Table 6.1. The IGS station coordinates used were the ITRF93 [Boucher, et al., 1994] mapped to September 1995 and are also listed in Table 6.1. Double differenced pseudorange measurements were formed using L1 from the Collins receiver and ionosphere-corrected pseudorange (L1/L2) from the IGS stations. For the TurboStar, double differenced L1/L2 pseudorange and double differenced L1/L2 carrier phase measurements were formed with the like measurements from the ground network of IGS. The DD measurements used for this calibration test were made during the same one hour period that was used for the in-flight calibration test, described in the previous chapter.

Table 6.1 IGS Network Stations Used in STS-69 Analysis

All Stations Listed Use TurboRogue GPS Receivers			
Station	x	y	z
Algonquin, Ontario	918129.525	-4346071.353	4561977.980
Fairbanks, Alaska	2281621.496	-1453595.799	5756962.090
Goldstone, California	2353614.197	4641385.422	3676976.500
Kokee Park, Hawaii	-5543838.257	-2054587.381	2387809.711
Kootwijk, Netherlands	3899225.344	396731.824	5015078.453
Madrid, Spain	4849202.490	-360329.139	4114913.132
Santiago, Chile	1769693.329	-5044574.253	-3468321.113
Tidbinbilla, Australia	-4460996.187	2682557.163	-3674443.897
Tromso, Norway	2102941.176	721569.691	5958194.461
Usuda, Japan	-3855262.980	3427432.584	3741020.313
Wettzell, Germany	4075578.612	931852.679	4801570.064
Yaragadee, Australia	-2389025.496	5043316.952	-3078530.911
Yellowknife, NWT	-1224452.536	-2689216.146	5633638.443

The orbit determination was performed with the University of Texas/Center for Space Research software MSODP (Multi-Satellite Orbit

Determination Program) described by Rim [1992]. Each orbit determination of the combined vehicle (Endeavour/WSF-02) was performed in exactly the same way for all cases with one exception: locations of the antennas with respect to the combined vehicle CM were different. The processing of the Collins/IGS DD used the position vector from the combined vehicle's center of mass to the upper-hemi, because all of the measurements common to the TurboStar and Collins were made from the upper-hemi rather than the lower-hemi. The TurboStar/IGS DD used the position vector from the Endeavour/WSF-02 center of mass to the WSF-02 GPS antenna. These position vectors are listed in Table 6.2, with the vectors originating at the CM, where $\hat{x}$ is a unit vector in the direction of the combined vehicle velocity, $\hat{y}$ out the Shuttle's belly and $\hat{z}$ pointing down to the Earth. Calculations for Table 6.2 used the Shuttle CM position, namely $1097.90\,\hat{x}_{OSRS} - 0.03\,\hat{y}_{OSRS} + 377.53\,\hat{z}_{OSRS}$ inches, where OSRS is a Shuttle-fixed coordinate frame described in Section 5.2.3. A table of the CM position history for STS-69 can be found listed in Appendix 6.

Table 6.2 Combined Vehicle's Center of Mass to Antenna Position Vectors

Antenna	$\hat{x}$ (m)	$\hat{y}$ (m)	$\hat{z}$ (m)
WSF-02	-12.791	-1.178	-11.344
Upper-hemi	0.001	-3.108	-15.004

The Shuttle force model was generally consistent with the IERS Standards [McCarthy, 1992], except the gravity field was JGM-3 [Tapley, et al., 1996] and the atmospheric density model was the Density and Temperature Model, DTM [Barlier, et al., 1978]. The IERS standards include solid Earth and ocean tides, as well as luni-solar perturbations. The GPS ephemerides were determined by JPL for the IGS GPS week 818 (Crustal Dynamics Data Information System). No adjustment of the GPS ephemerides was performed in the Shuttle solutions. All cases estimated the position and velocity of the combined vehicle in a batch mode, along with a bias (or phase ambiguity). Atmospheric drag was modeled, but a drag parameter was not estimated because of the short arc duration. As

noted previously, the arc length was about one hour, which is less than one orbital revolution. The specific force models are listed in Table 6.3.

Table 6.3 Forces Modeled in MSODP

Force	Models
Gravity	JGM-3 70 x 70
Tides	Solid Earth and Ocean
Luni-solar	DE 200 (JPL Ephemeris)
Drag	DTM Model CD = 2.2 Area = 266 m^2 Mass = 108294.5 kg
Radiation pressure	Constant Area Model CR = 0.3

6.2 RESULTS

6.2.1 Collins Clock Correction Issue

MSODP uses the observed DD calculations to estimate a spacecraft's orbit in a dynamic sense instead of solving for a position solution and clock correction kinematically, as discussed in Section 3.1. Even though clock errors cancel in double differencing, the DD_{obs} time tags must be corrected to GPS Time. As demonstrated in Figure 2.4 , the TurboStar clock corrections were smaller than a microsecond and thus considered negligible for the time tag. The Collins clock corrections computed from the pseudoranges, however, were approaching a 100 ms level so it was presumed that the correction was needed for the DD_{obs}. time tag. After applying the time tag correction, a TurboStar phase determined orbit and a Collins pseudorange determined orbit were then produced with MSODP. Their differences in radial, transverse and normal residuals are shown in Figure 6.1.

Figure 6.1 shows a large difference in the transverse component between the Collins and TurboStar determined orbits. The transverse component appears

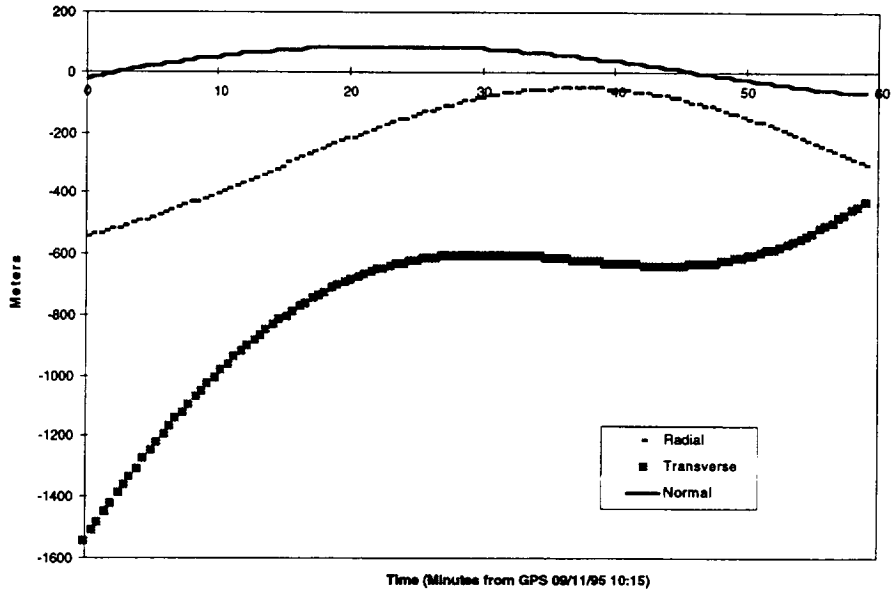

Figure 6.1 Orbit Difference Between Collins Clock Corrected Pseudorange Determined Orbit and TurboStar Phase Determined Orbit

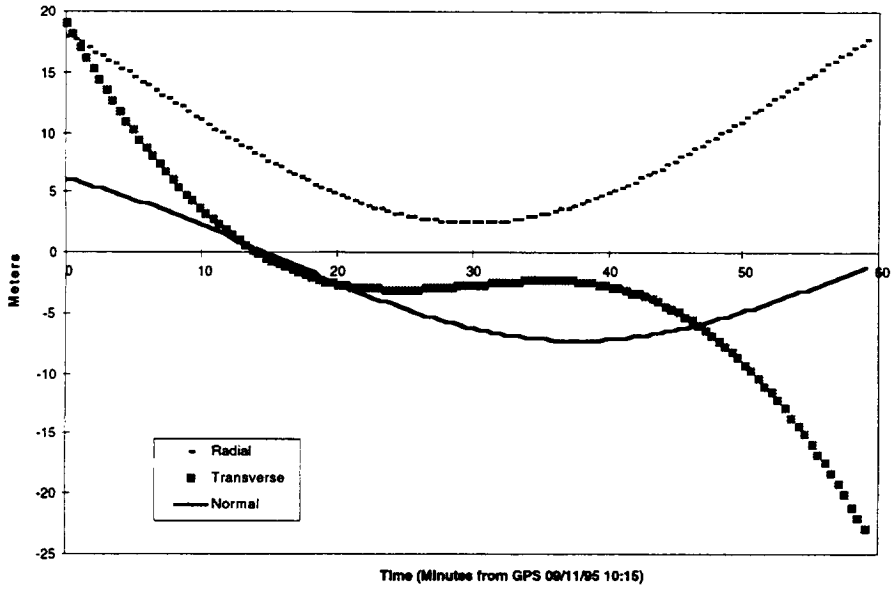

Figure 6.2 Orbit Difference Between Collins Uncorrected Pseudorange Determined Orbit and TurboStar Phase Determined Orbit

to be offset by about 700 m. Knowing that the time tag correction to the Collins DD_{obs} measurements was on the order of 100 ms, and roughly speaking, the velocity of the combined vehicle was 7,000 m/s, it was then concluded that this transverse offset was caused by a timing error. In other words, a 100 ms timing error at 7,000 m/s would produce about a 700 m offset. The Collins pseudorange-determined orbit was estimated again but without the time tag corrections. Figure 6.2 shows the orbit difference that resulted.

It was this analysis that lead to the realization that the time tags in the Collins data had already been adjusted to account for the receiver clock error. It was later confirmed that the spread sheet cell "GPSTIME" shown in Appendix 1 was indeed a time compensated for the receiver clock offset (see Appendix 9). However, it is important to note that the pseudorange measurements are negative, which implies that these quantities are not consistent with the interpretation that the time tag is GPS Time. For consistency, the pseudoranges should have been adjusted also, which would have resulted in positive values rather than negative. However, any adjustment in the pseudoranges would cancel when the double differences are formed; thus, the pseudorange correction is irrelevant with double differencing.

It should also be noted that the results in Chapters 4 and 5 were obtained with the knowledge of the interpretation of the orbit comparisons. All results in these chapters were obtained under the assumption that the Collins time tag was GPS Time.

6.2.2 Precision Orbit Determination

The evaluation of the ephemeris accuracy on TOPEX/POSEIDON (T/P) was made possible by the use of different tracking systems and comparing the results. This result was described by Tapley, et al., [1995], by using ephemerides resulting from Satellite Laser Ranging (SLR), a French doppler system known as DORIS, and GPS. Based on the comparison of ephemerides derived from these systems and from independent software, it was concluded that the orbit accuracy

on T/P was 2-3 cm in the radial component and less than 10 cm in the horizontal (along-track and cross-track) components.

In the case of WSF-02, the assessment of orbit accuracy must be made solely from the observation residuals. Unfortunately, the experiences gained from analysis of T/P GPS data and simulated low Earth orbiter GPS data [Rim, 1992; Davis, 1996] show that there is not a one-to-one interpretation of DD residuals and orbit accuracy. Based on these analyses, the orbit accuracy has been observed to be four to five times higher than the phase DD residuals, where the residuals are formed between the low Earth orbiter GPS data and the ground IGS data.

Using the force models for the combined vehicle given in Table 6.3, the DD residuals obtained from a converged orbit are shown in Table 6.4. The DD in Table 6.4 were formed using single frequency Collins pseudorange and dual frequency ground IGS pseudorange data. Furthermore, double difference bias parameters were estimated for each combination of satellite pairs and Collins/IGS pairs. This strategy was adopted in order to accommodate the channel biases found to exist in the Collins data inferred from ground and calibration in-flight tests.

Table 6.4 Combined Vehicle POD DD Residuals

Data	rms
Collins Pseudorange	3.17 m
TurboStar Pseudorange	3.20 m
TurboStar Phase	0.34 m

For the TurboStar, dual frequency data for pseudorange and carrier phase were used. In the case of carrier phase, the ambiguity terms were estimated for each satellite pair and TurboStar/IGS receiver pairs, similar to the treatment of the Collins data.

Since the arc length for the orbit solution was about one hour, only the combined vehicle position and velocity at the initial time were estimated. The phase DD from the TurboStar reflect the most accurate determination of the

combined vehicle's orbit. The pseudorange DDs are dominated by measurement noise, but the phase precision is a few millimeters, thus the phase residuals more clearly reflect force model errors and measurement model errors.

If the 34 cm phase DD residual shown in Table 6.4 is scaled by five to represent orbit error, the estimated orbit accuracy of the combined vehicle is 1.70 m in an rms sense. Experience with TOPEX/POSEIDON and high fidelity simulations of low Earth orbiters suggest this is a reasonable estimation of the accuracy of the Shuttle for the one hour arc. This result is especially important since it suggests that large, unmodeled forces do not exist for this time period. Furthermore, the results suggest that meter-level POD of the Shuttle is obtainable if a high precision GPS receiver is available.

The expected sources of contributing error to the 34 cm phase residuals are given in Table 6.5. As noted in Table 6.5, the dominant error source is expected to be the Earth gravity model. Using the JGM-3 covariance matrix, a state of the art gravity model [Tapley, et al., 1996], the predicted error is about two meters. For a one hour arc, the influence of drag can not be adequately separated from the epoch position and velocity, thus a drag parameter was not simultaneously estimated. The level of errors shown in Table 6.5 for other contributors was determined from simulations that have been conducted with other satellites and are intended to simply provide an order of magnitude effect.

Table 6.5 POD Error Sources for Combined Vehicle at 400 km, i = 28.5°

Source	Description	Estimated rms Error
Gravity	Based on JGM-3 covariance	1 - 2 m
Tides	Modeled	< 1 m
Luni-solar	Modeled	< 1 cm
Drag	Modeled, accommodated in position/velocity estimate	< 1 m
Radiation pressure	Modeled, accommodated in position/velocity estimate	< 1 m
Attitude	Mismodeling will produce error in ECF antenna locations (Appendix 5)	< 2 m
Summary		3-4 m

Based on the ground tests and the in-flight comparisons between the Collins and TurboStar, an estimate of the Collins L1 pseudorange precision is about 5-6 meters, yet the DD rms was about 3 meters. One explanation is the ground and in-flight tests used much more data. The fit with a dynamic model was based on a data interval of 30 seconds, about one sixth the amount of data in the other tests.

As noted previously, it is expected that the TurboStar phase-determined orbit will be the most accurate. For this reason, the TurboStar phase-determined orbit was used to compare against the Collins pseudorange-determined orbit. After determination of the orbit from the respective receivers, the ephemerides were differenced, as shown in Figure 6.2. The ephemeris differences were resolved into RTN components as given in Table 6.6. These rms differences show that the Collins result compared to the more accurate phase-determined orbit using the TurboStar agrees to better than 10 m. This result implies that through bias estimation with the pseudorange data, the Collins receiver is capable of orbit determination better than 10 m, which far surpasses the orbiter's several kilometer precision requirement.

Table 6.6 RMS Differences Between Collins-determined Orbit and Turbo-Star Determined Orbit

Radial (R)	3.07 m
Transverse (T)	5.95 m
Normal (N)	4.16 m

6.3 SUMMARY

Both the ground tests and the in-flight calibration tests showed the existence of pseudorange biases, i.e., biases dependent on the particular GPS satellite being tracked. These biases are believed to occur in the Collins 3M receiver, based primarily on the ground tests. As a consequence, orbit determination using pseudorange measurements from the Collins receiver should be performed with bias estimation, similar to that used with carrier phase. Using

the two separate receivers on the combined Endeavour/Wake Shield-02 vehicle, it was shown that the orbits determined by each receiver agreed to better than 10 meters, further showing that the effect of the Collins pseudorange biases can be mitigated to this level. Remaining error sources that could improve the results include the proper modeling of the vehicle attitude. Finally, using carrier phase measurements from the TurboStar, the results suggest that meter level POD is attainable for the Shuttle, when a high precision GPS receiver is available.

Chapter 7

Conclusions

On September 7, 1995, the Space Shuttle Endeavor on STS-69 was launched carrying with it a University of Houston free-flyer payload called the Wake Shield Facility (WSF-02). The main purpose of the WSF-02 was to grow thin wafers of semiconductor compounds, such as gallium arsenide, in an ultra-vacuum created in the wake region during the WSF-02 free flight. Additional experiments were carried on the WSF-02 including a flight version of the high precision TurboRogue GPS receiver, known as the TurboStar. The presence of a high precision GPS receiver on board the WSF-02 at Shuttle altitude ($\approx$ 400 km) provided many unique opportunities for research. This report summarizes the results of such opportunities afforded by STS-69.

One opportunity included the use of GPS to accomplish relative positioning between two objects in space (the Shuttle and the WSF-02). This experiment was enabled by the presence of a Collins 3M GPS receiver on the Shuttle, as well as the WSF-02 receiver. However, little experience has been acquired with the Shuttle using the Collins. Therefore, in order to best interpret the relative positioning results, an analysis of the performance of the Shuttle receiver was also required. This latter objective lead to an assessment of the Shuttle receiver's ability to perform precision orbit determination.

Calibration tests in a controlled environment was conducted as a validation tool to establish respective receiver performance characteristics. In pre- and post-flight calibration tests, ground tests were conducted using both the Shuttle and the WSF-02 GPS receivers. The pre-flight test had a short antenna separation (2.4 m) between the two receivers and the post-flight test had a common antenna (zero baseline) for the receivers. Double difference (DD) pseudorange residuals between the two receivers and two GPS satellites were formed to remove Selective Availability (SA) and other common error sources.

An additional calibration test was conducted in orbit during STS-69 while the WSF-02 was held by the Endeavour robot arm for a one hour period. For this in-flight case, DD residuals were computed as in the ground test analysis. However, the orbital motion produced time-varying positions in an Earth-fixed reference frame. Therefore, the position vector between the two antennas was determined from the robot arm flight record, resulting in a baseline of 13.4 m.

In all three tests, biases up to 140 m were observed in the double difference pseudorange measurements, implying that instrument-dependent characteristics exist which do not cancel in double differencing. Due to previous experience with TurboRogue receivers, these biases were initially assumed to exist in the Collins receiver. The effects of these biases were then mitigated by including bias parameters to accommodate for them in an estimation process. As it turned out, at the conclusion of the study, the existence of channel biases within the Collins was confirmed (Appendix 10).

Another observation was made from the three calibration tests: the biases were not constant. Mismodeling of the Shuttle attitude, doppler effects and even an unknown Collins timing issue were likely causes of the residual slopes. These slopes cannot be completely accommodated in bias estimation alone and require further investigation.

An additional ground test was then conducted after the mission in order to ensure confidence in the TurboStar. This test had a zero baseline between the TurboStar and an "off-the-shelf" TurboRogue ground receiver. The results confirmed the assumed performance of the TurboStar showing that the DD L1 pseudoranges were unbiased.

The final relative positioning test was carried out using the one hour period of data when WSF-02 was attached to Endeavour with the RMS. In this case the orbit of the combined Endeavour/WSF-02 was determined independently with each receiver. The analysis was performed in a manner similar to that used for the precision orbit determination of TOPEX/POSEIDON [e.g., Schutz, et al., 1994]. The one hour arcs were based on forming double differences with 13 TurboRogue receivers in the global IGS network. In an attempt to compare these

two orbits and their accuracy, the Shuttle remote manipulator system data was incorporated as another source of information to determine the relative position between the two receivers (13.4 m). In the Collins case, the double differences were formed with pseudorange but the TurboStar case was performed with carrier phase. Pseudorange biases were estimated with the Collins and phase ambiguities were estimated with the TurboStar.

Various analyses suggest that the accuracy of the Endeavour/WSF-02 orbit for the one hour period as determine by the TurboStar is better than two meters. This result is based on the extrapolation of the 0.34 m DD phase residual rms to account for errors in the force modeling, especially gravity, and other effects.

The orbit determined using the Collins receiver was compared with the TurboStar phase-determined orbit. The rms differences between the two independently determined orbits was better than 10 meters. This final test demonstrated the accuracy of the Collins-determined orbit to be better than 10 m as well as the accuracy of the relative positioning using these two receivers.

The results of the study demonstrated the feasibility of relative positioning between two GPS receivers in low Earth orbit. The results also indicated that the Collins receiver has the capability to support a semi-precision orbit determination at a level exceeding its original design requirements. This conclusion also shows that the Collins 3M receiver can support Shuttle applications, such as scientific experiments with an improved spaceborne scientific platform.

Future endeavors could include improvements in the analysis of the STS-69 data to include factors such as refined modeling of the Shuttle attitude. An additional future goal should be to test the TurboStar and Collins in a similar manner as presented here during NASA Shuttle mission STS-80 to fly in November of 1996. This would allow the opportunity to request Collins' channel bias outputs and account for these channel biases rather than estimating them. By continuing to investigate the Collins, the residual slope issue could be resolved as well as verifying the raw data interpretation. Once the Collins is completely understood, its orbit determination capability may be pushed to levels of accuracy significantly better than 10 m, perhaps at the meter-level.

Appendix 1

Collins Raw Data Spread Sheet

The raw data from the Collins used in this study was received in a spread sheet format. The following is an example corresponding to one data record "near" GPS time 95 9 11 11 0 54.9508563. This is referenced as "near" GPS time since the interpretation of the time cells is not completely understood.

GPSTIME	TIMETAG	#MEAS	MT1	MT2	MT3	MT4	MT5	MT6	MT7	MT8	MT9
126054.9509	347521.74	8	1	1	1	1	9	2	2	2	2

MT10	MT11	PR1	PR2	PR3	PR4
10	0	-4077183.38	-5032639.996	-4219820.498	-6989795.783

PR5	DR1	DR2	DR3	DR4
-5032641.456	1720.427246	1494.609863	-4743.848633	-1050.212036

DR5	DR6	PPR1	PPR2	PPR3	PPR4
1494.633789	0	-4077180.441	-5032639.748	-4219818.303	-6989795.105

PPR5	PDR1	PDR2	PDR3	PDR4
-5032640.373	1720.51001	1494.698364	-4743.83252	-1050.203003

PDR5	PDR6	IDSAT1	IDSAT2	IDSAT3	IDSAT4	IDSAT5	CH1DR5
1494.698364	0	19	12	15	2	12	344.429382

CH2DR5	CH3DR5	CH4DR5	CH5DR5	CH1DR4	CH2DR4
299.502655	-948.48822	-209.31691	299.50827	344.269196	299.22168

CH3DR4	CH4DR4	CH5DR4
-948.642883	-209.676682	299.210449

The labels indicated are identical to labels provided in the spread sheet; however, little information was available on their interpretation. The following interpretation of selected labels has been made:

GPSTIME: time tag for the measurements given as seconds into the GPS week and in GPS Time. It was assumed that this time tag applies to all measurements in this record.

PR1 to PR5: Pseudorange measurements in meters from channels 1 to 5 respectively.

IDSAT1 to IDSAT5: PRN of the satellites with measurements PR1 to PR5 in the corresponding channel.

An interpretation of the other quantities has not been made.

Appendix 2

Flight Hardware Integration Summaries

This appendix contains unedited trip summaries prepared shortly after the respective trips.

Orlando, April: WSF-02 GPS Equipment Integration Summary

Houston/Orlando Trip 04-17 to 04-20 04-22-95

Monday noon, we, Dr. Schutz and Christie Schroeder, flew out of Austin and into Houston to travel to NASA Johnson Space Center (JSC) and pick up the recorder and GPS receiver. We met with Samantha McDonald, the GPS recorder engineer, and finalized all details about the tests, the software, and precautions of traveling with the flight hardware.

Tuesday morning, 8:30 am, we arrived at the security gate to be badged. Unfortunately Mike Exner had not yet been cleared so we were delayed a bit getting to Hangar AE. Eventually we met up with Nick Combs and the Wake Shield Facility staff after 9:00 am.

Mike worked with McDonnell Douglas people (Oscar and Mitch) to set up the GPS antenna and choke ring on top the roof of the hangar. Mike was concerned with the messy environment on top the roof. There were some obstructions, other antennas and even a transmitter.

We obtained a +28 Volt power supply needed to power up the recorder for the bench test and proceeded to the clean room after suiting up in 'bunny' suites. The recorder was unpacked and connected to the power supply and computer (see Figure A2.1) enabling the first acceptance test to be initialized at 11:20 am. Mean while, Mike set up the receiver for its initial test.

The recorder passed its first acceptance test! The recorder's sequence number was counting implying the recorder was processing. The drive temps 1

and 2 read 256 and 257 (hex) respectively which is nominal and the sector count went to zero since there was no data present as a result of the reformatting of the disk before Houston departure. The next step was to hook up the GPS receiver to make sure the data could get to the recorder.

The receiver was powered via the recorder but the data port of the receiver was connected to Mike's laptop still trying to lock on to satellites. As of 2:50 p.m., we still were not tracking enough satellites. At times we had one or two locks but no more; therefor most of the afternoon was spent trouble shooting the tracking problem.

Mike concluded that maybe the cable used to link the antenna to the receiver had a substantial amount of loss in it. The signal to noise ratio was extremely low: values of 6 to even 1 when we were expecting values of 30 to 40. Mike decided to increase the gain of the signal to the receiver by 26 dB. This enabled the receiver to lock on to four satellites. Another 26 dB and the receiver had six by 4:00 p.m.

Shortly afterwards the recorder data port (P3) was hooked up to the receiver to catch the data. For the next half hour, the disk drive temperatures were a nominal 25e and 25f (hex), there were absolutely no write errors or buffer over-flows, and the receiver was at times tracking up to eight satellites to give us both navigation states and pseudo-range data.

We disabled the recorder and off-loaded the data onto the hard drive of the computer using the command 30 in the GPS Ground Support Engineering (gpsgse) software. We recorded 115 sectors worth of data ($\approx$ 60 kB) but unfortunately messed up the conversion from hex to decimal and down loaded 1123 sectors! The error caused some extra time copying all the empty sectors (about 1 sector/sec) but Mike Exner was able to edit the file. Analysis later that night at the hotel showed the data looked fine.

We started the next day (04-19) with the agenda of 1) quantifying the loss in the main cable from the roof antenna to the receiver, 2) figuring out how to keep the signal strength up as we moved the equipment from the bench to the WSF, and 3) perform the final tests. While Mike worked with McDonnell

Douglas people on the antenna/receiver situation, Space Industry Inc. (SII) people and Christie donned the WSF-02 with the recorder and the receiver.

Mike was able to acquire a signal generator and a spectrum analyzer and measure the loss of the co-axial cable used the day before. A signal was sent up a neighboring cable, that went to the roof, to which was connected to our cable by a jumper. Measuring the signal strength coming back via our cable, we hoped to quantify the signal loss and verify our results from the day before. For a typical RG9 cable (?), the loss between the two was expected to be about 5 dB. We discovered only 4 dB. This meant that something else was causing our problems and a new cable wasn't going to fix it.

Meanwhile, the recorder was being hooked up via the WSF-02 power (P4) to initialize its last acceptance test. It was noticed that the cable connections on the recorder were mis-marked. As a precaution, SII personnel, Rob, checked the polarity of the switched connections and re-labeled them. Unfortunately no power was getting to the recorder due to a blown fuse in the WSF. SII people Rob and Jan found the fuse, replaced it and then got the test running. The ground support software to be used during the flight (fltgse) did not initialize correctly at first. After a bit of trouble shooting, it was discovered that the port was set incorrectly on the laptop. In Houston we initialized with port 1 and figured it worked but in reality it is port 0. It should be noted that this is indigenous to the laptop being used so the value may change. The recorder finally passed the acceptance test.

The next step was to connect the receiver to the recorder so the remainder of the tests could be achieved, however, the receiver was still only tracking two satellites. By 11:00 am, the spectrum analyzer showed signals crowding the area around the antenna. The domain around 1.2 GHz was terribly messy! There was our problem. As it turned out, Patrick Air Force Base, 8 - 12 miles away, was transmitting a FAA dual channel radar of frequencies 1.345 and 1.265 GHz. There was also a transmitter very near to our receiver at a frequency of 1.8 GHz. The two satellites that we *were* receiving were probably because of their stronger signal strength due to geometry.

There were several ideas to handle the frequency interference problem. The first was to tilt the antenna away from the radar source. A McDonnell Douglas personnel, Mitch, went to the top of the roof with a walkie-talkie to position the antenna in different directions. Pointing the antenna away from the radar source and the 1.8 GHz transmitter helped a little but not enough. He next moved the antenna below the roof line out of sight from the Patrick AFB radar but that didn't seem to help - nor did moving the antenna as far away from the 1.8 GHz transmitter using an extra 95 ft cable. We even had sheet metal made to shield the antenna but it never came to that. We decided to run a cable out of the clean room through a nearby portal to an exit door. The antenna ended up on the driveway outside the hangar which resulted in a much cleaner environment.

At 3:30 p.m. we finally hooked up the receiver to the antenna, however we noticed there was no power again. At the time we didn't realize that the grid to the recorder had been turned off so we instead used the portable +28 V power supply. After about six crashes, the receiver locked onto four satellites. A little after 4:00, and we were ready to start running our final tests. Unfortunately it was at this time that Rob accidentally tripped over the +28 V power supply, knocking it off the table and to the ground. The power supply was broken.

We quickly unhooked the power and re-connected to the WSF: the recorder seemed to be okay after the acquisition command was initiated but the receiver was not registering. Mike, and then Rob, both measured the voltage across the receiver-to-recorder-power port (P1) and noted that instead of getting +15 V, we were getting 0.77 V. A call was made to Samantha and by 5:00 p.m. we had the recorder open and searching for the problem.

Samantha hoped it would be either a blown surge protector diode or power converter. Either one would not be too much of a problem to fix. The diode was perfect with no charred residue so after some voltage measurements across the board, Mike and Jan concluded it was a blown converter. Samantha Federal Expressed us a replacement part that night and Nick assigned Jan to fix it in the morning.

Thursday, 04-20, we called Federal Express first thing and found out that the part had left Memphis, the central hub, around 3:30 am and was to be in Orlando shortly. Christie drove to the Cocoa Beach FedEx location and picked it up personally to expedite its delivery. Meanwhile, Mike and Dr. Schutz set up the antenna again outside but this time on a stairwell instead of in the middle of the driveway and ran a test for a couple of hours.

By 10:00 am, SII personnel, Jan, was swapping the converters. By 11:00 am, we powered up the recorder on the bench and ran an acceptance test and checked the voltage out of the receiver-to-recorder port (P1): +15 V and a passed acceptance test! Jan then proceeded to make the recorder flight ready by wiping it down and torquing the screws.

At 12:30 the recorder and the receiver were hooked up to the WSF-02 and each other. Everything was looking good! The recorder was getting GPS data with no write errors and apparently no buffer overflows. Both navigation states and pseudo-range data were being received. One thing to note, when the recorder is initially turned on and down counting to its next available sector to record to, it can not take data. Once data was being recorded, we let it run for an hour and went to lunch.

Upon our arrival back, we noted that the recorder was maintaining a data-rate of about 1.5 MB/hour. We ended up with 3054 sectors ($\approx$ 1.5 Mb) and no write errors! The next test was the high-rate/low-rate toggle, or the 159 command. The fltgse software showed a successful toggle as did Mike Exner's software. SII personnel, Art, got a small error but it didn't seem to be a problem. Christie later checked with Samantha and she agreed with Art's assessment:

Error Message	What That May Mean
NO REPLY TO THE SC2	Either the receiver did not reply to the command at all or it did not reply in the allotted amount of time. Either way, the command was initiated and the receiver got it.

XNEXT PACKET ASKED FOR	After waiting for the reply, the recorder continues its business and asks for the next data packet.
CRC ERROR	The next packet it did get was longer in bits than it expected. Art figured the reply from the receiver was tacked onto the next packet thus causing the error.

It was noted that this toggle is a high-rate to low-rate only. It does not work the other way. It was also noted that the toggle has orbital (not ground) GPS receiver configurations attached to it, therefor, Mike cut the power to the recorder-receiver set up before the receiver got too lost.

By 2:30 p.m., we had the gpsgse software hooked directly to the recorder in order to down-load the data recorded over lunch and during the toggle test. Unfortunately the download was aborted by power interruptions caused by either the RS422-232 converter being loose, the power connection to the outlet being weak, or the laptop acting a bit quirky. Once fixed we started again but a quarter of the way through, the process seemed to crash. We tried this twice which ate up a lot of time since transferring the data went at a rate of 1 sector/sec and we had over 3000 sectors! It was later realized after calling Samantha that Christie forgot the recorder had to be disabled for the command 30 to work (downloading the disk to a file).

Finally at 4:00 p.m., the recorder computer port (P2) was hooked back up to the WSF-02 for the final re-format command. This process could have been done directly from the gpsgse software with the laptop connected to the recorder, however, if we wanted to clean the disk one last time before flight, we needed to test Art doing it via the WSF. If it didn't work, we were there to use the gpsgse software. It was noted that each time the recorder is powered up (which it will be

several times before it goes up since it is on a power line connected to other experiments still to be checked out), it will be recording. The default mode for the recorder is 'on'. Even when the receiver is not giving it any data, it will be recording; however, this 'data' will be garbage and very minimal. If Art can re-format the disk prior to flight, we will have a virtually clean disk.

The reformat command was initiated via three commands: 7, 25, and 93. Each took about 8 or 9 seconds to register on the fltgse software but all went well. The sectors started at zero and started erasing its way up to number 163839. The filled sectors took longer but once the recorder reached blank or empty sectors, the process almost doubled in rate.

By a quarter to 5:00 (with a plane to catch at 7:10 p.m.), it didn't look as if the disk would be done formatting for another 20 minutes so we loaded a copy of the fltgse software on to a SII laptop and showed Art how to make sure the reformatting worked. The task was very simple and everything looked like it was running great so we felt that this was acceptable. The only thing left for Art to do after we left was to make sure the recorder did indeed reformat all 163839 sectors. This was done by cycling the power to the recorder and letting it initialize itself by counting down its sectors to the next available recording space. If the reformat worked, it should count down to sector zero.

At the conclusion of the trip, we felt pretty confident that everything was going to work just fine. Even if it turned out that the reformatting failed, Mike Exner is going back in mid-May to update the receiver software and re-configure it for orbital tracking rather than ground tracking. He can perform the reformat with his copy of the gpsgse software that he obtained from Dr. Schutz.

Both carry cases were brought back along with all the bench test cables to be returned to Samantha before the launch. This included the cable and converter needed to hook up Exner's computer to the recorder in the event he needs to reformat the recorder's disk by hand. The blown power converter was also brought back and will be delivered to Samantha the following week (04-26) for analysis by the manufacturer to determine what caused the short.

TESTING APPARATUS AND CONFIGURATION

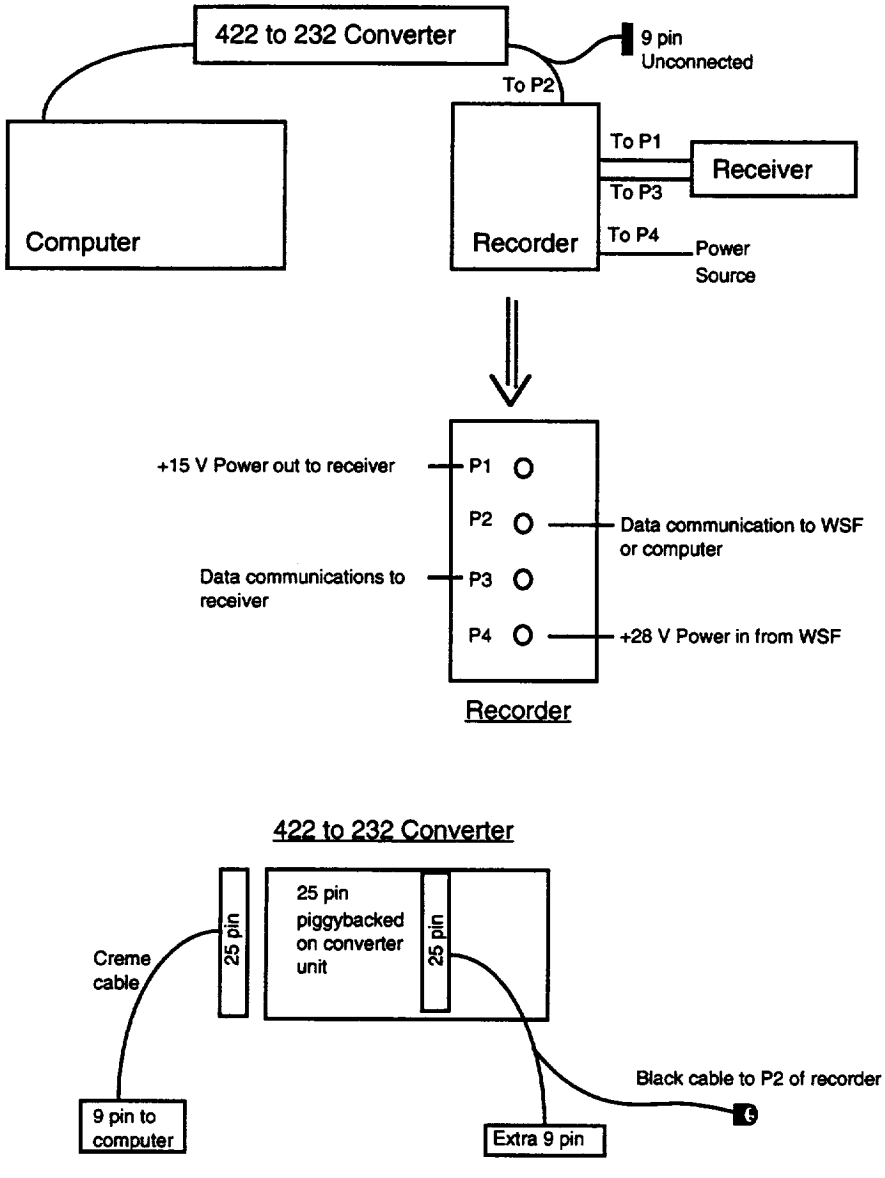

Figure A2.1 Recorder Test Integration Schematic

Orlando, May: Final WSF-02 Integration Summary

May 18

Arrived at Hangar AE at approximately 8:30 am with Exner. Russell Carpenter et al. from JSC arrived earlier--had their real-time activity set up. Informed by WSF-02 folks about schedule that indicated we could not get complete access until CHAWS completed test/installation. Schedule allowed us access around 2 pm. We were able to initiate receiver late morning using version of software left in receiver in April. Receiver acquired and locked on 8 satellites within a short time.

Antenna set up at same location as final April tests. Cable taken through side door into clean room. WSF-02 in different orientation than April--located in carrier and some 8 meters above floor. Obtained additional coax and extended cable to reradiator. Reradiator c-clamped near WSF-02 antenna. Only Exner allowed into clean room.

A signal splitter was used to allow the Collins and TurboRogue to share the same antenna (zero baseline). In general, the Collins receiver performed well, although the signal was weak from time to time. The Collins generally tracked 4 satellites and the fifth channel roved around the available satellites, sometimes tracking one of the same satellites that were in the primary four channels.

Recorded TurboRogue data through sector 4720 (2.88%) of flight recorder, terminated recording at about 3:15 pm.

Exner downloaded latest version of receiver software from GPS/MET POC and loaded into receiver at approximately 15:30. Reacquisition appeared to be nominal, but slow.

During this time, the JSC Real Time GPS (RGPS) was receiving no data from the Wake Shield telemetry (although the FLTGSE software was receiving). At approximately 6 pm, the Turbo Rogue tracking dropped from 8 satellites to 1 satellite. After approximately 1 hour it was determined that this event was probably correlated with turn-on of an S-Band transmitter for Wake Shield

communications. The transmitter/antenna was located approximately 1-2 meters from the GPS antenna. This RF problem had not been encountered during the April tests because the WSF-02 was mounted in a separate stand. This RF anomaly was peculiar to operation while the WSF-02 was mounted in the cross-bay carrier and is not expected to occur during flight. No further significant tracking was acquired until about 21:00, but everything was shut down at 22:00 (because of security agreement). At shutdown, the Turbo Rogue was performing marginally.

From approximately 17:00 to 21:00, Mission Specialist Jim Newman was assisting in the debug of RGPS. After he left, it was determined that the problem was caused by a synchronization problem on the Wake Shield side. After recycling the WSF-02 telemetry, the problem disappeared and telemetry appeared in the RGPS laptops.

WSF-02 powered down at 22:00.

At approximately 22:30, met up with WSF-02 flight crew at Castaways for food and drinks. Informed Newman of the status. Remaining problem, no telemetry flowing between RGPS laptops.

May 19

Arrived at Hangar AE at approximately 8:00. Wake Shield and Turbo Rogue had been powered up at 7:30. Recorder had completed countdown to first available sector, 4750, but no telemetry was flowing into the computers. Exner was contacted at the hotel since it was thought that the receiver should have locked on by this time, however, we did not have direct access to the receiver and had no way of evaluating the performance other than through the telemetry. When Exner arrived and connected his computer, he confirmed that the receiver was tracking only 1 or 2 satellites. The JSC group was waiting for telemetry to confirm their communication. Before starting this series, an LNA was added to the antenna path to boost the signal to the receiver.

Around 9:15, the Turbo Rogue began tracking and within a short time was tracking 8 satellites. Telemetry began flowing and the JSC group was able to

receive it and conduct state differencing between the Turbo Rogue and the Collins receiver.

At around 10:15, the receiver ops were terminated. In the next 30 min Exner configured the receiver for flight, placing the software into the "orbit mode".

SUMMARY

At the conclusion of the tests, the Turbo Rogue had tracked up to 8 satellites for an hour. With this period of tracking, the receiver obtained a good determination of the clock and rates. The receiver was operating extremely well at this conclusion. It was placed into the orbit mode, so it is now configured for flight.

It was decided not to reformat the recorder. The recorder was left for flight with approximately 3.97% used (through sector 5750). These numbers should show on GPSGSE in flight when the GPS experiment is activated.

LESSONS LEARNED

1. The Turbo Rogue may be completely lost when powered up in flight, which may require some time to lock on. Allow the receiver adequate time to start-up, perhaps at least one hour (PATIENCE!--we haven't had an identifiable receiver problem yet). Recycle power as a last resort, and only after giving the receiver at least one hour to acquire.

COMMENTS

1. Exner confirmed that thermal cover was in place. Temperature sensor has been installed between GPS and another payload.

2. Exner confirmed that visual inspection showed all cable connections in place. Also that receiver was left in the mode where it is configured for flight.

Bob Schutz, June 4, 1995

Appendix 3

Recorder Failure Analysis

Date: Thursday Oct 12 11:35:46 1995

The preliminary survey of the data recorder has been completed. The cabling and its supports were all intact and secure. The workmanship on the replacement DC/DC converter and reassembly of the recorder were superb. All connector sockets were properly inserted. Conductivity between the cabling and connectors was fine.

If you haven't guessed, all of the good news is in the first paragraph. The problem is with the DC/DC converter. Voltage is seen into the EMI filter, out of the EMI filter, into the DC/DC converter, and 0.003V out of the converter. That should be approximately 15.0V. From looking at my notes, it looks like the same results as after the problem at the Cape.

I'd like the remove the converter from the recorder and send it with the original converter to Interpoint for analysis. Hopefully, they can tell us what happened. I will have to cut all of the power cabling to do this so please let me know if this is okay.

Guess it could have been worse.

Samantha

(S. McDonald, JSC, personal communication, 1995)

Date: Tuesday, 30 Jan 1996 13:31:00 CST

Gentlemen,

Last week I finally received the failure analysis of the converters which were damaged during the development and flight of the GPS data recorder for Wake Shield 2. My summary of the report is that the failure was caused by noise or a sinusoidal wave form appearing on the sync input of the converter. This input was tied to the output common of the converter for the data recorder design per Interpoint technical support instructions. Since no isolation circuitry was

used, the sync was essentially floating allowing it to pick up any noise that was present. The corrective action on Interpoint's part is to include an application note with the specifications sheet stating that if the sync is not used, it should be connected to the input common of the converter.

Please feel free to distribute this information to anyone you think may benefit from it. If a copy of the failure report is desired, let me know your fax number and I will send a copy.

Samantha McDonald

From: "Samantha L. McDonald (Sam) 244 - 5877"

(S. McDonald, JSC, personal communication, 1995)

Appendix 4

DD Residual Sample Calculations

Sample Pre-Flight DD Residual Calculation

Table A4.1 through A4.5 lists the given information for a sample DD residual calculation assuming the pre-flight scenario presented in Chapter 4. Table A4.1 lists the receiver coordinates with respect to the Earth Centered Earth Fixed frame (ECF). The coordinates used were the result of numerous tests held on the rooftop of Building 18 at JSC and are expected to be accurate in an absolute sense (WGS-84) to better than 10 m. These coordinates were assumed to be the same for the Collins and the TurboStar. In other words, as stated in Chapter 4, a zero baseline was assumed.

Table A4.1 Assumed TurboStar and Collins Coordinates (m)

Receiver Coordinates		ECF Frame (x_R, y_R, z_R)
-492931.00600000	-5530652.0910000	3127843.3240000

The DD residual that will be calculated in this example is between PRN 28 and 15. Therefore, the pseudorange measurements for each receiver to the PRNs are listed in Tables A4.2 and A4.3. These measurements correspond to the receiver time tags listed in the header of the table in the form of year, month, day, hour, minute, and second.

Table A4.2 Collins Pseudorange Data Sample (m)

Collins	95 4 13 17 59 54.7378006000
PRN 28 Pseudorange	-5161025.6170000
PRN 15 Pseudorange	-5302458.7030000

Table A4.3 TurboStar L1/L2 Pseudorange Data Sample (m)

TurboStar	95 4 13 17 59 55.0000000000
PRN 28 Pseudorange	24159398.559000
PRN 15 Pseudorange	24017674.915400

The broadcast ephemeris (BC) information relevant to this problem is given in Table A4.4 where TOE is the time in seconds with respect to the current GPS week at which the BC information is valid. The variables a, b, and c are the transmitting clock correction parameters. Each GPS satellite has a different clock error so their respective clock correction parameters will be different as shown in Table A4.4.

Table A4.4 Data Sampling of Broadcast Clocks

Broadcast Ephemeris	95 4 13 18 00 00.0000000000	
GPS Week	796	
TOE (seconds)	0.41040000000D+06	
a (PRN 28, PRN 15)	0.83968043327D-05	0.17678132281D-03
b (PRN 28, PRN 15)	0.45474735089D-12	0.34106051316D-11
c (PRN 28, PRN 15)	0.00000000000D+00	0.00000000000D+00

Table A4.5 Useful Constants

Constants	
Earth angular rate (rad/s)	7.2921151467000D-05
speed of light (m/s)	299792458.D0

Each pseudorange listed in Tables A4.2 and A4.3 is a function of a different transmit time. There are two reasons for this. Because the receivers are recording measurements at different times (the Collins is at about 54.7 s and the TurboStar at 55.0 s), the transmit time from the same GPS satellite to each receiver will be different. Also, because each GPS satellite clock is a little

different, the transmit times from two GPS satellites to a single receiver will also be different. Thus there will be four different transmit times. Table A.6 and A.7 first lists the four GPS satellite coordinates in the ECF frame at the "true" transmit time. The true transmit time is a GPS satellite transmit time corrected to GPS time with respect to the current GPS week. Remember that GPS satellite clocks are not perfectly synchronized with GPS time and must be corrected by applying the respective broadcast constants a, b, and c as listed previously in Table A4.4.

Tables A4.6 and A4.7 give the GPS satellite coordinates transferred to a nonrotating frame (NF) chosen to be aligned with the ECF frame at the beginning of the current GPS week. Because Eq. (3-23) requires that the GPS satellite and receiver states be in the same nonrotating frame, the receiver coordinates in ECF will be transformed to the same nonrotating frame aligned with ECF at the beginning of the current GPS week. These coordinates are listed in Table A4.8.

Table A4.6 PRN Coordinates During Signal Transmission to Collins (m)

PRN 28 Coordinates		ECF Frame (x_{28}, y_{28}, z_{28})
(For True Transmit Time wrt GPS wk of BC: 410394.75500899 s)		
14551139.982631	-3474362.3295848	21922022.633578
PRN 15 Coordinates		ECF Frame (x_{15}, y_{15}, z_{15})
(For True Transmit Time wrt GPS wk of BC: 410394.75531092 s)		
15271215.132415	-20720456.971106	-6880362.5521439
PRN 28 Coordinates		NR Frame (X_{28}, Y_{28}, Z_{28})
(For Transfer Angle of 29.926458091273 rad)		
-2280769.2862747	-14785295.392861	21922022.633578
PRN 15 Coordinates		NR Frame (X_{15}, Y_{15}, Z_{15})
(For Transfer Angle of 29.926458113290 rad)		
-19411362.564237	-16904033.604786	-6880362.5521439

Table A4.7 PRN Coordinates During Signal Transmission to TurboStar (m)

PRN 28 Coordinates		ECF Frame (x_{28}, y_{28}, z_{28})
(For True Transmit Time wrt GPS wk of BC: 410394.91940598 s)		
14551260.602715	-3473920.5926907	21922009.507741
PRN 15 Coordinates		ECF Frame (x_{15}, y_{15}, z_{15})
(For True Transmit Time wrt GPS wk of BC: 4410394.91970888 s)		
15271342.009190	-20720524.271289	-6879863.7159225
PRN 28 Coordinates		NR Frame (X_{28}, Y_{28}, Z_{28})
(For Transfer Angle of 29.926475956305 rad)		
-2280141.9629216	-14785407.063769	21922009.507741
PRN 15 Coordinates		NR Frame (X_{15}, Y_{15}, Z_{15})
(For Transfer Angle of 29.926475956305 rad)		
-19411216.684692	-16904398.234148	-6879863.7159225

Table A4.8 Receiver Coordinates in Nonrotating Frame(m)

Collins Receiver Coordinates		NR Frame (X_{Rc}, Y_{Rc}, Z_{Rc})
(For True Receiver Time wrt GPS wk of BC: 410394.73780060 s)		
-5552416.4868700	42008.150322898	3127843.3240000
TurboStar Receiver Coordinates		NR Frame (X_{Rt}, Y_{Rt}, Z_{Rt})
(For True Receiver Time wrt GPS wk of BC: 410395.00000008 s)		
-5552417.2890462	41901.988733996	3127843.3240000
Note Clock Corrections (s)		
Collins = 0.00		TurboStar = -7.9754231141639D-08

The "true" receiver time shown in Table A4.8 is the receiver measurement time tag corrected to GPS time with respect to the current GPS week. As discussed in Chapters 2 and 6, the clock correction was already accounted for in the Collins receiver time tag, therefore, the clock correction is zero. It should be noted, however, that the pseudoranges are not consistent with the assumption that the time tag has been corrected. That is, if the time tag is GPS Time, then the pseudoranges must be positive, rather than negative since the clock corrections for the GPS satellites are small. The TurboStar clock correction, however, was solved using additional pseudorange measurements (not listed here) with the navigation solution methodology described in Chapter 3.

The final step is to plug all the appropriate values into the DD residual Eq. (3-23) and solve. This calculation can be broken up into two parts as shown in Eq. (3-21): DD_{obs} and DD_c. Carrying this out,

$$\begin{aligned} DD_{obs} &= \left(\rho^{PRN28} - \rho^{PRN15}\right)_{Collins} - \left(\rho^{PRN28} - \rho^{PRN15}\right)_{TurboStar} \qquad (3\text{-}19) \\ &= (-5161025.617 + 5302458.703)_{Collins} - \\ &\quad (24159398.559 - 24017674.9154)_{TurboStar} \\ &= -290.55760000274 \\ DD_c &= \left(\rho_c^{PRN28} - \rho_c^{PRN15}\right)_{Collins} - \left(\rho_c^{PRN28} - \rho_c^{PRN15}\right)_{TurboStar} \qquad (3\text{-}22) \end{aligned}$$

where, for example, $\left(\rho_c^{PRN28}\right)_{Collins}$ is written as,

$$\begin{aligned} &= \left[\left(X_{Rc}(T_R) - X_{28}(T_T)\right)^2 + \left(Y_{Rc}(T_R) - Y_{28}(T_T)\right)^2 + \left(Z_{Rc}(T_R) - Z_{28}(T_T)\right)^2\right]^{1/2} \\ &= [(-5552416.48687 + 2280769.2862747)^2 + \\ &\quad (42008.150322898 + 14785295.392861)^2 + \\ &\quad (3127843.324 - 21922022.633578)^2]^{1/2} \\ &= 24161411.003653 \end{aligned}$$

and similarly,

$$\left(\rho_c^{PRN15}\right)_{Collins} = 24070789.401275$$
$$\left(\rho_c^{PRN28}\right)_{TurboStar} = 24161489.235775$$
$$\left(\rho_c^{PRN15}\right)_{TurboStar} = 24070679.511175$$

This results in a DD_c of,

$$\begin{aligned} DD_c &= (24161411.003653 - 24070789.401275) - \\ &\quad (24161489.235775 - 24070679.511175) \\ &= -188.12222139537 \end{aligned}$$

Putting it all together gives the final result of,

$$\begin{aligned} DD_{Residual}^{28/15} &= DD_{obs} - DD_c \\ &= -290.55760000274 + 188.12222139537 \\ &= -102.435378607363 \text{ m} \end{aligned}$$

The same procedure is followed for the post-flight test except that the assumption listed in Table A4.1 is now a fact since the post-flight test was indeed a zero baseline.

Sample In-Flight DD Residual Calculation

A sample calculation for the on-flight calibration test follows. Tables A4.9 through A4.14 contain exactly the same information as Tables A4.1 through A4.8 except that the antenna coordinates are now assumed different. Table A4.9 lists the antenna coordinates that were interpolated to GPS Time from the position ephemerides formed as discussed in Chapter 5. Note also these coordinates are in ECI (J2000) since the resulting ephemeris from UTOPIA is in ECI (J2000). Therefore, the receiver positions do not need to be rotated to a nonrotating frame.

Because the GPS satellites are in ECF, however, they still need to be rotated back to ECI (J2000). Here a simplification was assumed where the GPS satellite position vectors were rotated to ECI (TOD) rather than ECI (J2000) since ECI (TOD) is near ECI (J2000). Finally, Table A.16 is the results of the example calculation DD residual between PRN 17 and 5.

Table A4.9 Antenna Coordinates Interpolated From Position Ephemerides (m)

Upper-hemi		ECI Frame (X_R, Y_R, Z_R)
(interpolated to 95 9 11 10 20 9.9507766000)		
1019117.1161939	-5880039.9659277	-3209147.299857
WSF-02 (m)		ECI Frame (X_R, Y_R, Z_R)
(interpolated to 95 9 11 10 20 10.0000000000 -5.6187980073649D-07)		
1019470.4960550	-5879965.2920290	-3209163.140813

Table A4.10 Collins Pseudorange Data Sample (m)

Collins	95 9 11 10 20 9.9507766000
PRN 17 Pseudorange	-5879985.6540000
PRN 5 Pseudorange	-5827691.7400000

Table A4.11 TurboStar L1/L2 Pseudorange Data Sample (m)

TurboStar	95 9 11 10 20 10.0000000000
PRN 17 Pseudorange	21334559.627400
PRN 5 Pseudorange	21386539.098400

Table A4.12 Data Sampling of a Broadcast Ephemeris

Broadcast Ephemeris	95 9 11 10 00 00.0000000000	
GPS Week	818	
TOE (seconds)	0.122400000D+06	
a (PRN 17, PRN 5)	-.922502949834D-04	0.125166494399D-03
b (PRN 17, PRN 5)	-.102318153949D-11	0.216004991671D-11
c (PRN 17, PRN 5)	0.000000000000D+00	0.000000000000D+00

Table A4.13 PRN Coordinates During Signal Transmission to Collins (m)

PRN 17 Coordinates		ECF Frame (x_{17}, y_{17}, z_{17})
(For True Transmit Time wrt GPS wk of BC: 123609.97048237 s)		
-6707840.2975593	25339678.560473	-3657923.3387505
PRN 5 Coordinates		ECF Frame (x_5, y_5, z_5)
(For True Transmit Time wrt GPS wk of BC: 123609.97009052 s)		
-24098030.461843	11191291.577845	809584.82167432
PRN 17 Coordinates		ECI Frame (X_{17}, Y_{17}, Z_{17})
(For Transfer Angle of 15.097321380376 rad)		
-9034005.7766703	-24606526.992503	-3657923.3387505
PRN 5 Coordinates		ECI Frame (X_5, Y_5, Z_5)
(For Transfer Angle of 15.097321351802 rad)		
13326023.489618	-22986456.387935	809584.82167432

Table A4.14 PRN Coordinates During Signal Transmission to TurboStar (m)

PRN 17 Coordinates		ECF Frame (x_{17}, y_{17}, z_{17})
(For True Transmit Time wrt GPS wk of BC: 123609.92892782 s)		
-6707832.8431953	25339698.281924	-3657791.4302624
PRN 5 Coordinates		ECF Frame (x_5, y_5, z_5)
(For True Transmit Time wrt GPS wk of BC: 123609.92853702 s)		
-24098028.417421	11191304.831212	809453.91228852
PRN 17 Coordinates		ECI Frame (X_{17}, Y_{17}, Z_{17})
(For Transfer Angle of 15.097318350171 rad)		
-9034097.7548680	-24606511.500550	-3657791.4302624
PRN 5 Coordinates		ECI Frame (X_5, Y_5, Z_5)
(For Transfer Angle of 15.097318321673 rad)		
13325944.563245	-22986506.453336	809453.91228852

Table A4.15 Final DD Residual Results (m)

$\left(\rho_c^{PRN17}\right)_{Collins}$	21259068.563524
$\left(\rho_c^{PRN5}\right)_{Collins}$	21453196.385433
$\left(\rho_c^{PRN17}\right)_{TurboStar}$	21259328.186339
$\left(\rho_c^{PRN5}\right)_{TurboStar}$	21453026.299717
DD_{obs}	-314.44299999997
DD_c	- -429.70853158087
$DD_{Re\ sidual}^{17/5}$	115.26553158090

Appendix 5

Accounting For Attitude Variations In DD Measurements

If the coordinates for the Shuttle and WSF-02 are defined as shown in Figure A5.1 where OBAS is the Shuttle-fixed coordinate system defined in Chapter 5 as the Orbiter Structural Axis System, then,

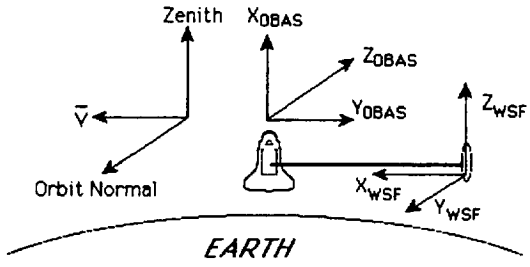

Figure A5.1 WSF-02 & Shuttle Coordinates

WSF-02 pitch = negative Shuttle yaw
WSF-02 roll = negative Shuttle pitch
WSF-02 yaw = Shuttle roll

Figure A5.1 demonstrates the shuttle in a gravity gradient (GG) orientation. One could define a coordinate frame aligned with this GG orientation (aligned with the OBAS frame in Figure A5.1) and call it the GG frame. However, as evident in Figure 5.5 and 5.17, the shuttle oscillates about this gravity gradient (GG) orientation or frame. In other words, OBAS is not in actuality aligned with the GG frame. Now the attitude of the Shuttle may be described by,

$$T_{OBAS}^{GG} = \left[T_{ORAS}^{OBAS}\left[ROLL_{Shuttle}\right]\left[YAW_{Shuttle}\right]\left[PITCH_{Shuttle}\right]\right]^{T}$$

where ORAS is the shuttle body-fixed Orbiter Rotation Axis System as described in Chapter 5. In the in-flight DD calculations it was assumed T_{OBAS}^{GG} was an identity matrix, or that the shuttle did not oscillate about its gravity gradient orientation. Therefore, the following resulted,

$$\bar{R}_{GG}^{STS/WSF} = \bar{R}_{OBAS}^{STS/WSF} \quad \Rightarrow \quad \bar{R}_{ECI_{Erroneous}}^{STS/WSF} = T_{RTN}^{ECI}\, T_{UNIT}^{RTN}\, T_{OBAS}^{UNIT}\, \bar{R}_{OBAS}^{STS/WSF}$$

In reality, however, if the actual gravity gradient attitude had been taken into account,

$$\bar{R}_{GG}^{STS/WSF} = T_{OBAS}^{GG}\, \bar{R}_{OBAS}^{STS/WSF} \qquad \bar{R}_{ECI_{Actual}}^{STS/WSF} = T_{RTN}^{ECI}\, T_{UNIT}^{RTN}\, T_{GG}^{UNIT}\, \bar{R}_{GG}^{STS/WSF}$$

where the UNIT and GG frames are assumed to be essentially aligned like the UNIT and OBAS frames in the previous analysis discussed in Chapter 5. Therefore, it follows that,

$$T_{OBAS}^{GG} = \left\{ \begin{bmatrix} -1 & 0 & 0 \\ 0 & -1 & 0 \\ 0 & 0 & 1 \end{bmatrix} \begin{bmatrix} 1 & 0 & 0 \\ 0 & c_{Y_{WSF}} & s_{Y_{WSF}} \\ 0 & -s_{Y_{WSF}} & c_{Y_{WSF}} \end{bmatrix} \begin{bmatrix} c_{-P_{WSF}} & s_{-P_{WSF}} & 0 \\ -s_{-P_{WSF}} & c_{-P_{WSF}} & 0 \\ 0 & 0 & 1 \end{bmatrix} \begin{bmatrix} c_{-R_{WSF}} & 0 & -s_{-R_{WSF}} \\ 0 & 1 & 0 \\ s_{-R_{WSF}} & 0 & c_{-R_{WSF}} \end{bmatrix} \right\}^T$$

The question about the effect that attitude mismodeling has on the DD measurements requires examination. If one looks at the difference between the actual and erroneous relative antenna positions in the OBAS frame, the magnitude of this difference can be interpreted essentially as a "delta-baseline". In relative positioning on non-zero baselines, the DD measurements will exhibit this baseline; therefore, the DD measurements will be in error by this delta-baseline. In other words,

$$\Delta \text{ baseline} = \left| \bar{R}_{OBAS_{acutal}}^{STS/WSF} - \bar{R}_{OBAS_{Erroneous}}^{STS/WSF} \right| \Rightarrow \text{excess DD}$$

Looking back at the attitude variations shown in Figure 5.4 and Figure 5.14, the pitch and roll both vary 2.5° while the yaw varies over 25° from the assumed values in the original calculations. Table A5.1 shows the variation in the baseline at maximum pitch and roll while the yaw increases.

Table A5.1 Variation Of In-Flight Baseline

Pitch (°)	Yaw (°)	Roll (°)	Δ baseline (m)
2.5	0	2.5	.56
2.5	10	2.5	2.4
2.5	20	2.5	4.6
2.5	30	2.5	6.8

In the worst case, the effect is about 7 m, but in an rms sense the effect will be less because of the diminishment that occurs with DD and the rms computation. Hence, in an rms sense, the effect on DD due to this error source is expected to be less than 2 meters.

Appendix 6

Shuttle Center of Mass History

The following Table A6.1 lists the Shuttle center of mass (CM) position vector in the Shuttle fixed OSRS frame (defined in Chapter 5). It also lists the corresponding "weight" of the Shuttle (B. Tracy, JSC, personal communications, 1995).

Table A6.1 STS-69 Center of Mass History

MET	Weight (lbs)	$\hat{x}_{OSRS}$ (in.)	$\hat{y}_{OSRS}$ (in.)	$\hat{z}_{OSRS}$ (in.)	Notes
2/13:48	238970	1102.47	0.31	377.51	
3/00:21	240439	1098.61	-0.05	377.94	post Spartan grapple
3/05:15	238602	1097.97	-0.05	377.94	
3/12:36	238565	1097.90	-0.03	377.53	vector used for MSOPD
3/22:32	234079	1100.36	-0.01	376.45	post WSF-02 release
4/05:13	234037	1100.24	0.02	376.44	
4/12:51	234022	1100.11	0.04	376.43	
4/20:40	233863	1100.17	0.08	376.45	
5/04:59	233624	1100.43	0.12	376.50	

Appendix 7

Lagrange Polynomial Interpolation

The method of Lagrange Polynomial interpolation constructs a polynomial of degree n as

$$p_n(x_k) = \sum_{j=0}^{n} f(x_j) P_j(x_k)$$

where x_j represents the $j = 1$, n data points. The data points, x, in this application is time. The function f is the satellite position value at the data point, x_k is the time of interpolation, and $P_j(x_k)$ is

$$P_j(x_k) = \begin{cases} 0, & k \neq j \\ A_j \prod_{\substack{i=0 \\ i \neq j}}^{n} (x_k - x_i), & k = j \end{cases} \qquad \text{where } A_j = \frac{1}{\prod_{\substack{i=0 \\ i \neq j}}^{n} (x_j - x_i)}$$

Because the positions for the WSF-02 and Shuttle antennas were three dimensional vectors, a single position at a given time required three interpolations for each component (x, y, z). Figure A7.1 is an example of Lagrange Polynomial interpolation used with the Shuttle upper-hemi ECI (J2000) X position component. The data used for Figure A7.1 is listed in Table A7.1.

Figure A7.1 Interpolated Upper-hemi ECI (J2000) X Component

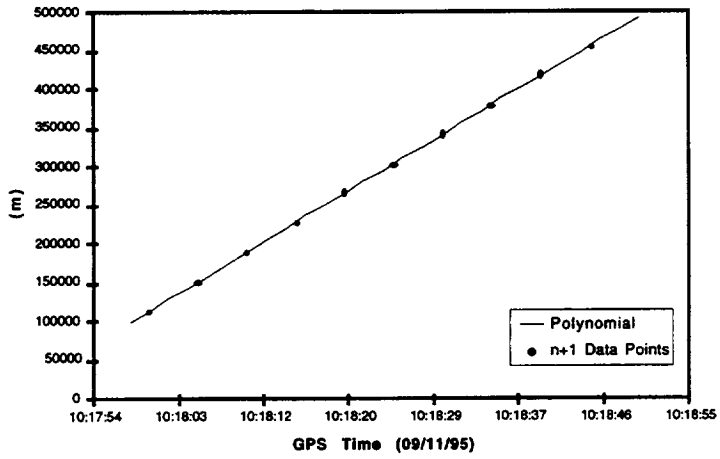

Table A7.1 Example Data Used For Lagrange Polynomial Interpolation

n	x	f(x)
1	10:18:00	111469.717
2	10:18:05	149461.087
3	10:18:10	187447.671
4	10:18:15	225428.253
5	10:18:20	263401.618
6	10:18:25	301366.548
7	10:18:30	339321.828
8	10:18:35	377266.244
9	10:18:40	415198.578
10	10:18:45	453117.618

Appendix 8

Shuttle Area Assumptions

The following information was received by B. Tracy, of JSC, 1995.

As far as frontal area goes, the 2750 ft^2 number is good for a side view (i.e. gravity gradient or there abouts). It is a good generic number that I use for flights with GG or if there are a lot of inertial attitude holds. For max area (ZVV) I use an area of 5600 ft^2 and a nose to the wind (+XVV) I use 1208 ft^2 (tail to wind I use 1301 ft^2). For the altitude we were flying on 69, area is not as big a player as it would be say for the rendezvous I did on STS-64 (~140 nm). If you plan to use constant area drag modeling, the 2750 is good.

Appendix 9

Confirmation of Collins Clock Correction

From: SMTP%"carpente@ollie.jsc.nasa.gov" 26-JAN-1996 13:56:44.96
Subj: 3M "measurement time tags" corrections

We have gathered the following evidence supporting our idea that the 3M receiver measurement times have indeed been compensated for receiver clock bias:

Young has compared the 3M receiver's own solution to the ground nav solutions based on C-band ground radar and TDRSS and found no obvious bias, whereas our filtered solutions computed from the 3M measurement data, show the 600 meter down track bias we discussed with you earlier. I also have noticed that the ranges between the WSF-02 and the Orbiter I get from your original sts254_4h and wsf254_4h seem too short compared with the rendezvous radar ranges by about 2000 feet. Finally, Ray Nuss and I confirmed with Charles Simmons of Collins just now that the parameter called GPSTIME in 3M output block 1022 is in fact a time compensated for the receiver clock offset.
Russell

Appendix 10

Confirmation of Collins Channel Biases

Date: Thu, 7 Mar 1996 16:24:50 -0600

Hi all,

Ray Nuss just came by and told me that when Collins was here today, they told him that there is a "Block 1100" which contains the interchannel bias information. Although this is a nonstandard block that did not get recorded during previous missions, Ray is going to try to get it added to the blocks recorded by his software for future flights, including STS-77 in May.

Collins suggested that if we want to find the interchannel bias from previous data sets, we should search for times when (H/W) channel 5 was tracking the same SV as one of the other (H/W) channels. They said the receiver should do this periodically to recalibrate its interchannel bias estimates. They also said that for the MAGR, interchannel biases are typically a meter or less, and that they were "bigger" for the 3M.

Russell

References

Astronomical Almanac for the Year 1995, U.S. Government Printing Office, Washington, D.C.

Engelkemier, B. S., Lagrangian Interpolation to an Ordered Table to Generate a Precise Ephemeris, Masters Thesis, The University of Texas at Austin, May 1992.

Barlier, F., C. Berger, J. Falin, G. Kockarts, G. Thuillier, Atmospheric Model Based on Satellite Drag Data, *Ann. Geophys.*, 34, 9-24, 1978.

Bertiger, W. I., et al., GPS precise tracking of TOPEX/POSEIDON: results and implications, *J. Geophys. Res., 99*, 24449-24464, Dec 1994.

Boucher, C., Z. Altamimi, L. Duhem, Results and Analysis of the ITRF93, IERS Technical Note 18, October 1994, Central Bureau of IERS/Observatoire de Paris.

Campion, E., J. Malone, "NASA Managers Delay Next Launch of Space Shuttle", NASA Press Release: 95-130, July 28, 1995.

Cheney, W., D. Kincaid, *Numerical Mathematics and Computing, Third Edition*, Brooks/Cole Publishing Company, Pacific Grove, California, 1994.

Cohen, C. E., E. G. Lightsey, W. A. Feess, B. W. Parkinson, Space flight tests of attitude determination using GPS, Proc. ION GPS-93, pp. 625-632, Sep, 1993.

Davis, G., GPS-Based Precision Orbit Determination for Low Altitude Geodetic Satellites, Ph.D. Dissertation, The University of Texas at Austin, May 1996.

Hajj, G., et al., Initial Results of GPS-LEO Occultation Measurements of Earth's Troposphere and Stratosphere Obtained with the GPS-MET Experiment, IUGG XXI General Assembly, IAG Symposium G2, Boulder, CO, July 1995.

Hoffman-Wellenhof, B., H. Lichtenegger, J. Collins, *GPS Theory and Practice*, Springer-Verlag, Wien-New York, 1992.

Hornbeck, Ph.D. R. W., Numerical Methods, Quantum Publishers, Inc., New York, New York, 1975.

Klobuchar, J. A., "Ionospheric Effects on GPS", GPS World, An Advanstar Publication, Cleveland Ohio, April, 1991.

McCarthy, D. (ed.), IERS Standards (1992), IERS Tech. Note 13, Observatoire de Paris, July 1992.

McKenna, J. T., "Wake Shield Tests Astronauts, Controllers", Aviation Week & Space Technology", September 18, 1995.

Melbourne, W. G., E. S. Davis, T. P. Yunk, B. D. Tapley, The GPS Flight Experiment on TOPEX/POSEIDON, *Geophys. Res. Lett., 21*, 2171-2174, 1994.

"Payload Deployment and Retrieval System Overview Workbook: PDRS OV 2102", Advanced Training Series, NASA Lyndon B. Johnson Space Center, Houston, Texas, February, 1988.

Rim, H., TOPEX Orbit Determination Using GPS Tracking System, Ph.D. Dissertation, The University of Texas at Austin, December 1992.

Rocken, C., C. Meertens, Monitoring Selective Availability Dither Frequencies and Their Effect On GPS Data, *Bulletin Geodesique* 65(3), 162-169, 1991.

Sandlin, A., K. McDonald, A. Donahue, "Selective Availability: To Be or Not To Be?", GPS World, An Advanstar Publication, Cleveland, Ohio, September, 1995.

Schroeder, C., B. Schutz, P. A. M. Abusali, "STS-69 Relative Positioning GPS Experiment", to appear in the Proceedings of AAS/AIAA Astrodynamics Meeting, Austin, Texas, February, 1996.

Schutz, B., et al., "GPS Tracking Experiment of a Free-Flyer Deployed from Space Shuttle", Proceedings of GPS-95, The Satellite Division of The Institute of Navigation 8th International Technical Meeting, October 1995.

Schutz, B., B. Tapley, P. Abuasli, H. Rim, Dynamic Orbit Determination Using GPS Measurements From TOPEX/POSEIDON, *Geophys. Res. Letters, Vol 21,* No. 19, 2179-2182, September 15, 1994.

Tapley, B., M. Watkins, J. Ries, G. Davis, R. Eanes, S. Poole, H. Rim, B. Schutz, C. Shum, S. Nerem, F. Lerch, J. Marshall, S. Klosko, N. Pavlis, R. Williamson, The JGM-3 Gravity Field, submitted to *Journal of Geophysical Research*, 1996.

Tapley, B., H. Rim, J. Ries, B. Schutz, C. Shum, The Use of GPS Data for Global Gravity Field Determination, Proceedings of the IAG Symposia G3,

Global Gravity Field and Its Temporal Variation, XXI General Assembly of IUGG, Boulder, Colorado, July 2-14, 1995.

Tapley, B., J. Ries, G. Davis, R. Eanes, B. Schutz, C. Shum, M. Watkins, J. Marshall, R. Nerem, B. Putney, S. Klosko, S. Luthcke, D. Pavlis, R. Williamson, N. Zelensky, Precision Orbit Determination for TOPEX/POSEIDON, *Journal of Geophysical Research,* Vol. 99, No. C12, 24383-24404, December, 1994.

Tapley, B. D., Statistical Orbit Determination Theory, Advances in Dynamical Astronomy, 396-425, B. D. Tapley and V. Szebhely (eds), D. Reidel Publ. Col, Holland, 1973.

TSGC (Texas Space Grant Consortium) World Wide Web Home Page (http://www.utexas.edu/tsgc/), University of Texas at Austin, , 3925 W. Braker Lane, Suite 200, Austin, TX 78759-5321.

Ware, R., M. L. Exner, et al., GPS Sounding of the Atmosphere From Low Earth Orbit: Preliminary Results, Submitted to *Bulletin of the American Meteorological Society*, 1995.

Yunck, T. P., "Recent Activities In Spaceborne GPS", Travaux de l'Association Internationale de Geodesie., pp. 152-161, Secretariat de l'Association, Paris, 1995.

Yunck, T. P., et al., First Assessment of GPS-based Reduced Dynamic Orbit Determination on TOPEX/POSEIDON, *Geophys. Res. Lett., 21*, 541-544, 1994.